

LEVEL III

12

A060942



RADC-TR-79-117
Final Technical Report
April 1979

**STUDY OF THE PHYSICS OF INSULATING FILMS AS RELATED TO THE
RELIABILITY OF METAL-OXIDE SEMICONDUCTOR DEVICES**

IBM T.J. WATSON RESEARCH CENTER

Sponsored by
Defense Advanced Research Projects Agency (DoD)
ARPA Order No. 2180

AD A 073300

APPROVED FOR PUBLIC RELEASE; DISTRIBUTION UNLIMITED

DDC
RECEIVED
AUG 30 1979
RECEIVED

A

The views and conclusions contained in this document are those of the authors and should not be interpreted as necessarily representing the official policies, either expressed or implied, of the Defense Advanced Research Projects Agency or the U.S. Government.

DDC FILE COPY

**ROME AIR DEVELOPMENT CENTER
Air Force Systems Command
Griffiss Air Force Base, New York 13441**

79 00 00 004

This report has been reviewed by the RADC Information Office (OI) and is releasable to the National Technical Information Service (NTIS). At NTIS it will be releasable to the general public, including foreign nations.

RADC-TR-79-117 has been reviewed and is approved for publication.

APPROVED:



JOHN C. GARTH
Contract Monitor

If your address has changed or if you wish to be removed from the RADC mailing list, or if the addressee is no longer employed by your organization, please notify RADC (ESR) Hanscom AFB MA 01730. This will assist us in maintaining a current mailing list.

Do not return this copy. Retain or destroy.

STUDY OF THE PHYSICS OF INSULATING FILMS AS RELATED
TO THE RELIABILITY OF METAL-OXIDE SEMICONDUCTOR
DEVICES

Z.A. Weinberg	D.R. Young
G.W. Rubloff	E.A. Irene
E. Bassous	H.Z. Massoud
J.M. Aitken	R. DeKeersmaecker
D.J. DiMaria	

ARPA Order Number: 2180
Program Code Number: 9D10
Program Element: 61101E
Name of Contractor: IBM T.J. Watson Research Center
Effective Date of Contract: 16 May 1976
Contract Expiration Date: 30 June 1978
Short title of work: Study of the Physics of Insulating
Films as Related to the Reliability
of Metal Oxide Semiconductor Devices
Contract Number: F19628-76-C-0249

Principal Investigator: Dr. Donald R. Young
914-945-1087

RADC Project Engineer: John C. Garth
617-478-2360

Period of work covered: 16 May 76 - 30 June 78

Approved for public release; distribution unlimited

This research was supported by the Defense Advanced
Research Projects Agency of the Department of Defense
and was monitored by John C. Garth (ESR), Hanscom AFB
MA 01730 under Contract F19628-76-C-0249

UNCLASSIFIED

SECURITY CLASSIFICATION OF THIS PAGE (When Data Entered)

REPORT DOCUMENTATION PAGE		READ INSTRUCTIONS BEFORE COMPLETING FORM
1. REPORT NUMBER RADC-TR-79-117	2. GOVT ACCESSION NO.	3. RECIPIENT'S CATALOG NUMBER 9
4. TITLE (and Subtitle) STUDY OF THE PHYSICS OF INSULATING FILMS AS RELATED TO THE RELIABILITY OF METAL-OXIDE SEMICONDUCTOR DEVICES		5. TYPE OF REPORT & PERIOD COVERED Final Technical Report 16 May 1976 - 30 June 1978
7. AUTHOR(s) Z.A. Weinberg, J.M. Aitken, E.A. Irene G.W. Rubloff, D.J. DiMaria, H.Z. Massoud E. Bassous, D.R. Young, R. DeKeersmaecker		6. PERFORMING ORG. REPORT NUMBER Scientific Report-4 7. CONTRACT OR GRANT NUMBER(s) F19628-76-C-0249
9. PERFORMING ORGANIZATION NAME AND ADDRESS IBM T.J. Watson Research Center P.O. Box 218 Yorktown Heights NY 10598		10. PROGRAM ELEMENT, PROJECT, TASK AREA & WORK UNIT NUMBERS 61101E 2180ARAE WARPA Order 2-184
11. CONTROLLING OFFICE NAME AND ADDRESS Defense Advanced Research Projects Agency 1400 Wilson Blvd Arlington VA 22209		12. REPORT DATE April 1979
14. MONITORING AGENCY NAME & ADDRESS (if different from Controlling Office) Deputy for Electronic Technology (RADC/ESR) Hanscom AFB MA 01730		13. NUMBER OF PAGES 11
15. SECURITY CLASS. (of this report) UNCLASSIFIED		15a. DECLASSIFICATION/DOWNGRADING SCHEDULE N/A
16. DISTRIBUTION STATEMENT (of this Report) Approved for public release; distribution unlimited		
17. DISTRIBUTION STATEMENT (of the abstract entered in Block 20, if different from Report) Same		
18. SUPPLEMENTARY NOTES RADC Project Engineer: J.C. Garth (ESR) (Related In-House 2306J301)		
19. KEY WORDS (Continue on reverse side if necessary and identify by block number) MOS Structures Band Gap Photo Conductivity Electron Traps Photo Transmission Exciton Generation		
20. ABSTRACT (Continue on reverse side if necessary and identify by block number) These papers discuss the effects of radiation, heat treatment, thickness, measuring temperature, impurity content on the electron trapping characteristics of SiO ₂ . The results of a comprehensive study of the photo conductivity and photo transmission of SiO ₂ are also included that make it possible to determine the band gap. The generation of donor states near the Si-SiO ₂ interface is described with a discussion of two alternate mechanisms involving excitons or hydrogen diffusion.		

349250

JB

I. TABLE OF CONTENTS

I.	Table of Contents	1
II.	Summary of Work Performed Under This Contract	2
III.	List of Contributors	9
IV.	Papers Published Under This Contract	11
V.	Papers Contributed With This Report	16
	A) Transmission, Photoconductivity, and the Experimental Band Gap of Thermally Grown SiO ₂ Films	16
	B) Radiation-Induced Electron Traps in SiO ₂	52
	C) Charge Trapping in Thermal Silicon Dioxide	70
	D) Electron Trapping in SiO ₂ at 295K and 77K	90
	E) Exciton or Hydrogen Diffusion in SiO ₂	128
	F) Radiation Damage in Silicon Dioxide Films Exposed to Reactive Ion Etching	145

Accession For	
MIS GMAI	<input checked="" type="checkbox"/>
DOC TAB	<input type="checkbox"/>
Unannounced	<input type="checkbox"/>
Justification	
By _____	
Distribution/	
Availability Codes	
Dist	Avail and/or special
A	

II. Summary of Work performed Under this Contract

The basic goal of this contract has been to investigate thin insulating SiO_2 films of the type used in modern metal-oxide semiconductor (MOS) devices. It is well known that important reliability exposures of these devices are due to various mechanisms leading to charge build up in these films. The advanced techniques that have been developed at the IBM Research Center have made it possible to clarify many of the physical mechanisms leading to these effects. In addition our studies have increased our understanding of the oxidation mechanisms that control the oxide growth rate. The initial proposal for this contract contained the following areas of work:

1. Determine the location of charge impurities, trapped holes and electrons using the photo I-V technique.
1. Study the effect of process technology and chemical compositions on the trapping of the various charge species using avalanche injection and photoelectric injection with automatic MOS C-V measurements.
3. Determine the effect of process technology and impurity content on the radiation sensitivity.
4. Use shallow buried junctions to study hole mobility and to permit separate measurements of hole and electron current. Relate this work to breakdown mechanisms.
5. Study the effect of oxide processing conditions on the trapping characteristics and radiation sensitivity.

6. Study detrapping effects as a result of temperature, electric field strength and optical excitation.
7. Study the reaction occurring at the metal-SiO₂ and metal-silicon interfaces using the techniques of Auger electron spectroscopy, x-ray diffraction and field dependent internal photoemission.

In the discussion that follows, the reference numbers will refer to the publication numbers contained in part IV of this report. The photo I-V technique for charge location developed by D. J. DiMaria²⁴ has been used extensively in numerous studies concerned with this work. The work of DiMaria, Weinberg and Aitken¹⁴ has shown that the positive charge generated in SiO₂ in response to radiation resides near the Si-SiO₂ interface (within 50 Å). Soloman and Aitken⁸ have studied the location of positive charge generated by the application of large electric fields and they have found that it resides at the Si-SiO₂ interface and at the Al-SiO₂ interface and not in the bulk of the SiO₂ as suggested by other workers. DiMaria, Young, Hunter and Serrano²¹ have studied the location of trapped electron charge, as a result of avalanche injection, in oxides containing implanted Al. The centroid of the trapped electronic charge is shown to be close to the centroid of the implanted Al. The work on implanted species has been extended in a subsequent paper by DiMaria, Young, DeKeersmaecker, Hunter and Serrano²² to include implanted P and As with reasonably good agreement between the measured trapped electronic centroids and the centroids of the implanted species. DiMaria²⁰ has also studied the location of the positive charge due to trapped N_A⁺ ions in SiO₂ and his work, in

agreement with the work of others, indicates that the N_A^+ ions are close to interfaces.

The effect of process technology on the trapping characteristics of SiO_2 has been studied in the paper by Young, E. A. Irene, Massoud, DiMaria, DeKeersmaecker²⁹ showing a significant difference between the trapping if the measurements are made at room temperature as compared to 77 K. The dominate traps for measurements at room temperature are distributed throughout the bulk of the SiO_2 . At 77K, the dominate traps are associated with the Si- SiO_2 interface. This paper also discusses some work on the generation of donor states in the vicinity of the Si- SiO_2 interface as a result of avalanche injection.

One of the important discoveries related to this work has been the observation by Aitken, Young and Pan³ that neutral electron traps are generated in SiO_2 as a result of the application of various types of radiation. The radiations used are similar to those encountered during the construction of useful devices by means of modern high density technology. The annealing conditions required to eliminate these traps have been investigated indicating that the temperature used for the conventional post metallization annealing treatments is not sufficient. Aitken²⁷ has extended this work to include samples with polysilicon gate electrodes as well as the Al gates studied earlier. It is more difficult to remove the "radiation damage" in these polysilicon gate samples with by annealing treatments. We also have used our automatic

avalanche injection apparatus to characterize the electron trapping resulting from Al implantation discussed in papers by Young, DiMaria, Hunter and Serrano.^{16,19} These studies have also been extended to include arsenic implantation by DeKeesmaecker and DiMaria¹⁰. We find implanted Arsenic is particularly effective as an electron trap. Electrons trapped on sites resulting from As and P implantation can be detrapped optically and this work has suggested a new device for charge storage that we call the LASD (Light Activated Storage Device) described in a recent paper by DiMaria, DeKeersmaecker and Young⁹.

Weinberg and Rubloff⁵ have made some interesting observations concerning effects appearing at the Si-SiO₂ interface as a result of the application of non penetrating vacuum ultraviolet radiation VUV. The important difference between their work and earlier workers is the use of a negative gate bias instead of positive gate bias. This has led them to propose an exciton model to explain their results. It has been shown that the effects on the Si-SiO₂ interface are similar to the effects previously mentioned in the paper by Young, Irene, Massoud, DiMaria and DeKeersmaecker²⁹ resulting from avalanche injection. Recent work by Weinberg, Young, DiMaria and Rubloff³⁰ has shown that the effect of both of these sources of stimulation (VUV and avalanche injection) can be increased if water is deliberately added to the SiO₂.

The avalanche injection apparatus can also be used to produced hole currents in SiO₂ if the proper wave form is used. Aitken and Young⁴ have used this technique to study the effect of processing conditions on hole trap-

ping. These results are similar to those of earlier workers who have studied the effect of oxide processing conditions on radiation sensitivity. This clearly indicates that hole trapping at the Si-SiO₂ interface is the important mechanism concerned with the positive charge build-up due to the application of radiation to MOS devices.

It has been possible, as shown by DiMaria, Young and Ormond¹⁸, to significantly improve the breakdown characteristics and decrease pre breakdown leakage currents in the oxide above polycrystalline silicon. Electron traps are deliberately added to the SiO₂. These traps charge up locally in the vicinity of the asperities of the polycrystalline silicon, reduce the enhanced electric field due to these asperities and nullify their effect. These observations offer a solution for the polysilicon-oxide problem and in addition may suggest an explanation for some observations concerning the breakdown of "normal oxides". Other contributions to high field breakdown are included in papers by DiStefano and Shatzkes¹³ and by Soloman and Aitken⁸.

Accurate studies of the oxide growth kinetics have been possible by the use of our automated in situ ellipsometer. This equipment has been used by Irene⁶ to study the initial oxidation regime and by Irene and Dong⁷ to study the oxidation of heavily B and P doped silicon.

The combination of careful studies of the optical transmission and photoconductivity of SiO₂ has led Weinberg, Rubloff and Bassous²⁶ to conclude that the band gap of SiO₂ is 9.3 eV. A wide scatter in the results of previous workers has suggested the need for this work. The electronic structure

of $\text{Si}_x\text{Ge}_{1-x}\text{O}_2$ compositions is described in a papers by Fischer, Pollak and DiStefano , Grobman, and by Pantelides, Fischer, Pollak and DiStefano.

Major Accomplishments Summarized

1. The photo I-V technique for charge location and the avalanche injection technique for trap characterization have been developed and applied to numerous problems.
2. The location of the charge centroid due to charge trapped on sites resulting from P, As and Al implantation coincides with the centroids of the implanted profiles.
3. The generation of neutral electron traps in SiO_2 as a result of radiation has been observed.
4. In "normal oxides" the dominate traps at room temperature are distributed throughout the bulk of the SiO_2 and the dominate traps at 77°K are located in the vicinity of the Si- SiO_2 interface.
5. Electrons can be detrapped optically from sites due to P and As implantation.
6. Traps can be used to improve the electric breakdown characteristic.
7. An exciton model has been proposed to explain effects resulting from the application of VUV.
8. The generation of donor states in the vicinity of the Si- SiO_2 interface has been observed as a result of the application of VUV or of avalanche injection.

9. The band gap of SiO_2 has been determined to be 9.3 eV.
10. The relationships between the oxide processing conditions and the electron trapping characteristic of normal SiO_2 has been determined.

III List of Contributors

J. M. Aitken
E. Bassous
N. A. BoJarczuk
R. F. DeKeersmaecker
D. J. Dimaria
T. H. DiStefano
D. W. Dong
B. Fischer
W. D Grobman
A. Hartstein
R. Huff
W. R. Hunter
E. A. Irene
H. Z. Massoud
D. W. Ormond
K. Pan
S. T. Pantelides
R. A. Pollak
G. W. Rubloff
C. M. Serrano
M. Shatzkes

Erhard Sirtle

P. M. Solomon

Z. A. Weinberg

D. R. Young

List of Contributors

J. M. Allen

B. J. Bracken

R. A. Brinkley

R. F. Burkhardt

B. J. Burns

T. H. Burton

L. W. Case

H. C. Case

W. D. Case

A. H. Case

E. Case

F. R. Case

D. A. Case

H. N. Case

G. W. Case

L. Case

S. L. Case

A. A. Case

G. W. Case

C. M. Case

M. Case

IV. Papers Published Under This Contract

1. "The Electronic Structure of SiO_2 , $\text{Si}_x\text{Ge}_{1-x}$, GeO_2 from Photoemission Spectroscopy", B. Fischer, R. A. Pollak, T. H. DiStefano and W. D. Grobman, *Phys. Rev.* **B15**, 3193 (1977).
2. "The Electronic Structure of SiO_2 , GeO_2 and Intermediate $\text{Si}_x\text{Ge}_{1-x}\text{O}_2$ Compositions: Experiment and Theory, S. T. Pantelides, B. Fisher, R. A. Pollak and T. H. DiStefano, *Solid State Comm.*, **21**, 1003 (1977).
3. "Electron Trapping in Electron-Beam Irradiated SiO_2 ", J. M. Aitken, D. R. Young, K. Pan, *J. Appl. Phys.*, **49**, 3386 (1977).
4. "Avalanche Injection of Holes in SiO_2 ", J. M. Aitken and D. R. Young, *IEEE Trans. Nucl. Si.*, NS-24, 2128 (1977)
5. "Exciton Transport in SiO_2 as a Possible Cause of Surface-State Generation in MOS Structure", Z. A. Weinberg and G. W. Rubloff, *Appl. Phys. Lett.*, **32**, 184 (1978).
6. "Silicon Oxidation Studies: The Initial Oxidation Regime", E. A. Irene, *J. Electro Chem. Sci.*, **25**, 1708 (1978).
7. "Silicon Oxidation Studies: The Oxidation of Heavily B and P Doped Single Crystal Silicon", E. A. Irene and D. W. Dong, *J. Electro. Chem. Sci.*, **125**, 1146 (1978).

8. "Current and C-V Instabilities in SiO₂ at High Fields", P. M. Solomon and J. M. Aitken, *Appl. Phys. Lett.*, **31**, 215 (1977).
9. "Light Activated Storage Device (LASD)", D. J. DiMaria, R. F. DeKeersmaecker and D. R. Young, *J. Appl. Phys.*, **49**, 4655 (1978).
10. "Electron Trapping and Detrapping Characteristics of Arsenic Implanted SiO₂ Layers", R. F. DeKeersmaecker and D. J. DiMaria, Not yet published (to be submitted to *J. Appl. Phys.*).
11. "Centroid Location of Implanted Ions in the SiO₂ Layer of MOS Structures Using the Photo I-V Technique", D. J. DiMaria, D. R. Young, R. F. DeKeersmaecker, W. R. Hunter and C. M. Serrano, *J. Appl. Phys.* **49**, 5441 (1978).
12. "Photodepopulation of Electrons Trapped in SiO₂ on Sites Related to As and P Implantation", R. F. DeKeersmaecker, D. J. DiMaria, and S. T. Pantelides in The Physics of SiO₂ and its Interfaces, Proc. Internatl. Topical Conference, Yorktown Heights, March 22-24, 1978, ed. S. T. Pantelides (Pergamon Press, NY, 1978) p. 189.
13. "Dielectric Breakdown Phenomena in SiO₂", T. H. DiStefano and M. Shatzkes, in Semiconductor Silicon, ed. by Howard R. Huff and Erhard Sirtl, (Published by the Electrochemical Society, Princeton, (1977) pp. 332-341.

14. "Location of Positive Charges in SiO₂ Films on Si Generated by VUV Photons, X-rays, and High-Field Stressing", D. J. DiMaria, Z. A. Weinberg, and J. M. Aitken, *J. Appl. Phys.* **48**, 898 (1977).
15. "Electron Injection Studies of Radiation Induced Positive Charge in MOS Devices", by J. M. Aitken, D. J. DiMaria and D. R. Young, *IEEE Trans. Nuc. Si.*, NS-23 1526 (1976).
16. "The Electron Trapping Behavior of Silicon Dioxide with Ion Implanted Aluminum", D. R. Young, D. J. DiMaria and W. R. Hunter, *J. Electron. Mat.* **6**, 569 (1977).
17. "Electron Trapping Characteristics of W in SiO₂", D. R. Young, D. J. DiMaria, and N. A. Bojarczuk, *J. Appl. Phys.* **28**, (1977).
18. "Use of Electron Trapping region to Reduce Leakage Currents and Improve Breakdown Characteristics of MOS Structures", D. J. DiMaria, D. R. Young, and D. W. Ormond, *J. Appl. Phys. Lett.* **31**, 680 (1977).
19. "Characterization of Electron Traps in Aluminum-Implanted SiO₂", D. R. Young, D. J. DiMaria, W. R. Hunter, and C. M. Serrano, *IBM J. Res. Develop.* **22**, 285 (1978).
20. "Room Temperature Conductivity and Location of Mobile Sodium Ions in the Thermal Silicon Dioxide Layer of a Metal-Silicon Dioxide-Silicon Structure", D. J. DiMaria, *J. Appl. Phys.* **48**, 5149 (1977).

21. "Location of Trapped Charge in Aluminum-Implanted SiO₂", D. J. DiMaria, D. R. Young, W. R. Hunter, S. M. Serrano, *IBM J. Res. Develop.* **22**, 289 (1978).
22. "Centroid Location of Implanted Ions in the SiO₂ Layer of MOS Structures Using the Photo I-V Technique", D. J. DiMaria, D. R. Young, R. F. DeKeersmaecker, W. R. Hunter, and C. M. Serrano, *J. Appl. Phys.*, *Sept. 1978*.
23. "The Properties of Electron and Hole Traps in Thermal Silicon Dioxide Layers Grown on Silicon", D. J. DiMaria, in the Proceedings of the International Topical Conference on the Physics of SiO₂ and Its Interfaces, ed. by S. T. Pantelides (Pergamon Press, NY 1978), p. 160.
24. "Evidence for a Band Tail on the Conduction Band Edge of Thermal SiO₂ from Photon Assisted Tunneling Measurements", A. Hartstein, Z. A. Weinberg, and D. J. DiMaria, in Proceedings of the International Topical Conference on the Physics of SiO₂ and Its Interfaces, ed. by S. T. Pantelides (Pergamon Press, NY 1978), p. 51.
25. "Use of Photocurrent-Voltage Characteristics of MOS Structures to Determine Insulator Bulk Trapped Charge Densities and Centroids", D. J. DiMaria, Z. A. Weinberg, J. M. Aitken, and D. R. Young, *J. of Elect. Mat.* **6**, 207 (1977).

26. "Transmission, Photoconductivity and the Experimental Band Gap of Thermally Grown SiO₂ Films", Z. A. Weinberg, G. W. Rubloff, E. Bassous, To be submitted for publication.
27. "Radiation Induced Electron Traps in SiO₂", J. M. Aitken to be published *J. of Electronic Materials*.
28. "Charge Trapping in Thermal Silicon Dioxide", D. J. DiMaria. to be published *Jap. J. of Appl. Phys.*
29. "Electron Trapping in SiO₂ at 295K and 77K", D. R. Young, E. A. Irene, H. Z. Massoud, D. J. DiMaria, R. F. DeKeersmaecker. To be submitted for publication.
30. "Exciton on Hydrogen Diffusion in SiO₂?", Z. A. Weinberg, D. R. Young, D. J. DiMaria, and G.W. Rubloff. To be submitted for publication.
31. "Radiation Damage in Silicon Dioxide Films Exposed to Reactive Ion Etching", D.J. DiMaria, L.M. Ephrath, and D.R. Young, to be published in *J. of Appl. Phys.*

TRANSMISSION, PHOTOCONDUCTIVITY, AND THE EXPERIMENTAL
BAND GAP OF THERMALLY GROWN SiO_2 FILMS*

**
Z.A. Weinberg, G.W. Rubloff, and E. Bassous

IBM Thomas J. Watson Research Center

P.O. Box 218

Yorktown Heights, New York 10598

ABSTRACT

Optical transmission and photoconductivity spectra (7-14 eV) and the field dependence of photoconductivity are presented for thermally-grown (amorphous) SiO_2 films. It is argued that the clearest experimental determination of the band gap in SiO_2 can be obtained from the field dependence of photoconductivity and its similarity to internal photoemission; a band gap of 9.3 eV for amorphous SiO_2 is deduced from the data. In view of this result some recent experimental band gap determinations are criticized and the literature on this subject is examined.

The transmission experiments were performed on thin thermally-grown (amorphous) SiO_2 films (450 Å - 5000 Å) produced by etching off the silicon substrate and using a fabrication method which is described in detail. The photoconductivity measurements were performed on

*This work was supported in part by the Defense Advanced Research Projects Agency, the Department of Defense, and monitored by the Deputy for Electronic Technology (RADC) under contract No. F19628-76-C-0249.

**Present address: Electrical Engineering Department, Technion, Haifa 32000, ISRAEL

Al-SiO₂-Si structures (SiO₂: 600 Å - 3500 Å). Diode experiments for detecting photoluminescence and possibly excitons are also described. The upper limit on photoluminescence yield was determined as ~10⁻⁴.

I. INTRODUCTION

The experimental determination of the band gap of SiO_2 is a difficult task because of its long absorption tail and the presence of exciton effects in its optical spectra. It is not surprising, therefore, that the experimental band gap is found to vary quite widely in the literature. In this paper we review the subject and propose that the field dependence of photoconductivity can be used to deduce a band gap of 9.3 eV for SiO_2 ¹ (for more discussion of this value see section III). This method is quite different from the conventional procedure of extracting a threshold from spectral data, a procedure which is subject to many complications as is explained throughout section II. This section also describes in some detail our measurements on transmission and photoconductivity of thermally grown SiO_2 films.

In spite of the considerable attention devoted to studies of SiO_2 , the character of its band gap remains unresolved both experimentally and theoretically and its experimental value is found to vary anywhere from 5 to 12 eV in recent literature²⁻⁴. In order to further illuminate this issue, we present below a review of the experimental values of the band gap, found scattered in the literature, including the newer results which are not confirmed by our data. On the theoretical side, Griscom⁵ has published an excellent review of the electronic structure of SiO_2 and its spectroscopic aspects; an elegant summary of theoretical advances has been offered by Pantelides⁶; and for more recent advances the reader is referred to ref. 7. For the sake of completeness we shall mention here, only briefly, the recent theoretical predictions regarding the SiO_2 band gap. Mott, in his review article⁸, estimated the band gap to be at about 10.6 eV, i.e. above the first peak in the optical spectra (10.45 eV in Fig. 4); however, he has since accepted the view that the band gap is at about 9 eV (largely on the basis of the data presented in this paper and in ref. 1) and he proposes that it is indirect with the 10.45 eV peak being a direct gap exciton⁹ (presumably below a higher lying direct gap). Chelikowski and Schlüter's band structure calculation¹⁰ for crystalline α -quartz yielded an indirect band gap of 9.2 eV and the lowest direct gap was found to be 9.8 eV¹¹. Schneider and Fowler¹² and

Calabrese and Fowler¹³ find the band gap to be direct forbidden. Ciraci and Batra¹⁴ have computed a direct gap at 9.8 eV for the idealized form β -cristobalite. While all the above band structure calculations neglect the important electron-hole interaction, it has been incorporated into the calculation of the optical absorption spectrum for the first time by Pantelides¹⁵, who finds that electron-hole interactions have a strong effect so that excitonic peaks dominate the entire spectrum.

One of the earliest measurements of absorption in quartz (extended to 8.44 eV) was reported by Groth and Weysenhoff¹⁶ and their data was the basis for Williams's band gap estimation of 8 eV¹⁷. Photoemission of holes from silicon into thermally grown SiO₂ was reported by Goodman¹⁸, with the energy difference between the conduction band edge in the silicon and the valence band edge in the oxide given by about 4.9 eV. This yields a band gap of 8.0-8.1 eV when combined with the energy difference between the conduction band edges of silicon and SiO₂, which has been much more firmly established at 3.1-3.2 eV^{19,20}. The earliest reflectance spectrum of SiO₂ (in the form of natural brazilian quartz) was reported by Loh²¹; he identified the first spectral peak (~ 10.4 eV) as excitonic and crudely estimated the band gap to be above it, at about 11 eV. The excitonic assumption was further strengthened by the observation of Platzöder²², on α -quartz, that the first two reflectance peaks are temperature dependent. More refined reflectance spectra of crystalline and fused (amorphous) quartz were published by Philipp^{23,24}. Although Philipp did not attempt to estimate the band gap energy from his spectra, Powell and Derbenwick²⁵ used Philipp's results to conclude that the fundamental absorption edge of SiO₂ is at approximately 9 eV. In the same paper²⁵ the authors suggest a band gap of 8.8 eV from their measurements of hole trapping in thermally grown SiO₂ films illuminated by vacuum-ultraviolet (VUV) photons.

Until recently, the most accepted band gap value was due to DiStefano and Eastman²⁶, who determined an interband gap of 9.0 eV by fitting their photoconductivity spectra (performed on a 5000 Å thermally-grown SiO₂ film) to a parabolic absorption edge character-

istic of an indirect band gap. They also determined a band gap of 8.9 ± 0.2 eV from photoemission of electrons from SiO_2 into vacuum (for which they place the threshold at 10.2 eV) and similarly from silicon through 150 Å of SiO_2 into vacuum (for a review of these results see ref. 5). We note in passing that the 8.9 eV value would be revised upward to 9.3 eV if one assumes that the valence band edge of SiO_2 lies at 10.6 eV below vacuum, as indicated by Ibach and Rowe²⁷ from electron energy-loss spectroscopy measurements on thermally grown SiO_2 films.

In contrast to the above trend, the region for creation of electron-hole pairs has been placed much higher (above 12 eV) by Zakis *et. al.*²⁸ (see also Trukhin, below) – and on the other hand much lower band gap values were proposed by Stephenson and Binkowski². The latter authors observed a soft shoulder in their X-ray photoelectron spectroscopy (XPS) data obtained on α -quartz and fused silica, but this was absent in OH-rich silica glass. They propose the following lower and upper limits on the SiO_2 band gap: 5.55-7.8 eV for α -quartz, 5.05-7.3 eV for fused silica, and up to 8.3 eV for OH-rich silica. These results have already been criticized by Griscom⁵ on the basis of defects introduced in the surface of the sample during its preparation by vacuum milling. We add here that such low band gap values would imply unreasonably low barriers for hole injection from the electrodes into SiO_2 in metal-oxide-silicon (MOS) structures. These have not been observed although such low barriers would have been easily seen because holes conduct quite readily in SiO_2 at room temperature^{29,30}. Interestingly, in contrast to Stephenson and Binkowski, Kaminow *et. al.*³¹ find that the absorption edge of their dry silica occurs at an energy 0.2 eV higher than for their wet silica.

More recently, Trukhin⁴ published photoconductivity spectra of crystalline quartz, fused silica, and thermally grown SiO_2 films on silicon. For all his samples the data show an exponential rise from about 8.8 eV with some rounding observed above 12 eV (Fig. 5 in ref. 4). Trukhin interprets his data as evidence for a direct band gap of 12 eV and a lowest band

gap of 9.5 eV. Trukhin's photoconductivity spectra and likewise the earlier photoconductivity results of Zakis *et. al.*²⁸ are completely inconsistent with our results (see Fig. 7) and those of DiStefano and Eastman²⁶. Appleton *et. al.*³² have measured transmission and photoconductivity of α -quartz and vitreous SiO₂, and suggest, following Mott⁸, a direct band gap of 10.6 eV with the possibility of a lower indirect band gap of about 9 eV.

In a more elaborate band gap determination Powell and Morad³ obtain a value of 8.0 ± 0.2 eV, which is the same threshold they find in the absorption coefficient, photoconductivity spectra, and positive charging effects of thermally grown SiO₂ films. We find ourselves in disagreement with this result. First, the thresholds in these spectra cannot be determined very accurately because of interference and internal photoemission effects, as is described in section II; and secondly, the threshold of spectral data may not represent the band gap, as is explained in section III.

In addition to the above literature, many papers have dealt with the optical absorption edge of various glasses, which is generally sensitive to impurities and radiation damage. References on these subjects can be found in the reviews by Sigel³³ and Lell *et. al.*³⁴.

II. EXPERIMENTAL RESULTS

Initially, the transmission experiments (section IIA) and photoconductivity measurements (section IIB) were motivated by the need for accurate data on the optical absorption coefficient and on electron-hole separation in SiO₂ to supplement our experiments on the possibility of exciton migration^{1,35}. It developed that our results did not confirm the band gap determination presented in recent publications²⁻⁴, and therefore, we shall emphasize in this section the points of disagreement and the difficulties in extracting a threshold from the spectral data. Instead, we propose that the field dependence of photoconductivity (section IIC) may be a better means for band gap determination.

The three device structures used in our study are illustrated schematically in Fig. 1. Thin oxide membranes (Fig. 1a) were used for transmission measurements, MOS structures (Fig. 1b) were employed for photoconductivity studies, and the diode structures (Fig. 1c) were used in an attempt to detect excitons and photoluminescence. More experimental details are found in the appropriate section below.

In each of the experimental arrangements the incident ultraviolet photon flux was monitored by the fluorescence of a sodium salicylate layer³⁶ which is assumed to have an approximately flat conversion efficiency of VUV to lower energy photons, which are then detected by a photomultiplier. VUV light was obtained from a McPherson model 225 monochromator equipped with a H₂ discharge lamp and an Al/MgF₂-coated grating of 1200 lines/mm. The samples were mounted approximately 3 cm away from the monochromator's exit slit, which was open to 1.0 mm, giving a wavelength resolution of 8 Å (FWHM).

A. TRANSMISSION THROUGH THIN OXIDE MEMBRANES

1) Membrane Preparation.

As described by Powell and Morad³ (abbreviated herein as PM), thin oxide membranes produced by the anisotropic etching of silicon,^{37,38} can be used for measuring optical transmission. PM have used the simplest technique of membrane preparation where the initial thick oxide used as an etching mask is also the final oxide to be studied (reduced in thickness during the silicon etching). Although we have also tested this technique, a more elaborate fabrication method was adopted in order to retain better control over the processing and thickness of the final oxide. The technique employs a layer of Si₃N₄ for protection, as described below. Oxides, 400 – 600 Å thick, were thermally-grown in dry O₂, steam, or dry O₂ with HCl (4.5%) ambients. These ultrathin membranes are suitable for measuring transmission in the strongly absorbing region of SiO₂ (\lesssim 10 eV). To extend the measurement to the less absorbing region, membranes with about 1000 Å and 5000 Å of dry oxide were also prepared. A photograph of a typical membrane is shown in Fig. 2. It was found that the elongated

structure gives better support to the membrane and that the sinusoidal pattern produced by interference (due to the slight wrinkling of the film) is a good indication of the membrane integrity. These membranes have exhibited a remarkable resilience during final fabrication and handling steps. We proceed to describe the membrane preparation method in some detail since it includes a few novel steps.

Silicon wafers 57 mm in diameter, 0.4 mm thick, polished on one side, (100) oriented, 2-5 Ω -cm p-type were thermally oxidized to a thickness slightly above the final desired value. The oxidation conditions investigated were: dry O_2 at 1000°C; dry O_2 with 4.5% HCl at 1000°C; and wet oxidation at 800°C. The oxides were then coated with 1500 Å of CVD Si_3N_4 deposited from SiH_4 and NH_3 at 800°C. The purpose of the Si_3N_4 film is to protect the initial SiO_2 during the anisotropic etching of the silicon. A second wet oxidation was performed to grow 5000 Å of SiO_2 on the unpolished back-side of the wafers. Using standard photolithography, a pattern of rectangular openings (1.42mm \times 0.81mm) and a grid defining chip sizes were etched in the back-side oxide with the pattern aligned parallel to the wafer flat or $\langle 110 \rangle$ direction. The silicon was then etched through this pattern by an anisotropic etching solution containing 12 gm pyrocatechol, 75 ml ethylene diamine, 6 ml of H_2O_2 (30%), and 18 ml of water. At its boiling point of $118 \pm 1^\circ C$, the solution etches (100) silicon at about 130 μ m per hour which is approximately twice the rate of the more commonly used etchant^{39,40} without H_2O_2 . Etched cavities were formed with the 4 convergent {111} walls inclined at 54.7° with respect to the wafer's surface. The wafers were removed from the etching solution when the etched silicon thickness reached 3-10 μ m as determined by monitoring the membrane transparency under a microscope. To form the free SiO_2 membrane, the Si_3N_4 film was etched in boiling H_3PO_4 at 180°C followed by removal of the underlying thin silicon by the anisotropic etchant. The latter step was carefully controlled to minimize etching of the back side of the SiO_2 . Since the etching rate of SiO_2 is slow (approximately 130 Å per hour), we estimate that at most a 5 Å layer of SiO_2 might be removed in this step. The wafers were then separated into chips by breaking them along the grid lines defined by the etching. The yield of good

membranes was about 20%. The oxide thickness ($\pm 1\%$) was measured by ellipsometry on each chip, adjacent to the membrane, after the transmission experiment was completed.

2. Experimental Results

Several chips were mounted in a rotary holder, with their oxide side facing the light source, as shown schematically in Fig. 1(a). One of the chips had its oxide etched off to serve as a reference. The transmission data were obtained by dividing the oxide signal by the reference signal after each had been corrected for the scattered light contribution. Corrections for small differences in membrane sizes were done, initially, by etching the oxide off and calibrating the aperture's transmission relative to the reference. Alternatively, a simpler procedure was adopted (which is probably more accurate): where the transmission was normalized to unity at the interference peak at low photon energies, which is the theoretical value for a transparent film. Such transmission data are shown in Fig. 3 for three oxide thicknesses of 436, 1100, and 5110 Å.

The absorption coefficient (α) was evaluated by an iterative procedure from the transmission (T) using the exact formula as described in Appendix A. In the calculation the initial values of k were taken from Philipp⁴¹ while his values of n were assumed throughout, where $n-ik$ is the complex index of refraction. For the range where $T < 0.2$ the error resulting from the use of Philipp's data for n is small: a $\pm 10\%$ change in n yields a change of $\pm 2\%$, or smaller, in α . The absorption coefficient is shown in Fig. 4 and the tail region is shown on an expanded scale in Fig. 5. Fig. 4 gives a comparison between our results for a 436 Å SiO_2 film, Philipp's Kramers-Kronig analysis of fused silica reflectance data, and PM's results for a 580 Å SiO_2 film. We have found it necessary to shift Philipp's data by +.075 eV to align the position of his first peak with ours and that of PM. It is not clear whether this small shift is due to a real difference between thermally-grown SiO_2 and fused silica or to errors resulting from the Kramers-Kronig analysis. As seen in Fig. 4, good agreement is found between Philipp's data and our results over an appreciable energy range. The discrepancy above about

11.5 eV might be due to the appreciable scattered light correction in our data in this region. The discrepancy below about 10 eV, again, is due to either real differences between the oxides or to errors in Kramers-Kronig analysis. The discrepancy between our result and that of PM is much larger than our experimental error and, in our opinion, cannot be explained by differences in oxide processing. The accuracy of α in our data is estimated to be better than $\pm 2\%$ for the region where $T < 0.2$, which applies from about 9.2 eV for the 5110 Å film to about 11.3 eV for the 436 Å film. Above 11.3 eV the scattered light correction becomes appreciable and the error could be as high as 10%. The reproducibility of α among membranes of various oxide thicknesses and processing, as described in the previous section, has been within $\pm 5\%$.

The absorption tail region is shown in expanded scale in Fig. 5 and a few points from measurements on thin vitreous silica by Appleton *et. al.*³² are also shown. In our results it is evident that when the transmission approaches unity (Fig. 3) the errors in α become larger and interference effects cannot be entirely corrected by the use of Philipp's optical constants. Therefore, we consider our results to be reliable only down to about 9.2 eV for the 5110 Å film. Similarly, the Kramers-Kronig analysis of Philipp's data is also questionable in the tail region. The data of PM show much stronger absorption than even the data of Appleton *et. al.* on vitreous SiO₂, which is not reasonable considering the high purity of thermally-grown SiO₂.

We conclude this section by remarking that the 8 eV threshold determined by PM (Fig. 2 in ref. 3) from a square root fit of the absorption tail seems very doubtful in view of the low reliability of the measurement in the absorption tail on ultrathin films, as discussed above.

B. PHOTOCONDUCTIVITY SPECTRA

1) Experimental

MOS capacitors were mounted in a manner shown schematically in Fig. 1(b). The photocurrent flowing in the oxide was measured on the substrate side (1) and a mask was employed to shield the unmetallized regions of the SiO₂ and to collect secondary emitted

electrons. The use of a mask is important since VUV light impinging on the exposed regions of the oxide will charge up these regions and cause current to flow through the oxide, resulting in erroneous current readings. Similarly, erroneous readings will occur if secondary photoemitted electrons can reach the contact region where the current is measured. The proper functioning of the mask has been verified by checking that varying the mask voltage did not affect the current readings, especially at low photon energies where the oxide currents are small. As a matter of routine the mask was held at +15 V with respect to the gate. An *in situ* calibration of the light intensity was obtained by rotating the sample holder away from the beam and using the same detection method as explained in the introduction to section II.

The oxides were thermally grown on (100), 2 Ω -cm, p-type, silicon wafers. Thicknesses up to about 1000 \AA were prepared by a dry oxidation followed by 5 min. anneal in an argon ambient. Higher thicknesses were prepared by a dry-wet-dry oxidation with a similar anneal, all done at 1000°C. The wafers were all metallized together with a pattern of aluminum dots, 1.25 mm in diameter and about 160 \AA thick. The contact was initially made on a thicker Al pad but it was found that direct bonding to the thin Al is simpler and serves equally well.

2) Results and Discussion.

The spectral dependence of photoconductivity is shown in Fig. 6 for three oxide thicknesses of 575, 1015, and 2310 \AA , with the region at low photon energies multiplied by 10 for clarity. As explained below, the tail also contains photocurrent contributions resulting from internal photoemission (IPE) from the aluminum. The data shown are uncorrected for reflectance or interference effects. Such corrections were attempted but have been found inadequate, presumably because a 3-layer structure requires a more precise knowledge of all optical constants.

The data of Fig. 6 show a more complete and a more complex behavior than previously published. Clearly, the determination of a threshold, or a band gap, from such data is difficult

in view of the obvious strong interference effects and appreciable internal photoemission contribution at low photon energies. It is interesting to compare our results with the literature. DiStefano and Eastman²⁶ extracted a 9 eV band gap by fitting a portion of their photoconductivity data, obtained on a 5000 Å SiO₂ film, to a parabolic absorption law. However, we have determined that interference effects persist even for higher thicknesses (measurements were carried up to 3500 Å and absorption calculations up to 6000 Å); therefore, their fitting procedure is somewhat unreliable. Powell and Morad³, on the other hand, observed an 8 eV threshold in their photoconductivity measurements on 1034 Å of SiO₂; again, interference effects and IPE contributions make the agreement between this value and their absorption coefficient threshold seem quite coincidental. Trukhin's⁴ photoconductivity spectrum shows a plateau that begins only above 12 eV. We think that his results are erroneous because his samples were covered with LiF and also possibly because of inadequate shielding against secondary electrons which interfere with the current readings.

The data of Fig. 6 exhibit an approximate plateau above about 10 eV, with the structure in this region being partially due to variations in reflectance (especially near 10.5 eV) and partially due to a varying loss of carriers by recombination near the aluminum as light is absorbed closer or further from this electrode. Nevertheless, the photoyield in this region is approximately unity, as determined from an absolute intensity calibration of the detector, performed at a lower photon energy (~ 5.5 eV). This high yield rules out the explanation offered by Mott⁸ that the currents below about 10.5 eV result from excitons which migrate to the aluminum and give up their energy to electrons in the electrode, thereby injecting some of them into the oxide (this mechanism, similarly to IPE, should have quite a low yield).

C. PHOTOCONDUCTIVITY FIELD DEPENDENCE

In view of the difficulties with the spectral dependence, more insight can be gained by examining the dependence of the photocurrents on the electrical field. This is shown by the series of curves in Figs. 7-9, for photon energies in the range of $2.6 \text{ eV} < h\nu < 11.1 \text{ eV}$ which extends from below the energy barrier for IPE to above the main threshold of photoconductivity in the oxide. The curves of Fig. 7 were obtained with a visible-UV monochromator and those of Figs. 8 and 9 in the VUV monochromator. All data were taken on the same device and normalized to unity at their highest point. Measurements on samples with other oxide thicknesses gave the same results, hence the data shown are free of interference effects. The data were taken with a negative bias on the Al electrode and are discussed below. For positive bias, the following observations were made: For $h\nu > \sim 10 \text{ eV}$, the currents display a complicated dependence on time and field, due to hole trapping at the interfaces^{29,43}. For $\sim 8.5 \text{ eV} < h\nu < \sim 10 \text{ eV}$, the currents are steady and equal to the negative bias case, which is consistent with absorption mainly throughout the SiO_2 bulk. For $h\nu < \sim 8.5 \text{ eV}$, the currents are smaller than for negative bias since they originate from IPE from the silicon.

The change in curvature in Fig. 7 is associated with the transition from mainly photon assisted tunneling⁴⁴ to IPE which, as has been shown by Powell,²⁰ occurs at $h\nu \sim \phi_B$, where ϕ_B (3.15 eV) is the barrier height between the Al Fermi level, E_F , and the oxide conduction band. In Fig. 7 the square root of the yield is plotted since in the simplest form of IPE, the yield Y is given by

$$Y = A(h\nu - \phi_B + \Delta\phi)^m \quad (1)$$

where A is a constant, $\Delta\phi$ the image force barrier lowering, and m is a parameter which characterizes the energy distribution of the photoexcited electrons. It was previously concluded from IPE⁴⁵ and photon assisted tunneling experiments⁴⁴ that for injection from Al into SiO_2 $m \sim 2$, which corresponds to the photoexcited electrons being uniformly distributed in

energy up to $E_F + h\nu$. The field rather than its square root, as predicted by the classical image force theory, has been used in the figures, since the latter tends to exaggerate the relatively unimportant low field portion of the curves.

The transition from IPE to absorption and photoconductivity in the oxide is apparent in Fig. 8. At 7.72 and 8.34 eV the curves display a behavior which is due mainly to IPE (which increases only weakly with field); in contrast, the curve at 8.63 eV shows a sharp increase of current at higher fields which indicates that oxide photoconductivity becomes larger than IPE.

The general behavior of the curves in Fig. 9 is similar to that of Fig. 7. This is not surprising since the separation of an electron from the hole within the oxide is not too different from the separation of an electron from the screened hole in the metal. Aside from the more subtle differences between the two cases, associated with the escape probability (dielectric constant, energy levels, etc.), the energy distribution of the photoexcited electrons is certainly different. For absorption, the distribution in energy is probably fairly narrow which leads to a uniform distribution in the component of momentum in the direction of escape parallel to the field; this in turn gives $m=1$ in eq. (1). Therefore we chose to plot the yield rather than its square root in Figs. 8 and 9. Similarly to IPE (Fig. 7), where the change in curvature is associated with the barrier height, we associate the change in curvature seen in Fig. 9 with the SiO_2 band gap and deduce that $E_g \sim 9.3$ eV. This association and the 9.3 eV value are, obviously, subject to a more detailed modeling of the problem.

D. DIODE EXPERIMENTS

A schematic illustration of the diode experiment is shown in Fig. 1c. Shallow junctions ($\sim 1 \mu\text{m}$) were fabricated by standard diffusion processes in the silicon substrate, and the oxide was grown over them. Both n/p and p/n diodes²⁹ were used and the oxide was unmetallized. Several oxide thicknesses in the range 450-1350 Å were used. The diode's contacts were

shielded from light and from secondary electrons and the current (I) was the signal induced by the VUV light.

The diode, obviously, is a detector for photons and in principle could detect excitons too, provided that excitons diffusing in the SiO_2 can cross the Si-SiO₂ interface. Such excitons would separate in the silicon into free electrons and holes and be detected much the same as photons which are absorbed in the silicon near the Si-SiO₂ interface.

Because it is difficult to determine an absolute calibration for the diode signal, the data was normalized to the calculated transmission of the oxide in the transparent region (~ 8 eV). The diode signal was then compared with the calculated transmission for the rest of the spectrum (up to 12 eV). It was found that the diode signal was always larger by about a factor of 3-10 than that predicted from the calculated transmission in the absorbing region (over 9.8 eV). This "extra" signal was found to decay exponentially with the oxide thickness (in the range 450-1350 Å) and therefore could not be due to photoluminescence. A possible explanation of its origin is as follows: if only the initial "hot" excitons (i.e. before they recombine or relax to lower more stable energy levels) can cross the Si-SiO₂ interface, then the "extra" signal originates from a region near the Si-SiO₂ interface extended by the distance these "hot" excitons can travel. To explain the data this distance is about 150 Å. These findings merit further investigations.

The diode experiments provide, however, two useful results. They approximately confirm the transmission results of the membrane experiments and they provide an upper limit on photoluminescence. At 10.2 eV (the peak intensity of H₂ discharge) the diode with 1350 Å of SiO₂ showed a normalized signal of $\sim 10^{-4}$. Since the diode provides the best geometry for collecting photoluminescence, this value can be taken as an upper limit on photoluminescence. This result confirms the previous observation of one of us²⁹ that recombination is nonradiative in pure SiO₂. We point out here that PM's 5×10^{-4} limit on photoluminescence efficiency was computed erroneously because the geometrical arrangement of the membrane experiment does

not allow good collection of photoluminescence. The intrinsic limit on luminescence collection is placed by the Brewster angle (total internal reflection) given by $\theta_b = \arcsin(1/n)$ where n , the index of refraction of SiO_2 , is $\sim 1.94^1$ for $h\nu \sim 9$ eV. The solid angle defined by θ_b yields a photon escape efficiency from the membrane of only $(1 - \cos\theta_b)/2 = 0.075$ which rises to 0.13 for $n=1.5$ (in the visible).

III. DISCUSSION AND CONCLUSIONS

The presence of strong electron-hole interaction in a material like SiO_2 raises the question of whether a single value for the band gap is at all meaningful. In the amorphous form the disorder even further complicates this question. Obviously, we cannot resolve this issue here, but we point out that it is difficult to deduce the band gap solely from optical data, since excitonic and band-to-band absorption are indistinguishable in the optical spectrum. Band structure calculations for crystalline SiO_2 which neglect the electron-hole interaction predict various values for the band gap⁹⁻¹⁴ and, in addition, they point to a common conclusion that the onset of band-to-band absorption is weak (e.g. the one-electron joint density of state of ref. 9 Fig. 6), and that the first spectral peak (10.45 eV) and its long tail are predominantly excitonic. Higher peaks may have substantial excitonic origins as well¹⁵.

More insight concerning the band gap issue can be gained when experimental transport properties are taken into consideration. It is well known that thermally-grown SiO_2 possesses a well defined and sharp conduction band edge; evidence for this comes from the well defined barrier observed in internal photoemission (IPE) experiments^{20,46}, from the lack of thermal activation on electron mobility⁴⁷ (see discussion by Mott⁸), and from the relatively small electron trapping in dry SiO_2 ⁴⁸. Our photoconductivity field dependence data (section IIC) display a behaviour which is similar to IPE and which contains a transition energy at $h\nu=9.3$ eV. In analogy with IPE we identify this energy as the "barrier height" for photoionization (electron-hole separation) in thermally-grown (amorphous) SiO_2 and propose that this is the most direct experimental estimate of the band gap. Obviously, it is not possible to specify

whether this is a direct or indirect band gap or the sum effect of both, especially since these band gaps are found to be very close in self-consistent band structure calculations (9.2 and 9.8 eV, from refs. 10,11) for α -quartz, and may be even further intermixed in amorphous SiO₂. Regarding the nature of the experimental band gap it has been implicitly identified as indirect both by DiStefano and Eastman²⁶ (DE) and PM³ because they both fit portions of their data to a $(h\nu - E_g)^2$ behavior (see also ref. 5 section 4.2). DE obtain $E_g \sim 9$ eV by fitting photoconductivity data, while PM obtain $E_g \sim 8$ eV from absorption coefficient data. Our estimate of $E_g \sim 9.3$ eV is more consistent with DE although we find that interference effects do not permit definite conclusions to be drawn from such fits.

With $E_g \sim 9.3$ eV it remains to explain the absorption tail which extends down to at least 8.4 eV (see Fig. 5) and in various silica glasses to below 8 eV³². In our opinion the tail is due to one or both of the following edge-broadening effects:

1) An Urbach tail which originates from excitonic absorption which is broadened by electric microfields⁴⁹ (localized fields which fluctuate both in time and space and which originate from intrinsic effects such as disorder and phonons and from extrinsic impurities). Urbach tails⁵⁰ are exponential edges usually seen below the absorption edge of insulators⁵¹. While an extended exponential edge is not seen for SiO₂, our absorption coefficient data (Figs. 4,5) show approximately exponential behavior in the range ~ 9.2 eV $< h\nu < \sim 10.2$ eV, corresponding to about 2 decades in α .

2) Broadening due to band tailing at the valence band edge. Evidence for such band tailing comes from the work on hole conduction at various temperatures in thermally grown SiO₂ films^{30,52,53}. Mott⁸ estimates the range of band tailing to be only 0.1 eV; however, Curtis and Srour⁵³ model their data with extended trapping in the range of ~ 0.5 eV.

Aside from the band gap issue it is interesting to note that even at relatively high fields ($> 2 \times 10^6$ v/cm) the photocurrents of Fig. 9 do not saturate. This indicates that an appreciable fraction of the electron-hole pairs are not dissociated by the applied field, and by definition

remain then as excitons. The field dependence of Fig. 9 cannot be attributed to any other phenomena, such as trapping of free carriers (Schubweg effects) because of the low trapping of both electrons and holes in the bulk of dry SiO_2 ⁴⁸ (trapping of holes is strong near the interfaces only⁵⁴); neither can it be explained by recombination of free (separated) electron and holes because of their low volume densities ($\sim 10^4$ and $\sim 10^{10}$ cm^{-3} assuming mobilities of ~ 20 and $\sim 10^{-5}$ $\text{cm}^2/\text{v-sec}$. for electrons and holes at room temperature, respectively; with a current of 10^{-7} A/cm^2 and a field of 10^6 v/cm). The excitons do not recombine radiatively (see section IID) and some general features of their lifetime before self-trapping have been discussed by Mott and Stoneham⁵⁵. We have previously interpreted our findings of charging effects in MOS structures illuminated by VUV light with the Al electrode biased negatively as evidence for diffusion of such excitons from near the Al- SiO_2 interface to the Si- SiO_2 interface^{1,35}. However, we have found recently that the effect increases in samples treated in water, which raises an alternative possibility that the effect can be explained by diffusion of water-related species (such as hydrogen). This issue is presently unresolved.

In summary, extensive transmission and photoconductivity data for thin thermally-grown SiO_2 films have been presented and discussed. Threshold determination from spectral data has been criticized, and it is proposed that a band gap of 9.3 eV for SiO_2 can be extracted from the field dependence of photoconductivity.

Appendix A

The transmission (normal incidence) of a thin film of thickness d and complex index of refraction $n-ik$, suspended in vacuum, is given by⁵⁶:

$$T = \frac{a}{b_1 e^\sigma + b_2 e^{-\sigma} + b_3 \cos \gamma + b_4 \sin \gamma}$$

where,

$$\sigma = \frac{4\pi kd}{\lambda}; \quad \gamma = \frac{4\pi nd}{\lambda}; \quad \lambda: \text{ vacuum wavelength}$$

$$a = 16(n^2 + k^2)$$

$$b_1 = [(1+n)^2 + k^2]^2$$

$$b_2 = [(1-n)^2 + k^2]^2$$

$$b_3 = 2[4k^2 - (n^2+k^2-1)^2]$$

$$b_4 = 8k[n^2+k^2 - 1]$$

The absorption coefficient, α , was calculated from:

$$\alpha \equiv \frac{4\pi k}{\lambda} = \frac{1}{d} \ln \left[\frac{1}{b_1} \left(\frac{a}{T} - b_2 e^{-\sigma} - b_3 \cos \gamma - b_4 \sin \gamma \right) \right]$$

This equation was solved by iteration with Philipp's⁴¹ k values as the initial guess, and his n values as constants.

Acknowledgements

One of us (ZAW) is indebted to D. J. DiMaria for critical discussions and for experimental help in the IPE measurements; and to H. R. Philipp for supplying detailed tables of optical constants for SiO_2 , Si, and Al. For sample preparation we are grateful to K. E. Belcher, J. W. Kuran, E. J. Petrillo, H. Pinckney, and S. K. Tharas; and for experimental assistance to J. A. Calise, J. J. Donelon, A. Marx, and F. L. Pesavento.

References

1. Z. A. Weinberg and G. W. Rubloff, in The Physics of SiO₂ and its Interfaces, ed. by S. T. Pantelides, p. 24 (Pergamon, New York, 1978).
2. D. A. Stephenson and N. J. Binkowski, *J. Non-Crystalline Solids* 22, 399 (1976).
3. R. J. Powell and M. Morad, *J. Appl. Phys.* 49, 2499 (1978).
4. A. N. Trukhin, *phys. stat. sol. (b)*, 86, 67 (1978).
5. D. L. Griscom, *J. Non-Crystalline Solids* 24, 155 (1977).
6. S. T. Pantelides, *Comments Solid State Phys.* 8, 55 (1977).
7. S. T. Pantelides, The Physics of SiO₂ and its Interfaces, (Pergamon, New York, 1978).
8. N. F. Mott, *Advances in Physics* 26, 363 (1977).
9. N. F. Mott, in The Physics of SiO₂ and its Interfaces, ed. by S. T. Pantelides, p. 1 (Pergamon, New York, 1978).
10. J. R. Chelikowsky and M. Schlüter, *Phys. Rev. B* 15, 4020 (1977).
11. M. Schlüter and J. R. Chelikowsky, *Solid State Commun.* 21, 1123 (1977).
12. P. M. Schneider and W. B. Fowler, *Phys. Rev. Lett.* 36 (425) 1976.
13. E. Calabrese and W. B. Fowler, *Phys. Rev.* B18, 2888 (1978).
14. S. Ciraci and I. P. Batra, *Phys. Rev. B* 15, 4923 (1977).
15. S. T. Pantelides, in The Physics of SiO₂ and its Interfaces, ed. by S. T. Pantelides, p. 80 (Pergamon, New York, 1978).
16. W. Groth and H. V. Weysenhoff, *Z. Naturforsch.* 11a, 165 (1956).
17. R. Williams, *Phys. Rev.* 140, A569 (1965).
18. A. M. Goodman, *Phys. Rev.* 152, 780 (1966).
19. R. Williams, *Semiconductors and Semimetals*, ed. by R. K. Willardson and A. C. Beer (Academic, New York, 1970) vol. 6, p. 97.
20. R. J. Powell, *J. Appl. Phys.* 41, 2424 (1970).
21. E. Loh, *Solid State Commun.* 2, 269 (1964).
22. K. Platzöder, *phys. stat. sol.* 29, K63 (1968).

23. H. R. Philipp, *Solid State Commun.* 4, 73 (1966).
24. H. R. Philipp, *J. Phys. Chem. Solids*, 32, 1935 (1971).
25. R. J. Powell and G. F. Derbenwick, *IEEE Trans. Nuc. Sci.* 18, 99 (1971).
26. T. H. DiStefano and D. E. Eastman, *Solid State Commun.* 9, 2259 (1971).
27. H. Ibach and J. E. Rowe, *Phys. Rev. B* 10, 710 (1974).
28. Y. P. Zakis, A. N. Trukhin, and V. P. Khimov, *Soviet Physics-Solid State*, 15, 149 (1973).
29. Z. A. Weinberg, *Appl. Phys. Lett.* 27, 437 (1975).
30. R. C. Hughes, *Phys. Rev. B* 15, 2012 (1977).
31. I. P. Kaminow, B. G. Bagley, and C. G. Olson, *Appl. Phys. Lett.* 32, 98 (1978).
32. A. Appleton, T. Chiranjivi, and M. Jafaripour-Ghazvini, in *The Physics of SiO₂ and its Interfaces*, ed. by S. T. Pantelides, p. 94 (Pergamon, New York, 1978).
33. G. H. Sigel, Jr., *J. Non-Crystalline Solids*, 13, 372 (1973/74).
34. E. Lell, N. J. Kreidl, and J. R. Heusler, *Prog. in Ceramic Sci.* 3, 1 (1966).
35. Z. A. Weinberg and G. W. Rubloff, *Appl. Phys. Lett.* 32, 184 (1978).
36. J. A. R. Samson, *Techniques of Vacuum Ultraviolet Spectroscopy* (Wiley, New York, 1967).
37. C. W. Wilmsen, E. G. Thompson, and G. H. Meissner, *IEEE Trans. Electron Devices*, 19, 122 (1971).
38. K. E. Petersen, *Appl. Phys. Lett.* 31, 521 (1977).
39. R. M. Finne and D. L. Klein, *J. Electrochem. Soc.* 114, 965 (1967).
40. E. Bassous and E. F. Baran, *J. Electrochem. Soc.* 125, 1321 (1978).
41. We used values kindly provided in table form by H. R. Philipp. For the published data see refs. 23 and 24 above.
43. R. J. Powell, *J. Appl. Phys.* 46, 4557 (1975).
44. Z. A. Weinberg and A. Hartstein, *Solid State Commun.* 20, 179 (1976).
45. P. M. Solomon and D. J. DiMaria, private communication.

46. A. Hartstein, Z. A. Weinberg, and D. J. DiMaria, in The Physics of SiO₂ and its Interfaces, ed. by S. T. Pantelides, p. 51 (Pergamon, New York, 1978).
47. R. C. Hughes, *Phys. Rev. Lett.* **30**, 1333 (1973).
48. D. J. DiMaria, in The Physics of SiO₂ and its Interfaces, ed. by S. T. Pantelides, p. 160 (Pergamon, New York, 1978).
49. J. D. Dow, in Optical Properties of Highly Transparent Solids, ed. by S. S. Mitra and B. Bendow, p. 131 (Plenum, New York, 1975).
50. F. Urbach, *Phys. Rev.* **92**, 1324 (1953).
51. J. Tauc, in the Optical Properties of Highly Transparent Solids, ed. by S. S. Mitra and B. Bendow, p. 245 (Plenum, New York, 1975).
52. F. B. McLean, G. A. Ausman, Jr., H. E. Boesch, Jr., and M. McGarity, *J. Appl. Phys.* **47**, 1529 (1976).
53. O. L. Curtis, Jr. and J. R. Srouf, *J. Appl. Phys.* **48**, 3819 (1977).
54. D. J. DiMaria, Z. A. Weinberg, and J. M. Aitken, *J. Appl. Phys.* **48**, 898 (1977).
55. N. F. Mott and A. M. Stoneham, *J. Phys. C: Solid State Phys.* **10**, 3391 (1977).
56. G. Hass and L. Hadley, American Institute of Physics Handbook, 3rd edition (McGraw-Hill, New York, 1972), p. 6-120.

Figure Captions

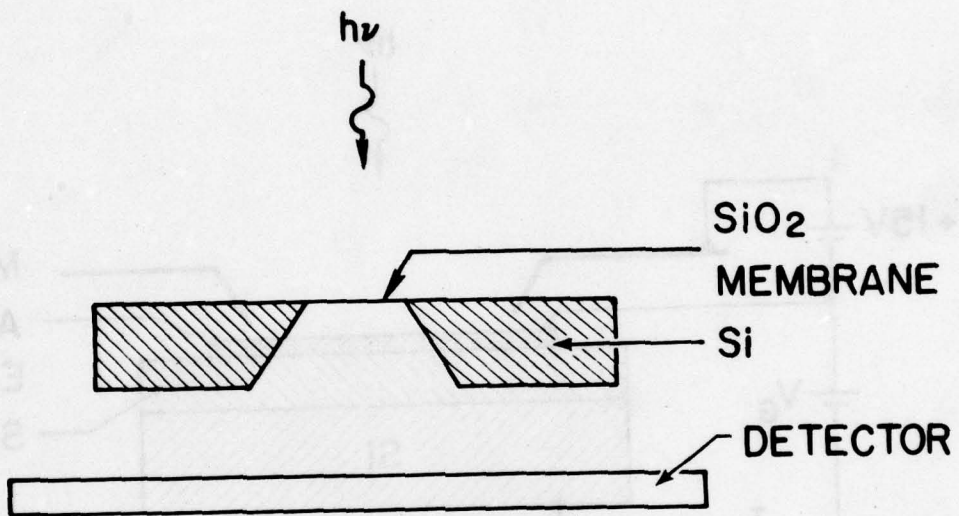
- Fig. 1. a) Schematic illustration of the transmission experiment with thin SiO_2 membranes. The detector was a sodium salicylate coating which converts the incident VUV light ($h\nu$) to lower energy photons detected by a photomultiplier.
- b) Schematic illustration of the photoconductivity experiments on MOS structures. The contact leading to the current meter (I) was completely shielded from secondary photoemitted electrons by the sample housing (not illustrated), and by the mask which also shields the unmetallized surface of the oxide. V_G was negative (Al-side) for the data of Figs. 6-9.
- c) Schematic illustration of the diode experiments for transmission, photoluminescence, and exciton detection.
- Fig. 2. Photograph of a membrane measuring 1.0×0.25 mm, showing the sinusoidal pattern produced by microscope light interference in the slightly wrinkled SiO_2 film.
- Fig. 3. Optical transmission data for 3 oxide thicknesses (for clarity, measured points are not indicated).
- Fig. 4. The absorption coefficient of amorphous SiO_2 (for the expanded tail region see Fig. 5). The 'present work' curve was calculated from the transmission data of Fig. 3, as explained in section IIA. Powell and Morad's curve was reproduced from Fig. 2 of ref. 3. Philipp's curve was obtained from his optical constants (calculated by Kramers-Kronig analysis of reflectance data, see ref. 41) and shifted by $+0.075$ eV to align the positions of the first peak (see text).
- Fig. 5. The absorption tail region. Note the expanded scale of α . Our data is considered reliable only in the range of $h\nu > 9.2$ eV for the 5110 \AA film; for lower $h\nu$, interference effects are clearly visible. A few points from Appleton et. al. (ref. 32) for vitreous SiO_2 , are added for comparison.
- Fig. 6. Normalized photoconductivity spectra. The currents were normalized to the incident photon flux and the scale shown corresponds to the range of actual meas-

urements. The data are not corrected for reflectance which is the cause of most of the structure for $h\nu > \sim 10$ eV. For $h\nu < \sim 10$ eV, interference effects are clearly visible and in the tail region (expanded by 10) internal photoemission of electrons from the Al is appreciable. The data were taken with an average field of 2×10^6 v/cm across the SiO_2 , with the Al biased negatively ($-V_G$ in Fig. 1b).

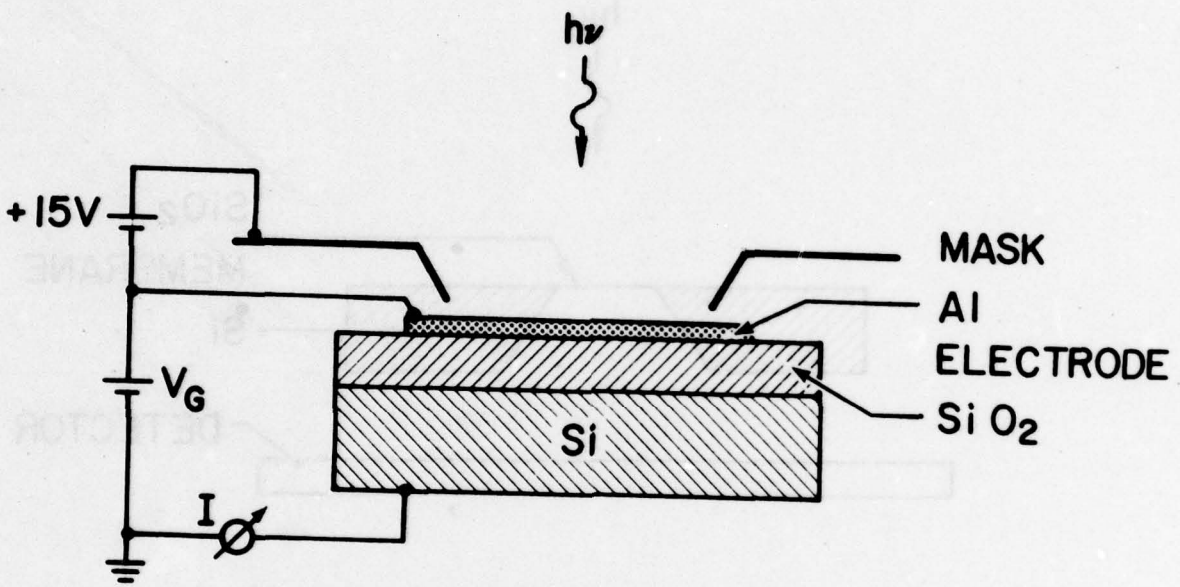
Fig. 7. The field dependence of photocurrents at various photon energies for electron injection from the Al ($-V_G$ in Fig. 1b) into the SiO_2 . The change of curvature at about 3.2 eV is associated with the barrier height between the Al Fermi level and the SiO_2 conduction band edge (see ref. 20). The reason for plotting (photocurrents)^{1/2} is explained in section IIC. The curves of Figs. 7-9 are all normalized to unity.

Fig. 8. The field dependence of photocurrents (Al-negative) at photon energies near the absorption edge of SiO_2 . At 7.72 and 8.34 eV the curves display mainly the behavior of internal photoemission (see Fig. 7 for $h\nu > 3.2$ eV) while at 8.63 eV photoconductivity (SiO_2 absorption) dominates at higher fields.

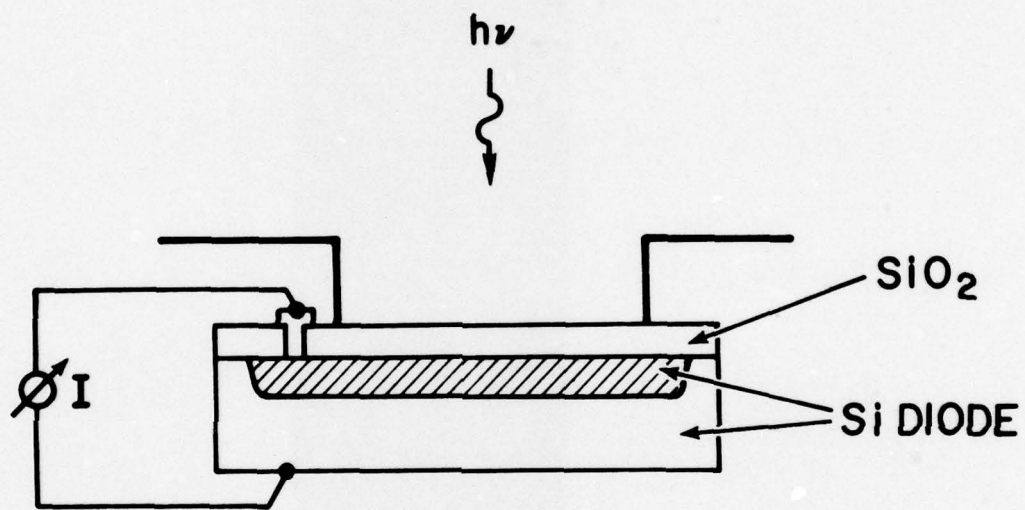
Fig. 9. The field dependence of photoconductivity (Al-negative) in thermally grown SiO_2 films (amorphous) at various photon energies above the absorption edge. As in Fig. 7, we associate the change of curvature at about 9.3 eV with a "barrier height" which we identify as the SiO_2 band gap (see sections IIC and III).



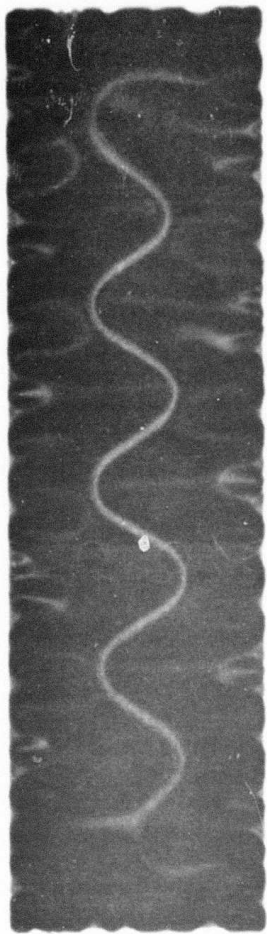
(a)

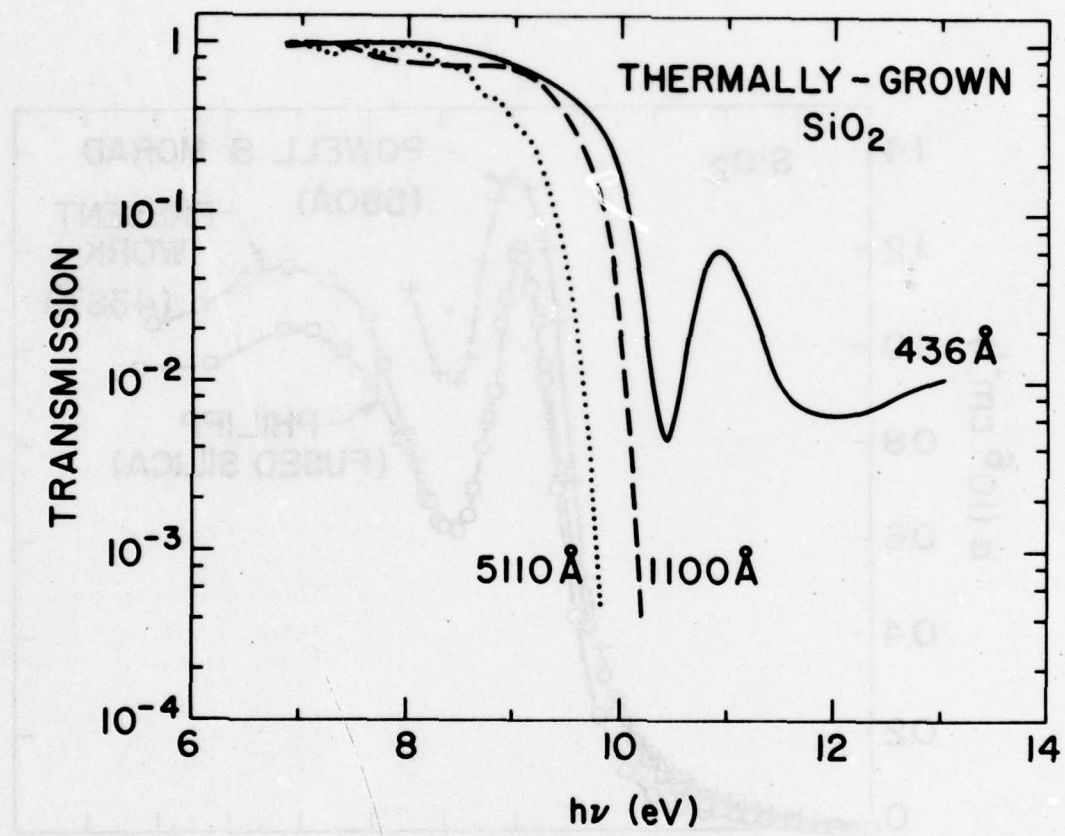


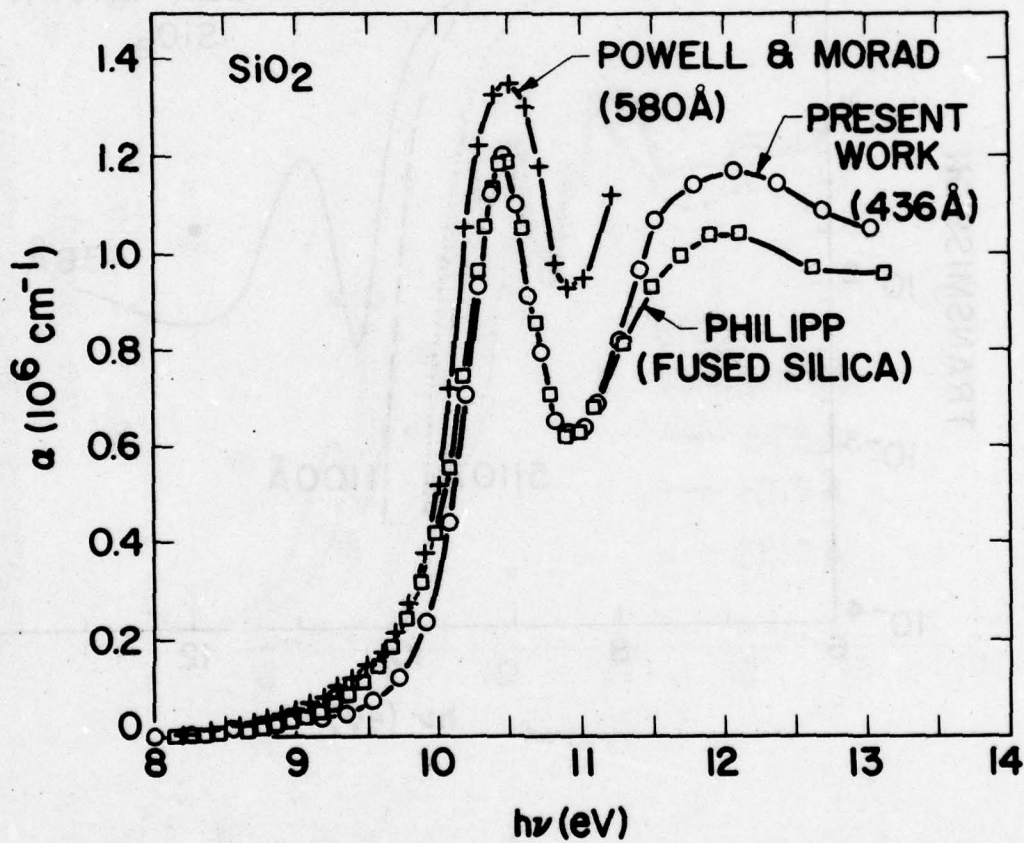
(b)

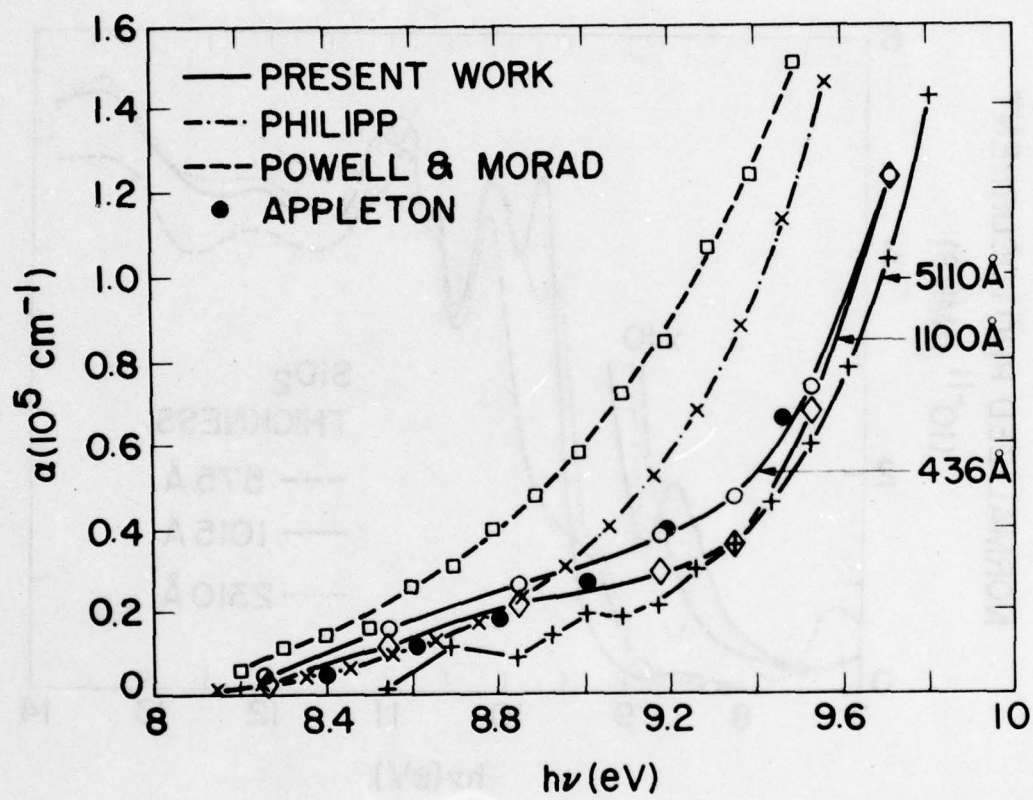


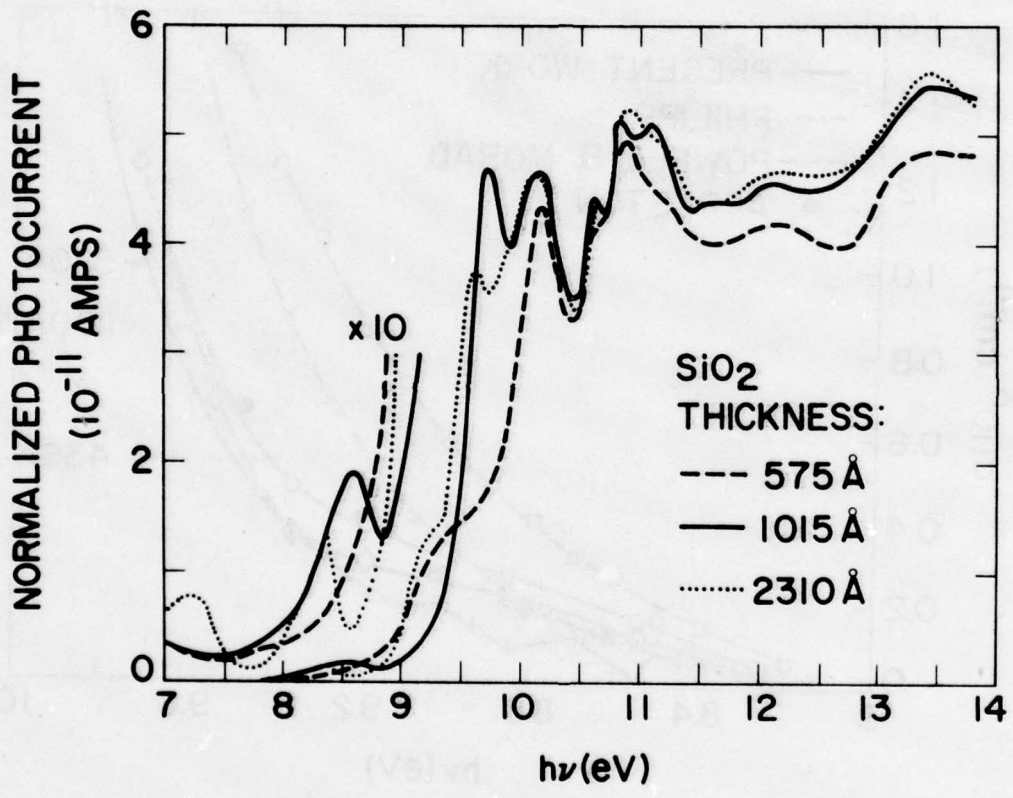
(c)

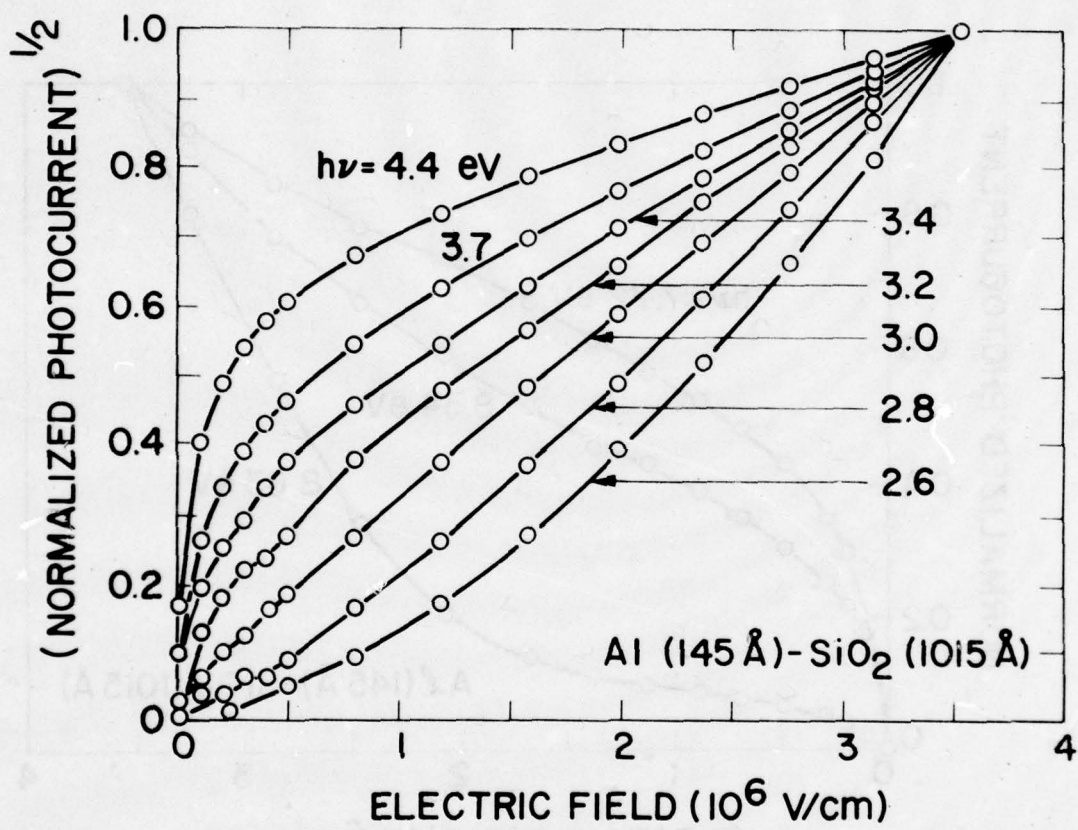


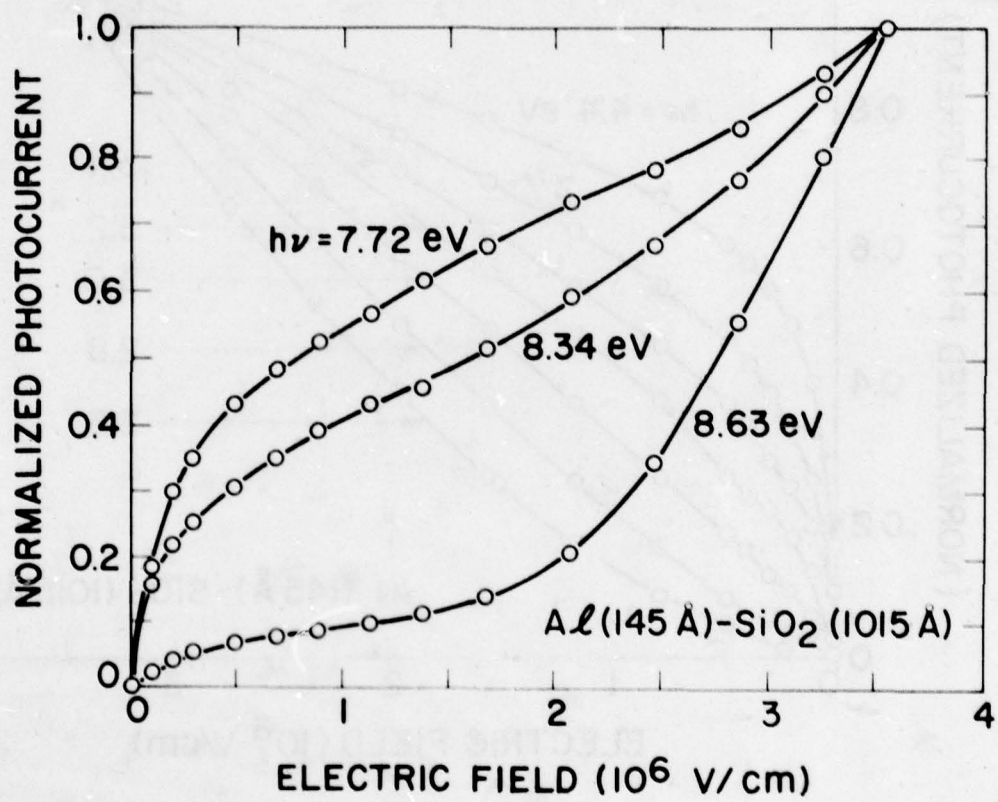


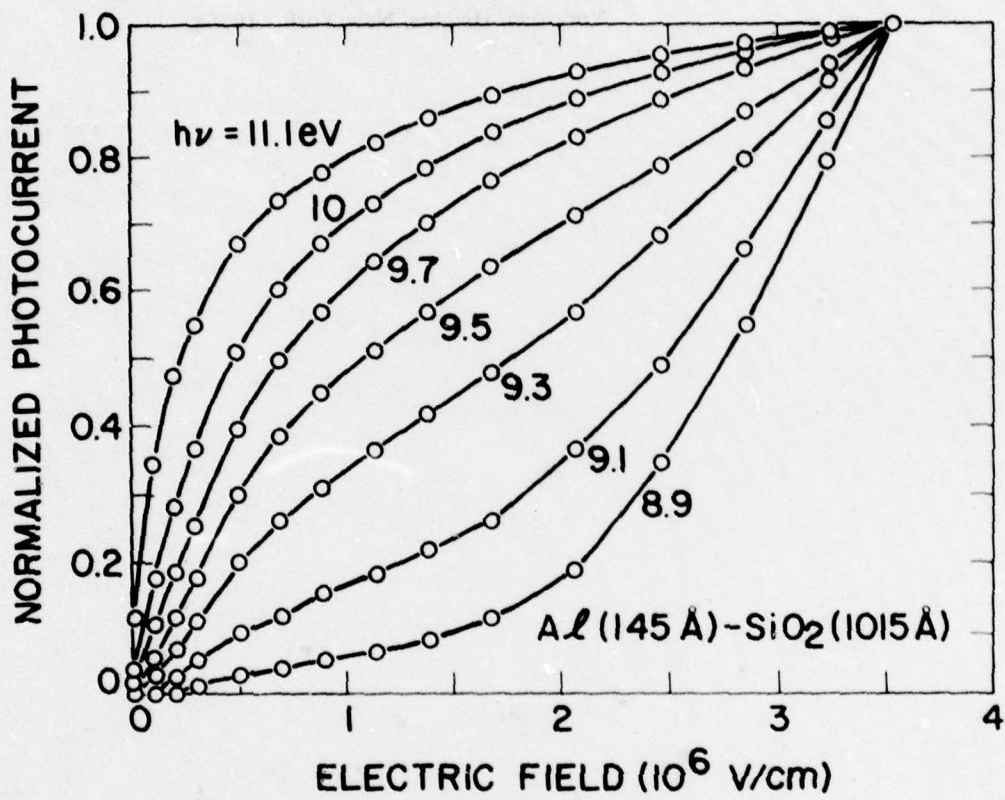










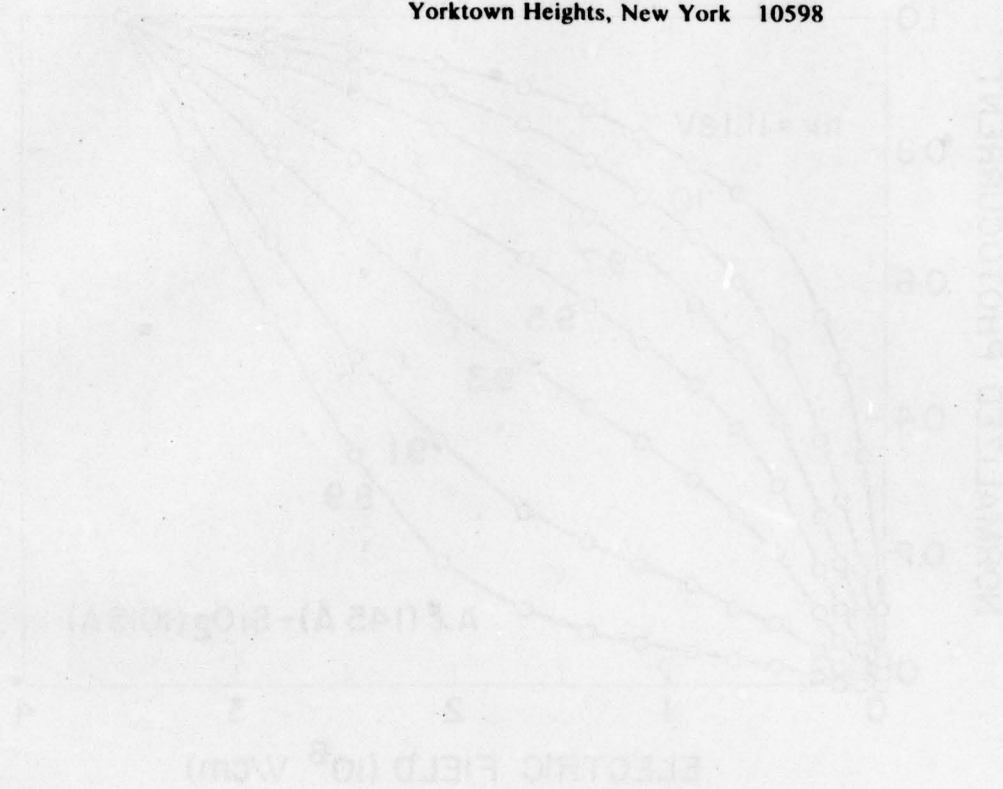


RADIATION-INDUCED ELECTRON TRAPS IN SiO₂

J.M. Aitken*

IBM T.J. Watson Research Center

Yorktown Heights, New York 10598



*This research was supported in part by the Defense Advanced Research Projects Agency, The Department of Defense, monitored by the Deputy for Electronic Technology (RADC) under contract No. F19628-76-C0249 Electronic Technology Laboratories.

Introduction

Semi-conductor processing environments in which ionizing radiation plays a direct role or appears as a by-product are being used to fabricate the next generation of MOSFET devices. Electron beam lithography and reactive ion etching, for example, allow the fabrication of dense arrays of small MOSFET's.¹ While ionizing radiation is known to cause a buildup of positive charge and surface states in the oxide layer of MOS devices, it is usually assumed that these changes are removed by thermal anneals at temperatures below 400 where metallurgical reactions between aluminum and silicon are unimportant². In this paper we investigate the annealing of radiation damage in SiO₂ and show that these low temperature anneals are not effective in completely removing radiation-induced positive and neutral electron traps from SiO₂. Such studies are important because emission of hot-electrons from the channel area during operation and subsequent trapping in the oxide layer at unannealed defects changes the device characteristics and can cause premature failure.³

Past studies have concentrated on the rate at which positive charges or surface states accumulate in optically fabricated devices operating in a radiation environment such as outer space⁴. Since annealing is not an easily practiced remedy in this instance, little effort has been made to study it. In a processing environment, however, thermal annealing is a practical step and is used to remove the "damage" introduced into the oxide by the ionizing radiation encountered in a particular processing step.

In addition the earlier studies have restricted themselves to MOS devices with aluminum gates. The newer FET technologies make extensive use of poly-silicon gates over the oxides. In this paper, annealing of damage in poly-silicon as well as aluminum gate devices is examined. The principal results show that in addition to the positive charge and surface states, neutral electron traps are also generated by the ionizing radiation and are removed only by anneals at temperatures above 550 C. Significant amounts of radiation induced positive charge

are also found in poly-silicon gated oxide films after a low temperature anneal which removes this charge from aluminum gated films.

Experimental Details

Both capacitor and FET structures were used in these experiments. Oxide films were grown in dry O_2 at 1000 C on p type substrates with a resistivity of 0.1 to 0.2 Ω -cm for the capacitors and .5 Ω -cm for the FET's. Such highly-doped material is necessary for the uniform injection of minority carriers at low applied fields.^{5,6} Two types of capacitors were formed by covering the oxide with a film of aluminum (MOS) or by a layer of phosphorous doped polysilicon covered by aluminum (MSOS). After deposition of the aluminum in a resistance heated evaporation system and definition of the capacitor gate area ($5 \times 10^{-4} \text{cm}^2$), the capacitors were annealed for 20 minutes at 400 C in forming gas to reduce the surface state density in the oxide. Subsequent to irradiation the aluminum was stripped from portions of the MSOS wafer to form SOS structures. The FET's consisted of large area ($5 \times 10^{-4} \text{cm}^2$) enclosed devices designed for trapping studies in oxides.⁷ The gate oxide was covered by a single poly-silicon layer (SOS) and was contacted by an aluminum pad in the thick oxide region away from the gate area. In all cases the poly-silicon was degenerately doped and was 350nm thick.

The densities of positively charged and neutral electron traps in the oxides were determined at various points in the experiments, i.e., before irradiation, after irradiation, and after a series of anneals designed to reduce the radiation damage. Although simple flat-band or threshold measurements give the positive charge densities in the samples, they do not reveal the presence of empty neutral electron traps. The densities of positively charged and neutral traps were determined by uniformly injecting hot electrons from the substrate into the oxide and measuring the shift of flat-band or threshold voltage which occurs as a small fraction of these carriers become trapped. The trapping cross-section observed is used to separate the traps into charged or neutral centers. The positive charge density determined from the

injection experiments provide a valuable check on the density determined by flat-band or threshold measurements. The electron currents through the oxide were generated by avalanche injection techniques in the capacitors^{5,6} and by optically induced hot electron injection in the FET's.⁷ Small currents (2×10^{-8} A-cm⁻²) were used to fill the traps with large cross-sections and as these saturated the current was gradually raised to populate the remaining traps at an acceptable rate.

A 25 KV electron beam was used to irradiate the samples. At this energy the beam penetrates the overlying layers of aluminum and polysilicon into the oxide⁸. In the capacitors, the thickness of the aluminum and polysilicon was adjusted so that the energy deposited in the SiO₂ underlying the aluminum contact in the MOS capacitor was the same as that deposited in the SiO₂ underlying the aluminum/poly-silicon contact in the MSOS capacitor. Dosages approximating those used to develop present day electron-beam resists were used. Anneals were carried out in a forming gas ambient for 30 minute intervals. As stated earlier, the SOS capacitors were formed by etching aluminum from the MSOS wafers prior to anneal. In the experiments comparing the annealing of the three kinds of capacitors, all three were annealed simultaneously in the same furnace to insure identical treatment. Anneal temperatures between 400 and 550 C were used. Penetration of aluminum contact metallurgy into diffusions presently limits post-metal sintering to temperatures below 450 C.⁹

Results and Discussion

The annealing of radiation induced positive charge in MOS, MSOS, and SOS structures is contrasted in Fig. 1. The samples were treated identically; the only difference being the metallurgy over the gate area during the anneal. Both the MOS and MSOS wafers were given a blanket exposure of 20μ coul-cm⁻². The aluminum and aluminum/polysilicon thicknesses were adjusted to give the same total thickness (750 nm) over the gate to allow equal penetration of the electron beam to the underlying gate oxide. The higher density of charge accumu-

lated in the poly-silicon gate capacitor is due to increased sensitivity of the gate oxide to ionizing radiation caused by the additional heat-treatment used to dope the poly-silicon gate.¹¹ This result shows that while the positive charge can indeed be removed from MOS or MSOS structures at 400 C, a small amount ($\sim 6 \times 10^{10}$) remains in the SOS structures. Note also that the anneal proceeds slower in the MSOS capacitor than in the MOS capacitor but that after 30 minutes the positive charge is removed in both. Anneals performed in pure hydrogen at this temperature exhibit the same end point densities although the rates of annealing are somewhat more rapid. The key ingredient to the effectiveness of the anneal appears to be the presence of aluminum over the gate during the anneal. Note however, that the aluminum is still effective when separated by 350 nm of poly-silicon from the oxide. Aluminum sintering at low temperatures has been long established as a process which improves surface state densities in aluminum gate devices. The special properties of this metal may be associated with its reactivity or its work function but are not understood. Surface reactions which produce some species effective in annealing could explain the similarity in annealing between the MOS and MSOS case. Aluminum does however penetrate easily through these poly-silicon films at this temperature¹⁰ so some other mechanism may be active.

Another experiment involving electron trapping in the oxides of these capacitors backs up these results. Electronic currents generated by avalanching the substrate into deep depletion were passed through the oxides of these capacitors. The shift in the flat-band voltage which occurs as electrons are trapped at positively charged traps is plotted in Fig. 2 against the number of electrons passed through the oxide per square centimeter of gate area. The electron capture cross-section and field dependence of positive charge in SiO_2 is well established and predicts that 1.5 MV/cm across the oxide during injection these traps saturate after 5×10^{13} electrons/cm² have been passed through the oxide¹². The greater shift evident in the sample annealed without aluminum over the gate at this value of injected charge further confirms the presence of positive charge in this sample. The initial flat-band voltages observed in these samples were consistent with the presence of positive charge in the amounts indicated by the

saturated shift in Fig. 2. Note that the control sample also exhibits a small amount of positive charge unrelated to the influence of radiation. Results in MOS capacitors are similar to those in the MSOS capacitors.¹³

In addition to the positive charge found in irradiated structures after annealing, unannealed neutral electron traps were also found. This point is illustrated in Fig. 3 which shows the shift in threshold voltage caused by trapping of optically injected electrons in the oxide layer of poly-silicon gated FET's which have been exposed to e-beam radiation and then annealed. The origin of this shift is identical to that shown in Fig. 2 although the mechanism by which the hot-electrons are generated is different and the field across the oxide is lower. As before the injected charge needed to saturate the positive charge in the oxide is calculated to be 5×10^{14} e/cm² for the indicated value of oxide field.¹² Note how the curves change slope at this point. The threshold shift at saturation corresponds very well with the low initial threshold voltage observed in these devices. The shift in threshold which occurs on further injection is associated with previously uncharged electron traps generated in the oxide by ionizing radiation. These traps are not evident from the initial threshold voltage of the device and become apparent only after electrons have been injected to fill them. Similar traps have been found in MOS, MSOS, and SOS capacitors injected with more than 10^{15} electrons/cm².¹³ The cross-section of these traps is approximately 10^{-15} cm². The additional lower cross-section traps which are also evident will not be discussed here but are treated in an earlier publication dealing with MOS capacitors.¹³ Ning has also observed similar results in FET's metallized in an e-gun aluminum evaporator where x-rays presumably cause the same phenomena.¹⁴

The temperature dependence of the annealing of the positive and neutral traps is also illustrated in this figure. After the chip was given in an initial 400 C anneal and measured, the temperature was raised 50 °C and another sample on the same chip was measured. This sequence continued until the wafer was annealed for 30 minutes at each of the temperatures shown on the figure. As evident from this figure, anneals at 550 C or over are required to

remove both the positive and neutral traps from the oxide once they are introduced. This work is consistent with earlier work on MOS capacitors¹³ and FET's.¹⁴ However, the densities of positive and neutral electron traps found in the FET's are 2 to 3 times larger than those found in capacitors. The additional processing steps to which FET's are subjected appear to increase the sensitivity of the oxide to these defects.

A summary of the densities of the positive and neutral electron traps observed in devices which were irradiated and then annealed for 30 minutes at 400 C in forming gas is given in Table I. The first column describes the gate structure during the anneal, the second gives the density of positive charge observed from flat-band voltage or trapping measurements, and the third the density of traps filled by electrons after a total electronic charge of 10^{16} e/cm² has been passed through the oxide. As evident from this table, the positive charge is more thoroughly removed from the MOS and MSOS structures. The neutral trap density appears to be the same for all the structures. Because the trap density is 2 to 3 times larger in the FET's than that observed in the capacitors, the values in Table I are quoted as lower limits for the neutral trap density and the positive trap density for the SOS structure. The upper limit quoted for the positive charge in the MOS and MSOS structure is from the maximum shift observed in a large number of measurements on these devices. It should also be noted that the neutral centers have a field dependent cross-section¹⁴ and that a number of other centers with lower cross-sections have also been observed.¹³

So far the properties of positive and neutral electron traps have been discussed principally through the effective trap density inferred from flat-band or the threshold voltage shifts. Both quantities are due to the influence of the trapped charged distribution on the silicon surface potential and are proportional to the total number of traps and the centroid of the distribution. They can however be separately determined by use of the photo I-V technique.¹⁵ The reader is referenced to reference 15 for an extended discussion of the principles of the measurement. In the experiments described the damage was introduced into the oxide with penetrating 25KV

electrons. These electrons interact weakly with the oxide and deposit energy uniformly in the bulk. The data presented in Fig. 4 shows the photo-emission characteristics from both interfaces on an capacitor before and after the residual neutral electron traps have been filled with electrons. In Fig. 4a the injecting interface is the silicon/SiO₂ while the gate is biased positively; in 4b it is the Al/SiO₂ interface while the gate is biased negatively. The capacitor was irradiated to a total dosage of 1000 μ C-cm⁻², and annealed at 400 C to remove the positive charge. The photo-emission characteristics were measured, the capacitor was injected with electrons to fill the residual neutral traps, and the photo-emission characteristics were measured again. As described in reference 15, the presence of the distribution of trapped charge alters the electric field near both interfaces. This in turn alters the photo-emission characteristics in a predictable fashion. Because the charge distribution shifts both characteristics (in 4a and 4b) about equally along the voltage axis the its effect on both interfaces must be the same. The result implies a uniform distribution of charge with its centroid in the middle of the film and is consistent with the damage created by penetrating radiation. In contrast with this result previous work on the centroid of radiation-induced positive charge shows it to be at the interfaces.^{11,16}

It should be noted that the photo-emission characteristics on an unirradiated control sample were identical with that observed in the irradiated and annealed oxide when the neutral traps were empty. Furthermore the injection and photo I-V measurement sequence was actually repeated twice on this sample. The traps with cross-sections less than 10⁻¹⁶ cm² were filled first and their centroid determined, the avalanche current was raised and those with cross-sections less than 10⁻¹⁸ cm² were filled. The centroids in both cases were found in the middle of the oxide.

Summary and Conclusion

In conclusion, the effects of ionizing radiation on electron trapping in SiO_2 have been examined with a viewpoint appropriate for semi-conductor manufacturing. Earlier conclusions about the nature of the damage and its annealability have been shown incomplete. Studies of poly-silicon gate structures show the important but still unexplained role played by aluminum in annealing of positive charge. Neutral electron traps have also shown to be a previously neglected form of the damage in the oxide.

The physical properties of these traps, charge state, capture cross-section, trap density, centroid and annealing behavior are clearly different and indicate a different physical mechanism is responsible for the centers. The role of the radiation also appears to be different in these two cases. In the case of the positive trap, it provides carriers to fill hole traps which pre-exist in the oxide at a density determined by its processing history.¹⁷ The neutral electron traps really are associated with "damage" in the sense that they are defects introduced into the oxide by the radiation. These defects may have a structural rearrangement associated with them as well. Eernisse et al have reported that the density changes induced in SiO_2 are not removed with anneals at 400 C but require temperatures of 600 C for removal.¹⁸ These results are consistent with those observed here for removal of the neutral trapping sites in the oxide.

Only the physical properties of the radiation induced electron traps have been discussed so far. A few comments on the impact of these traps on devices is in order. Processes such as reactive ion etching, x-ray, or e-beam lithography are used in the fabrication of small dimension devices. The results presented here indicate that the rate at which the electrons are trapped in the oxides of these devices will be increased by 2 or more orders of magnitude by the ionizing radiation used to fabricate them. This increase in trapping rate is a complicated function of the total exposure given the device, the processing steps, the annealing history, and the fields across the oxide during operation.

The traps can be removed if anneals at 600 C can be tolerated. This is usually the case. However, once aluminum metallurgy is deposited on the source-drain contacts, anneals at temperatures over 400 C can cause the aluminum to penetrate into the junction, shorting out the junction to the substrate. Other metallurgical systems more compatible with anneals at temperatures above 400 C are required to remove the traps by thermal anneals. Presently such metallurgical systems are not in common use. Some residual trap density is then expected in irradiated oxides. The increased rates of trapping and device degradation can be compensated by decreasing the hot-electron emission rate by increasing the channel length or lowering the voltage from source to drain. Such design procedures can compensate for the increase in oxide trapping rate expected in devices exposed to ionizing radiation in the course of fabrication. However because the hot-electron emission rates are generally higher in small channel length devices, the increase in oxide trapping is expected to aggravate any existing instability.

Radiation hardness in SiO_2 is notoriously dependent on oxide quality and processing. It is expected that annealing phenomena will also exhibit similar dependencies. Because of the many design and processing parameters which may influence the trap generation and annealing, it is recommended that hardware of a particular design, manufactured by a specific process be tested to determine the overall effect.

Acknowledgements

The author thanks the Silicon Process Studies Group at IBM for sample preparation, The Electron Beam Applications Group for sample irradiations, and D.J. DiMaria for the data presented in Figure 4.

References

1. H.N. Yu, R.H. Dennard, T.H.P. Chang, C.M. Osburn, V. Dilonardo, and H.E. Luhn, J. Vac. Sci. Technol., 12, 1297 (1975).
2. E.H. Snow, A.S. Grove, and D.J. Fitzgerald, Proc. IEEE, 55, 1168 (1967).
3. T.H. Ning, C.M. Osburn, and H.N. Yu, J. of Electronic Materials, 6, 65 (1977).
4. For review, see: K.H. Zaininger and A.G. Holmes-Siedle, RCA Rev, 28, 208 (1967).
5. E.H. Nicollian, A. Goetzberger, and C.M. Berglund, Appl. Phys. Lett., 15, 174 (1969).
6. E.H. Nicollian, C.N. Berglund, P.F. Schmidt, and J.M. Andrews, J. Appl. Phys. 42, 5654 (1971).
7. T.H. Ning, Sol. State Electronics 21, 273 (1978).
8. T.E. Everhart and P.H. Hoff, J. Appl. Phys. 42, 5387 (1971).
9. P.A. Totta and R.J. Sopher, IBM J. Res. Dev. 18, 228 (1969).
10. K. Nakamura and M. Kamoshida, J. Appl. Phys. 48, 5349 (1977).
11. J.M. Aitken, D.J. DiMaria and D.R. Young, IEEE Trans. Nucl. Sci., NS-23, 1526 (1976).
12. T.H. Ning, J. Appl. Phys. 47, 3203 (1976).
13. J.M. Aitken, D.R. Young, and K. Pan, J. Appl. Phys. 49, 3386 (1978).
14. T.H. Ning, J. Appl. Phys. 49, 4077 (1978).
15. D.J. DiMaria, Z.A. Weinberg, J.M. Aitken, and D.R. Young, J. of Electronic Materials 6, 207 (1977).
16. D.J. DiMaria, Z.A. Weinberg, and J.M. Aitken, J. Appl. Phys., 48, 898 (1977).
17. J. M. Aitken and D. R. Young, IEEE Trans. Nucl. Sci., NS-24, 2128 (1977).
18. E.P. Ernisse and C.B. Norris, J. Appl. Phys. 45, 5196 (1974).

Figure Captions

- Fig. 1 Removal of radiation induced positive charge from capacitor structures with the indicated contact metallurgies in place over the gate during the anneal. The total effective density of positive charge remaining after an anneal step at 400 C in forming gas is plotted against the anneal time. The oxides were 350 Å thick.
- Fig. 2 Capture of injected electrons by unannealed positive charge in the oxides of poly-silicon gate capacitors. The two uppermost curves were from capacitors exposed to an electron beam and then annealed as indicated. The bottom curve is from an unirradiated control on the same wafer. The flat-band voltage shift (left-hand axis) or effective trap density (right-hand axis) is plotted against the number of electrons injected per unit area into the oxides of the capacitors.
- Fig. 3 Capture of injected electrons by unannealed positive and neutral electron traps introduced into the oxide of poly-silicon gate FET's by electron-beam radiation. After fabrication the FET's were exposed to ionizing radiation and then annealed at various temperatures as described in the text; an unirradiated control sample from the same lot is included for comparison. The change in threshold voltage caused by the capture of injected electrons by the defects in the oxide is plotted against the number of electrons injected per unit area. The gate oxide was 350 Å thick.
- Fig. 4 The internal photo-emission characteristics of an irradiated aluminum gate capacitor, from which the positive charge has been completely removed by thermal anneal, are shown before and after the neutral electron traps have been populated with injected electrons. Fig. 4a shows the photo-emission characteristic from the silicon electrode (positive gate bias) and Fig. 4b shows the characteristic from the aluminum electrode (negative gate bias).

TABLE I

DENSITY OF RESIDUAL ELECTRON TRAPS
AFTER E-BEAM EXPOSURE^a AND ANNEAL^b

GATE STRUCTURE	POSITIVE (cm ⁻²)	NEUTRAL ^c (cm ⁻²)
MOS	<1 × 10 ¹⁰	<1 × 10 ¹¹
MSOS	<1 × 10 ¹⁰	>1 × 10 ¹¹
SOS	>5 × 10 ¹⁰	>1 × 10 ¹¹

a) 100 μ coul cm² at 25 KV

b) 400 C, 30 min forming gas

c) 10¹⁶ e/cm² injected into gate

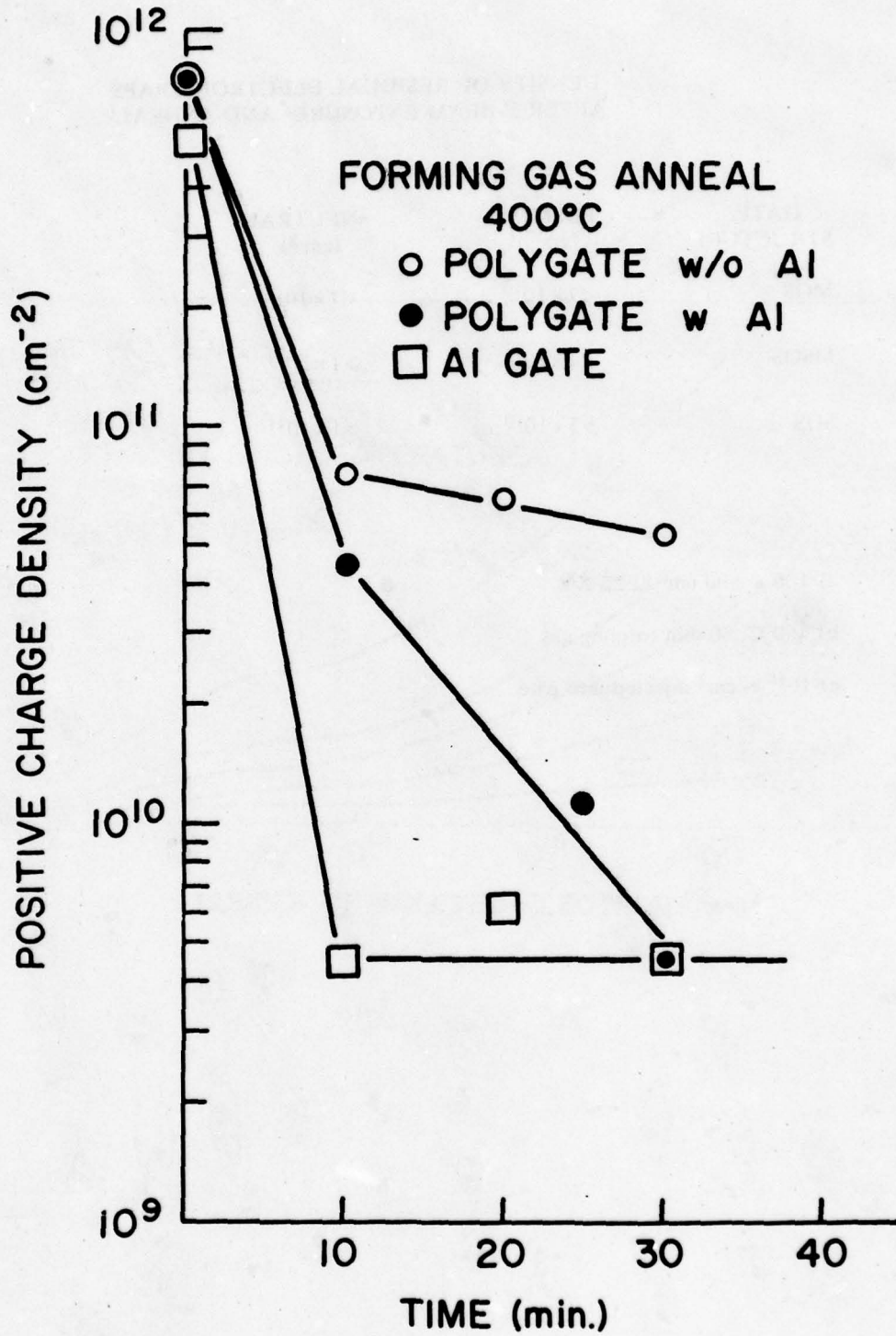


FIGURE 1

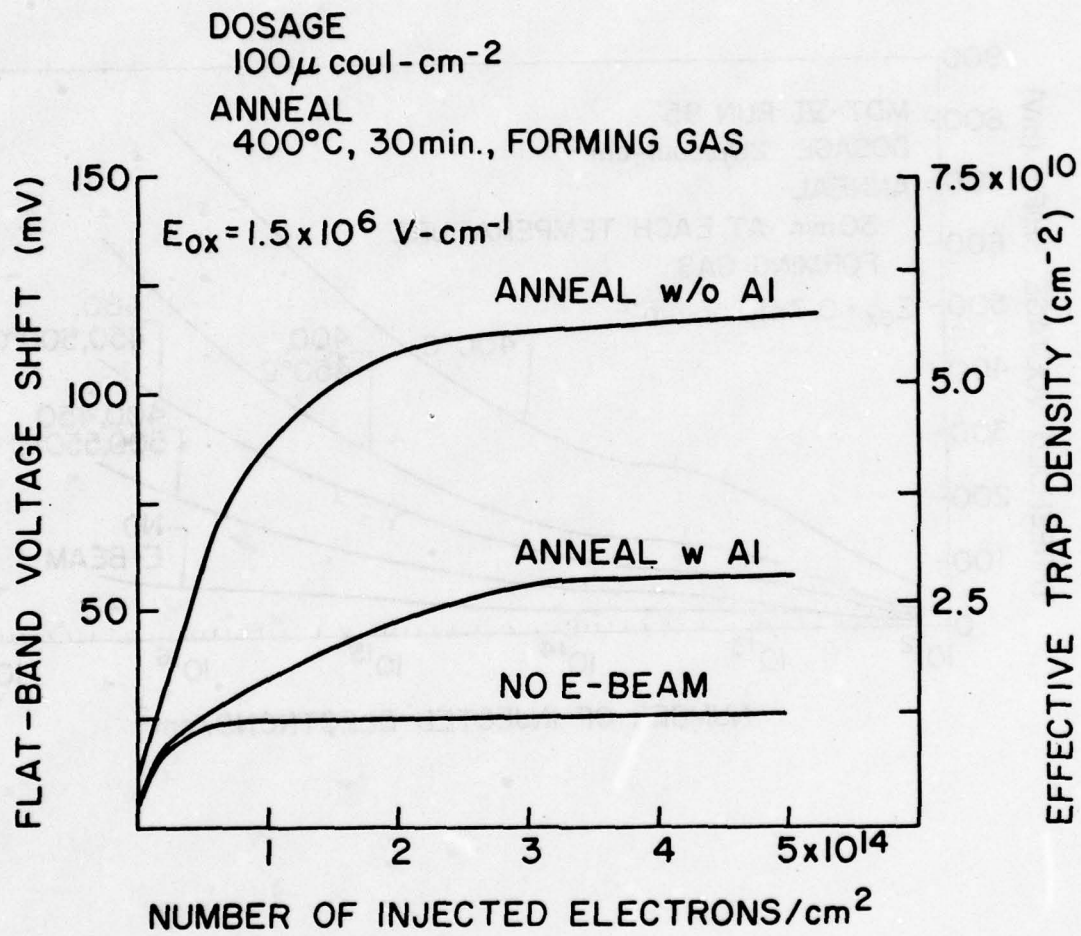


FIGURE 2

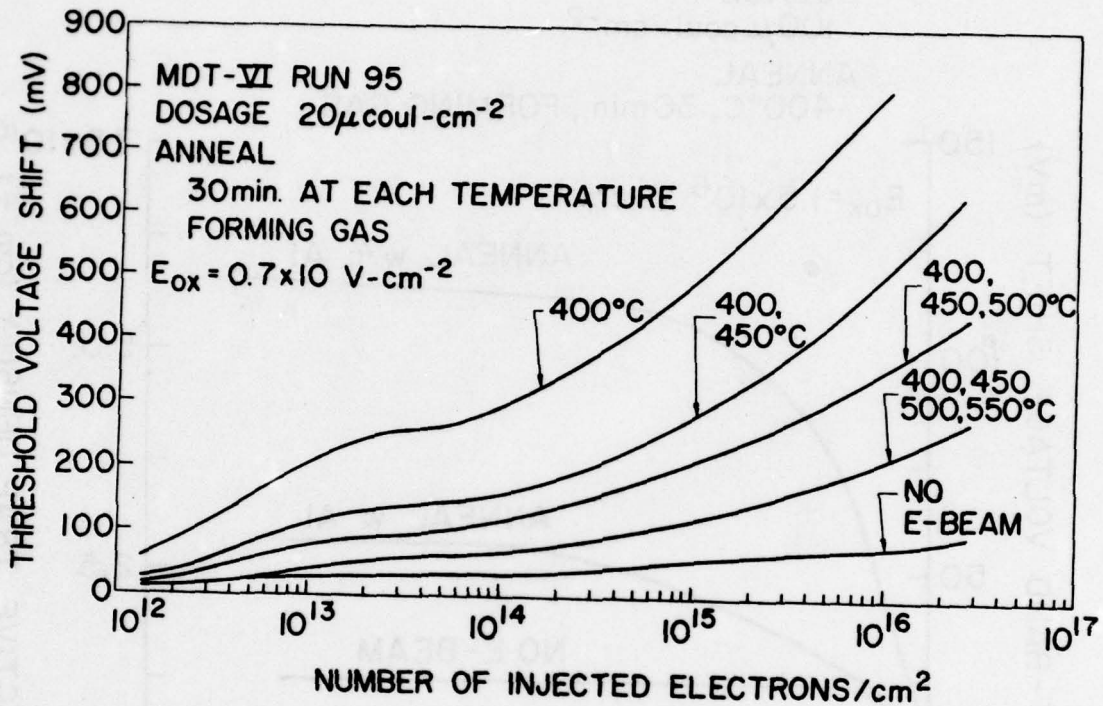


FIGURE 3

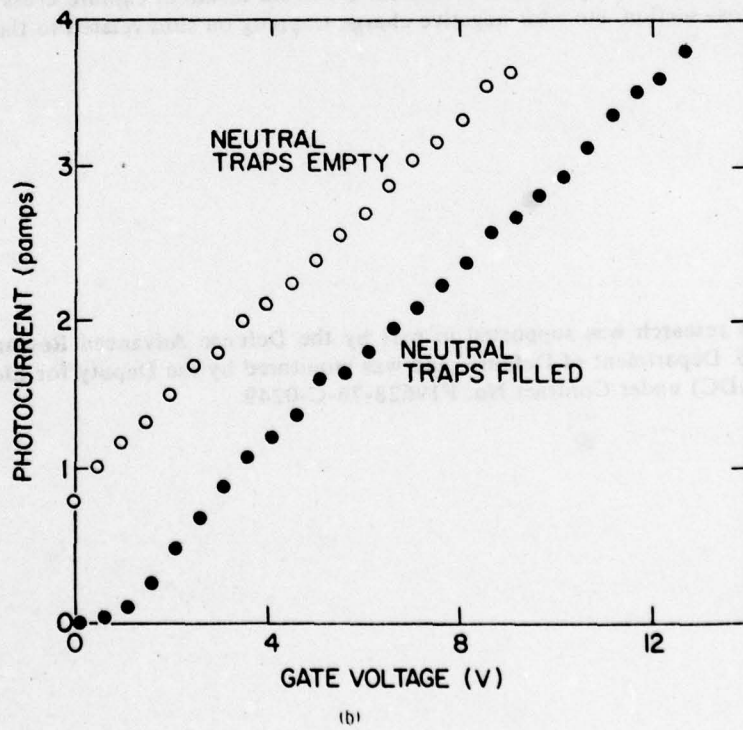
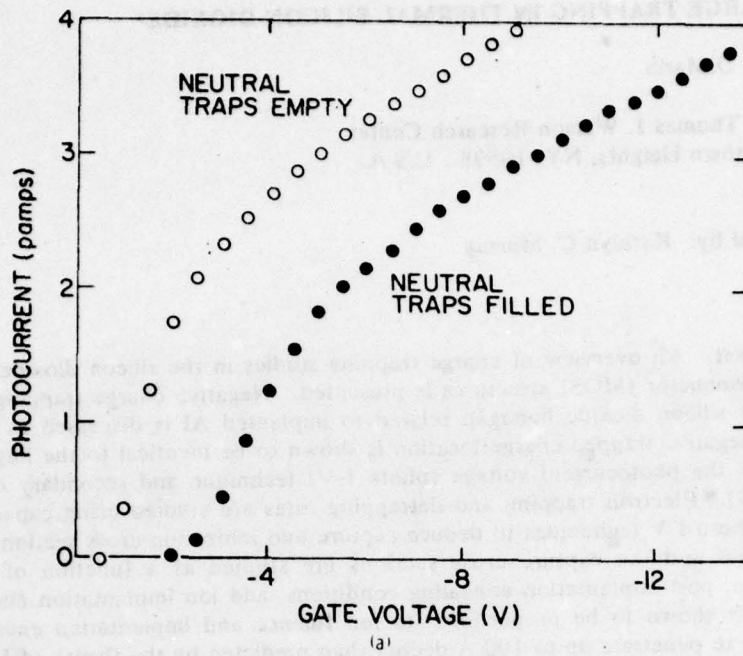


FIGURE 4

CHARGE TRAPPING IN THERMAL SILICON DIOXIDE*

D. J. DiMaria

IBM Thomas J. Watson Research Center
Yorktown Heights, NY 10598 U.S.A.

Typed by: Kathlyn C. Murray

Abstract: An overview of charge trapping studies in the silicon dioxide layer of metal-oxide-semiconductor (MOS) structures is presented. Negative charge trapping associated with sites in the silicon dioxide bandgap related to implanted Al is discussed in detail as an example. The negative trapped charge location is shown to be identical to the implanted Al location by use of the photocurrent-voltage (photo I-V) technique and secondary ion mass spectroscopy (SIMS). Electron trapping and detrapping rates are studied using capacitance voltage (C-V) and photo I-V techniques to deduce capture and ionization cross sections for these sites. The centroid and the capture cross sections are studied as a function of oxide thickness, ion fluence, post-implantation annealing conditions, and ion implantation energy. The number of traps is shown to be proportional to ion fluence and implantation energy. Implanted Al is shown to penetrate up to 100 Å deeper than predicted by the theory of Lindhard, Scharff, and Schiott (LSS). Comparisons between several implanted ions (Al, As, P, B) in SiO₂ are made with respect to the quantities of interest (centroid location, capture cross section, photoionization cross section, etc.) for negative charge trapping on sites related to the implanted ions.

- * This research was supported in part by the Defense Advanced Research Projects Agency, U. S. Department of Defense, and was monitored by the Deputy for Electronics Technology (RADC) under Contract No. F19628-76-C-0249.

§1. INTRODUCTION

Charge trapping in the silicon dioxide layer of metal-oxide-semiconductor (MOS) structures is of great importance in the electronics industry for two reasons:

(1) Build-up of trapped charge in the SiO_2 layer changes operating characteristics of devices like insulated gate field effect transistors (IGFET) [1]. An important example of this recently pointed out by Aitken et al. is the neutral centers created in the SiO_2 layer by x-ray or electron beam irradiation which only anneal out at high temperatures [2-4]. Electron beam lithography has been used to shrink the dimensions of IGFET transistors to increase performance, but unless the SiO_2 layer is properly annealed those structures will degrade more rapidly [3,4].

(2) Charge trapping or storage layers purposely incorporated into the insulating layers are currently used for non-volatile memory where information is stored as trapped charge for long periods of time. Examples of this are the dual-dielectric charge storage (DDC) cells which use less than a monolayer of W or WO_3 as a trapping layer interposed between thermal SiO_2 and CVD Al_2O_3 [5,6], and the floating gate avalanche injection MOS (FAMOS) structures which have a continuous polycrystalline Si layer for carrier storage interposed between SiO_2 layers [7].

In order to study charge trapping in SiO_2 , traps must be characterized by their spatial distribution, energy location in the ≈ 9 eV bandgap, relationship to impurities or defects, and trapping-detrapping characteristics which are most conveniently related to capture, thermal, and photoionization cross sections. In this review, trapping sites related to ion implanted Al will be discussed in detail as an example and compared to sites related to ion implanted As and P.

Ion implantation is a convenient way to add impurities to solids such as SiO_2 and Si, and it is extensively used in modern day processing. As will be discussed here, we have overcome

previous limitations of implanting ions into SiO_2 by using high temperature annealing after which carriers are trapped on sites related to the implanted ions and not on sites related to damage created as the energetic ions move through the film [8]. The overall program for studying charge trapping can be divided into the sample fabrication, charging the SiO_2 layer, sensing the trapped charge, and characterizing the traps by the quantities that can be measured.

§2. SAMPLE FABRICATION

After growth of a dry thermal SiO_2 film on Si at a temperature of usually 1000°C , ions are implanted into the SiO_2 film. If the traps created by the implantation are to be charged by avalanche injected electrons from the Si substrate which will be discussed in later sections, a p-type Si substrate is used with a resistivity of .1 to .2 Ωcm so that a uniform injection is achieved [9]. The outer surface of the SiO_2 is cleaned of any hydrocarbons or metals that could have been deposited during the implantation step using a procedure similar to that described by Irene [10] only with no HF. Then the samples are annealed in N_2 for 30 minutes at 1000°C to remove radiation damage except for cases where annealing conditions are studied. Finally, a capacitor structure is formed by depositing a thin, semitransparent (100-160 \AA) Al gate electrode on the top surface of the SiO_2 followed by a 400°C forming gas anneal for 20 minutes to reduce Si- SiO_2 interface states. After fabrication, the SiO_2 layer of the MOS structure is essentially in an uncharged state.

§3. TRAP CHARGING

For most experiments, traps in the SiO_2 layer are charged by avalanche injection [9,11] or by internal photoemission [12]. However, hot carriers from the Si can be injected by other methods which require more complicated transistor structures [13,14], or carriers can be generated across the ≈ 9 eV bandgap of the SiO_2 with vacuum ultraviolet (VUV) light which

requires a vacuum system [15]. High fields can also be used to inject carriers by Fowler-Nordheim tunneling [16], but this enhances the probability of oxide breakdown and electric field ionization of trapped carriers.

Internal photoemission uses light of energies between 2-5 eV to excite electrons from the contact at a negative voltage over the interfacial energy barrier into the oxide conduction band. The relevant energy barriers are shown in Fig. 1 for the condition of no voltage drop across a charge free oxide layer. With a voltage applied, the electrons then move towards and are collected by the contact that is at a positive voltage except for those electrons which may be trapped. Internal photoemission requires semitransparent metal electrodes to allow light penetration and can be used to inject carriers from either interface. Internal photoemission of holes without simultaneous injection of electrons (as can be seen in Fig. 1) is improbable for any metal gate contact because of the larger energy barriers for holes as compared to electrons. However, Goodman claims to have injected holes from the Si substrate by using a water electrode in place of the usual metal gate electrode [17].

Avalanche injection can also be used to inject carriers over the Si-SiO₂ interface energy barrier. By driving the Si into deep depletion by means of voltage pulses, a large electric field from ionized donors or acceptors is developed between the bulk of the Si and the Si-SiO₂ interface by depleting this region of mobile charge carriers (electrons or holes). For electron injection, thermal electrons in bulk p-type Si drift or diffuse into the high field region where they can gain energy from the field until they impact ionize and lose energy by creating another electron and a hole across the Si bandgap of 1.1 eV. This impact ionization process is multiplicative and gives a hot electron distribution in the Si at the Si-SiO₂ interface. Some of the electrons can surmount the interface energy barrier and move into the SiO₂ conduction band. A similar injection of holes can be accomplished with n-type Si [18-21].

§4. CHARGE SENSING

The build-up or decrease of trapped charge in the SiO₂ layer can be sensed by the electric field it creates. The two most widely used measurements which sense the electric fields near the contacts are the capacitance-voltage (C-V) [21] and photocurrent-voltage (photo I-V) [22,23] techniques. The C-V technique senses electric fields in the Si layer near the Si-SiO₂ interface due to the voltage dependent capacitance of this layer. The photo I-V technique senses electric fields in the oxide layer near either the Si-SiO₂ interface or the metal-SiO₂ interface, depending on voltage polarity, because of the contact limited nature of the internal photoemission currents. Typical C-V and photo I-V data for an SiO₂ layer implanted with 30 keV Al are shown in Figs. 2-4. As can be seen from these figures, the curves are shifted in a parallel fashion along the gate voltage axis after electronic charging of the bulk SiO₂ traps related to the implanted Al. These voltage shifts are the flat-band voltage shift ΔV_{FB} for the C-V curves and the photo I-V voltage shifts ΔV_g^+ (positive gate polarity-Si injecting) and ΔV_g^- (negative gate polarity-metal injecting). These shifts for bulk SiO₂ charge trapping are related to the charge centroid \bar{x} measured from the metal-SiO₂ interface and the total charge per unit area Q by the following relations obtained by integrating Poisson's equation [21-23]:

$$\Delta V_{FB} = - \frac{\bar{x}}{\epsilon} Q \quad (1)$$

$$\Delta V_g^+ = - \frac{\bar{x}}{\epsilon} Q \quad (2)$$

$$\Delta V_g^- = \frac{(L-\bar{x})}{\epsilon} Q \quad (3)$$

where L is the thickness of the SiO₂ layer and ϵ is the low frequency permittivity of SiO₂.

Obviously, Eq. 2 (or 1) and Eq. 3 can be solved for \bar{x} or Q to get the photo I-V relations

$$\bar{x} = L \left(1 - \frac{\Delta V_g^-}{\Delta V_g^+} \right)^{-1} \quad (4)$$

$$Q = \frac{\epsilon}{L} (\Delta V_g^- - \Delta V_g^+) \quad (5)$$

When the trapped charge is very near an interface (closer than 20 \AA), the photo I-V technique is not very sensitive to it and either Eqs. 2 or 3 is no longer valid for the entire range of gate voltages depending on which interface the charge is near [22-24]. However, the C-V technique would be most sensitive to a charge layer at the Si-SiO₂ (see Eq. 1). Therefore, the combination of C-V and photo I-V techniques can also be used to locate charges very near an interface (at least for the Si-SiO₂ interface).

§5. TRAP CHARACTERIZATION

In the previous section, two measurable quantities \bar{x} and Q to characterize traps were discussed. By monitoring the change in time of Q and \bar{x} as trapping or detrapping proceeds, other quantities to characterize trapping sites such as the capture cross section σ_c , total number of traps per unit area N_t , photoionization cross section σ_p , and the trap energy level E_t can be determined. The quantities usually are obtained from data fits to first order kinetic relationships like

$$Q(t) = qN_t (1 - \exp(-t/\tau_c)) \quad (6)$$

for trapping [25] where $\tau_c = q/J\sigma_c$, J is the constant current density, and q is the electronic charge; or data fits to

$$Q(t) = Q(0) \exp(-t/\tau_p) \quad (7)$$

for photodetrapping [25] where $\tau_p = (\sigma_p F_p)^{-1}$ and F_p is the photon flux. When more than one type of trapping center is present, traps can be separated by the magnitude of the cross-section by varying injected current densities for trapping and light energy for detrapping [25].

§6. Al IMPLANTATION

Charge trapping of electrons on sites related to ion implanted Al was studied as a function of post-implant annealing conditions, ion fluence, ion energy, and oxide thickness [26-28].

Figs. 5-8 show plots of ΔV_{FB} as a function of time under a constant avalanche injection electron current I depicting the dependence on these variables. Fig. 9 shows the dependence of the trapped negative charge centroid as determined with the photo I-V technique on the ion energy and oxide thickness. No noticeable charging was observed under similar conditions on unimplanted oxides. Several interesting conclusions are obtained from these data:

(1) Post-implantation annealing at 900°C or above tends to remove most (if not all) of the electron trapping due to radiation damage (see Fig. 5). All subsequent discussions will be limited to samples which were annealed at 1000°C in N_2 after implantation.

(2) The charge trapping is directly proportional to the ion fluence (see Fig. 6). Also it was observed that the centroid was independent of ion fluence as expected.

(3) The charge trapping is strongly dependent on the ion energy (see Fig. 7). If the average flat-band shifts from Fig. 7 are plotted as a function of energy as in Fig. 10, it is found that $(\Delta V_{FB})_{AVG} \propto V_1^2$ where V_1 is the implantation energy. Since $\bar{x} \approx V_1$ from the centroid data of Fig. 9, it is concluded that trapped charge and, therefore, the trap density is proportional to V_1 . The capture cross sections deduced from fitting the data of Fig. 7 to Eq. 6 were approximately independently of ion implantation energy. Young et al. have suggested that this dependence of the number of traps on implantation energy may be due to the role of vacancies created during the implantation into which Al atoms can move substitutionally and act as trapping centers [27]. Increasing the implantation energy would increase the number of vacancies and, therefore, the number of traps.

(4) For thin oxides, significant penetration of the Al into the Si substrate occurs which decreases the trap density and causes the centroid to become somewhat independent of implantation energy (see Figs. 8 and 9). Clearly from these figures Al is lost to the Si for all energies on the 490 \AA thick SiO_2 structures and for energies greater than 30 keV on the 730 \AA thick SiO_2 structures.

The curves in Fig. 9 are deduced from theoretical calculations for the ion distribution based on the work of Lindhard, Scharff, and Schiott (LSS) using the tables of Gibbons, Johnson, and Mylroie [29]. Corrections were made for the density of thermal amorphous SiO₂ as compared to the density of single crystal SiO₂ (density ratio .84) used in these tables. As can be seen in Fig. 9, the negative trapped charge centroid is fairly close to the predicted value of the ion centroid, but it seems to be in deeper (by 100 Å at most) from the Al-SiO₂ interface than the predicted value for the cases where the Al does not penetrate into the Si.

As an independent check to see if the negative trapped charge distribution is the same as the Al ion distribution, secondary ion mass spectroscopy (SIMS) was performed on a 20 keV Al implanted sample without the Al gate electrode. The SIMS profile for this sample and the corresponding LSS calculation are shown in Fig. 11 with the values of \bar{x} calculated from this data listed in Table I. The SIMS data were not very sensitive to post-implantation annealing conditions; therefore, this cannot explain the differences between experiment and theory in Fig. 11. Clearly the actual ion distribution is broader and in deeper than predicted by LSS theory and is essentially identical to the negative charge distribution. This is also seen in Fig. 9 for the 10-20 keV points where experimentally Al is lost to the Si where theoretically it should not be.

Capture cross sections were deduced from fitting data like that in Figs. 5-8 to Eq. 6. Values for the electron capture cross sections of the various traps associated with implanted Al are given in Table II. Also listed in this table are the number of traps per unit area associated with the 30 keV implant at a fluence of 1×10^{13} Al/cm². The capture cross sections are in the range from 10^{-15} to 10^{-18} cm² while the total trap density varies between 10^{12} to 10^{13} cm⁻² depending on ion energy for a fluence of 10^{13} Al ions/cm². As mentioned previously, total trap densities can be reduced if significant amounts of Al are lost to the Si substrate on thin oxide samples.

Once captured on an Al related site, electrons could not be photodetrapped with light energies up to 6 eV. In the next section where the characteristics of MOS structures with oxide layers ion implanted with As and P are discussed, it will be shown that electrons can be photodetrapped from sites related to these ions and photoionization cross sections and energy levels can be determined from data fits to Eq. 7.

§7. As and P IMPLANTATION

Ion implanted As or P related trapping centers will be discussed together because they are very similar except for their capture cross sections and sensitivity to annealing conditions. P related traps are more sensitive to annealing because with their smaller capture cross sections it is necessary to reduce background trapping in the SiO₂ layer more. The electron capture cross sections of the dominant trap (site which has the highest trapping probability) for As and P related sites are approximately $1 \times 10^{-15} \text{ cm}^2$ and $3 \times 10^{-17} \text{ cm}^2$, respectively [25]. The areal trap densities for these traps are not a function of the implantation energy in contrast to Al, are proportional to the ion fluence, and have a value of approximately half the value of the fluence [25]. The trapped electrons have the same centroid as the implanted ions [25], and the electrons can be detrapped with light [25]. The photoionization cross sections vary from 10^{-18} to 10^{-17} cm^2 with photon energy after threshold is reached which is approximately 4 eV [25,30] as is shown in Fig. 12. This threshold is consistent with theoretical predictions for substitutional P or As in an O site [30]. No pronounced temperature dependence of σ_p between 77°K and 300°K was seen [25]. For the As or P related sites, electrons could be thermally detrapped at temperatures between 100-350°C in N₂ with activation energies between .15 and .25 eV [25]. No significant electron detrapping for either As or P related sites with applied electric fields up to at least 3 MV/cm was seen [25]. As with the ion implanted Al case, the exact nature of these traps as related to the implanted impurity atoms is not known. Holes can also be trapped on ion implanted As and P related sites [25].

Ion implanted B in SiO₂ was also studied, but no noticeable trapping above the normal background trapping of the oxide layer itself was seen. It will not be considered further.

The characteristics for carrier trapping and detrapping on sites related to ion implanted Al, P, and As show a dependence on the column of the periodic table in where they appear (As and P are in the fifth column, while Al is in the third column). Except for the magnitude of the capture cross section for P related traps being smaller than that for As related traps, there is no dependence of the characteristics on the atomic mass (Al and P have about the same mass, while As is about twice as heavy) which further supports arguments against trapping on sites created by radiation damage (atomic displacement, radiation induced neutral centers, or trapped hole sites [25]).

§8. CONCLUSIONS

The trapping and detrapping of charge carriers on sites related to ion implanted Al, P, As, and B in SiO₂ have been discussed. Sample preparation, charge injection techniques, charge sensing techniques, and the measurable quantities of interest have been briefly reviewed. Other charge trapping sites either purposely introduced or normally present in thermal SiO₂ films are discussed in a recent review paper by this author [25]. Some of the other known traps are related to H₂O, Na⁺, Si, or produced by ionizing radiation [25]. As Si technology is pushed to its limits, charge trapping in the SiO₂ layer of devices like IGFET transistors will continue to increase in importance.

The author would like to acknowledge the critical reading of this manuscript by D. R. Young, R. F. DeKeersmaecker, and M. I. Nathan. The author is also deeply indebted to D. R. Young and R. F. DeKeersmaecker for helpful discussions of some of their trapping results used in this review.

REFERENCES

1. T. H. Ning, C. M. Osburn, and H. N. Yu, *J. Electron. Mat.* 6, 65 (1977).
2. J. M. Aitken and D. R. Young, *J. Appl. Phys.* 47, 1196 (1976).
3. J. M. Aitken, D. R. Young, and K. Pan, *J. Appl. Phys.* 49, 3386 (1978).
4. T. H. Ning, *J. Appl. Phys.*, (1978).
5. D. Kahng, W. J. Sundburg, D. M. Boulin, and J. R. Ligenza, *Bell Syst. Techn. J.* 53, 1773 (1974).
6. K. K. Thornber and D. Kahng, *Appl. Phys. Lett.* 32, 131 (1978).
7. D. Frohman-Benchkowsky, *ISSCC Dig. of Tech. Papers* 15, 80 (1971).
8. N. M. Johnson, W. C. Johnson, and M. A. Lampert, *J. Appl. Phys.* 46, 1216 (1975).
9. A. Goetzberger and E. H. Nicollian, *J. Appl. Phys.* 38, 4582 (1967).
10. E. A. Irene, *J. Electrochem. Soc.* 121, 1613 (1974).
11. E. H. Nicollian and C. N. Berglund, *J. Appl. Phys.* 41, 3052 (1970).
12. R. Williams, *Phys. Rev.* 140, A569 (1965).
13. J. F. Verwey, *J. Appl. Phys.* 44, 2681 (1973).
14. T. H. Ning and H. N. Yu, *J. Appl. Phys.* 45, 5373 (1974).
15. R. J. Powell and G. F. Derbenwick, *IEEE Trans. Nucl. Sci.* NS-18, 99 (1971).
16. M. Lenzlinger and E. H. Snow, *J. Appl. Phys.* 40, 278 (1969).
17. A. M. Goodman, *Phys. Rev.* 152, 780 (1966).
18. E. H. Nicollian, A. Goetzberger, and C. N. Berglund, *Appl. Phys. Lett.* 15, 174 (1969).
19. K. Nagai, Y. Hayashi, and Y. Tarui, *Jap. J. Appl. Phys.* 14, 1539 (1975).
20. J. M. Aitken and D. R. Young, *IEEE Trans. Nucl. Sci.* NS-24, 2128 (1977).
21. A. S. Grove, Physics and Technology of Semiconductor Devices (Wiley, New York, 1967), Chap. 9.
22. D. J. DiMaria, *J. Appl. Phys.* 47, 4073 (1976).
23. D. J. DiMaria, Z. A. Weinberg, and J. M. Aitken, *J. Appl. Phys.* 48, 898 (1977).
24. R. J. Powell and C. N. Berglund, *J. Appl. Phys.* 42, 4390 (1971).

25. D. J. DiMaria, in Proceedings of the International Topical Conference on the Physics of SiO₂ and Its Interfaces ed. by S. T. Pantelides (Pergamon Press, New York, 1978), p. 160 and references contained therein.
26. D. R. Young, D. J. DiMaria, and W. R. Hunter, *J. Electron. Mat.* 6, 569 (1977).
27. D. R. Young, D. J. DiMaria, W. R. Hunter, and C. M. Serrano, *IBM J. Res. Develop.* 22, 285 (1978).
28. D. J. DiMaria, D. R. Young, W. R. Hunter, and C. M. Serrano, *IBM J. Res. Develop.* 22, 289 (1978).
29. J. F. Gibbons, W. S. Johnson, and S. W. Mylroie, in Projected Range Statistics, Semiconductors and Related Materials, 2nd ed. (Halstead Press, Wiley, Somerville, N.J., 1975). Due to mistakes in the signs of pertinent equations on page 23 of these tables, calculated values for the ion centroids and distributions in references 26-28 are in error. The correct values are shown in Fig. 9 and 11 and in Table 1. However, this mistake does not change any of the relevant conclusions in refs. 26-28.
30. R. F. DeKeersmaecker, D. J. DiMaria, S. T. Pantelides, in "The Physics of SiO₂ and Its Interfaces", ed. by S. T. Pantelides (Pergamon Press, New York, 1978), p. 189.

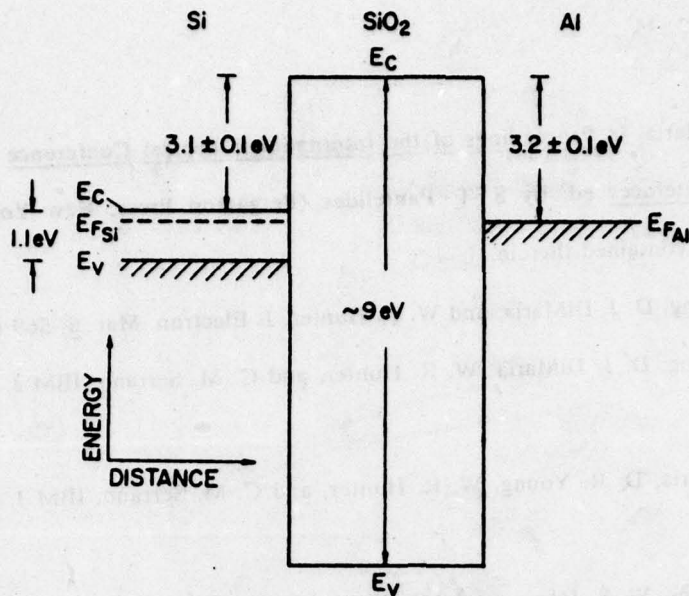


Fig. 1. Zero field energy band diagram of MOS structure taken from ref. 25.

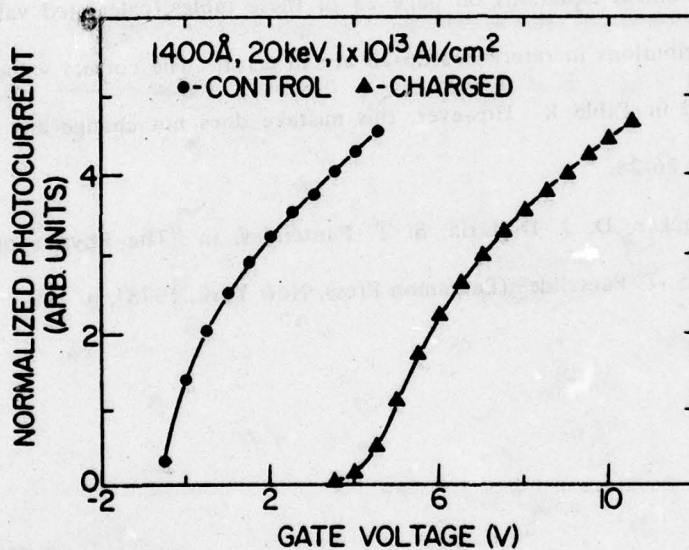


Fig. 2. Normalized photocurrent (photocurrent divided by area and light intensity) for 5 eV radiation as a function of positive gate voltage (Si-injecting): ●-uncharged control, ▲-charged by electron avalanche injection from the Si substrate. The MOS structure had a SiO₂ layer 1400 Å thick, 20-keV and 1×10^{13} Al/cm² implant, and was annealed at 1050°C for 30 min in N₂ after implantation prior to metallization. The average photo I-V voltage shift for positive gate polarity ΔV_g^+ is 5.34 ± 0.06 V. Taken from ref. 28.

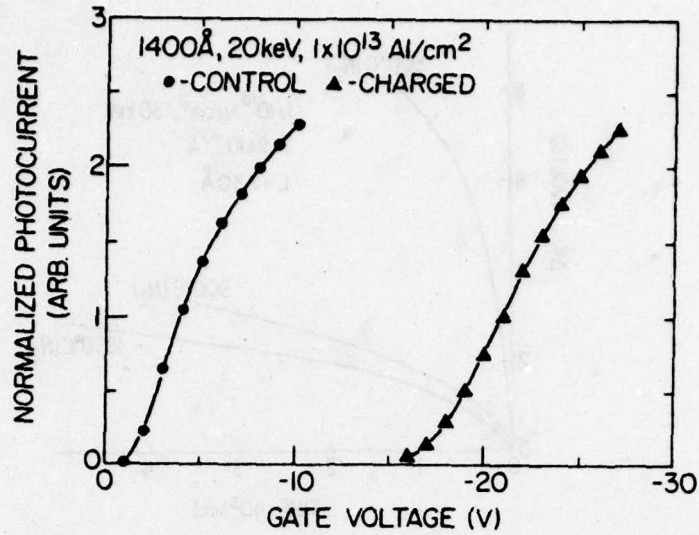


Fig. 3. Normalized photocurrent for 4.5 eV light as a function of negative gate voltage (Al injecting). Samples are the same as in Fig. 2. The average photo I-V voltage shift for negative gate polarity ΔV_g^- is -17.23 ± 0.11 V. Taken from ref. 28.

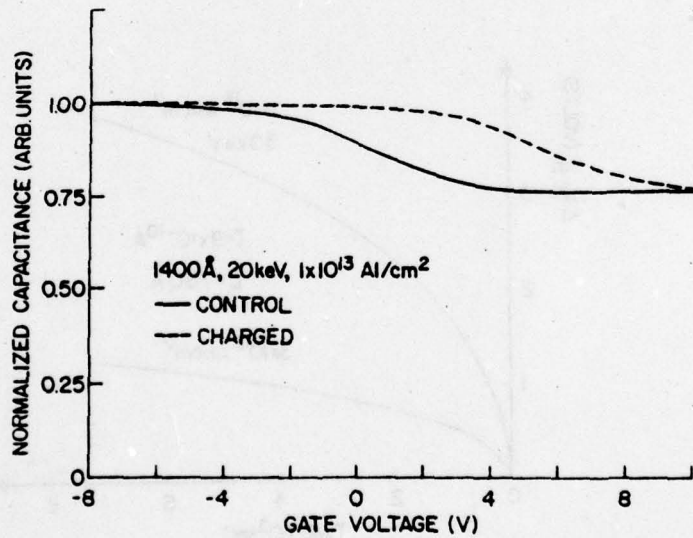


Fig. 4. Normalized capacitance (total capacitance divided by the oxide capacitance) as a function of gate voltage. Samples are the same as in Fig. 2, the solid and dashed lines representing the control and charged samples, respectively. The flat-band voltage shift ΔV_{FB} is 5.2 ± 0.1 V. Taken from ref. 28.

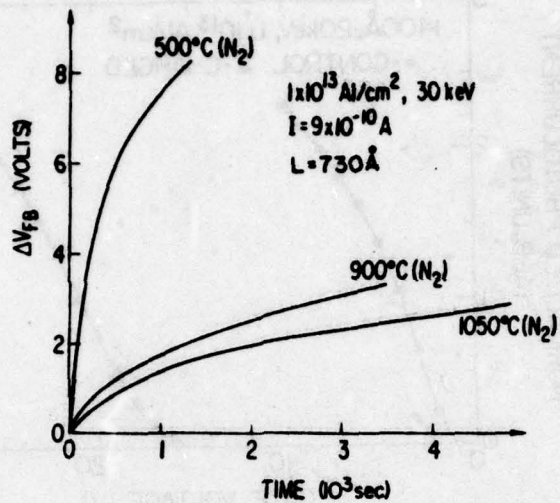


Fig. 5. Flat-band voltage shift as a function of time for various annealing temperatures. The annealing time is 30 min. Taken from refs. 26 and 27.

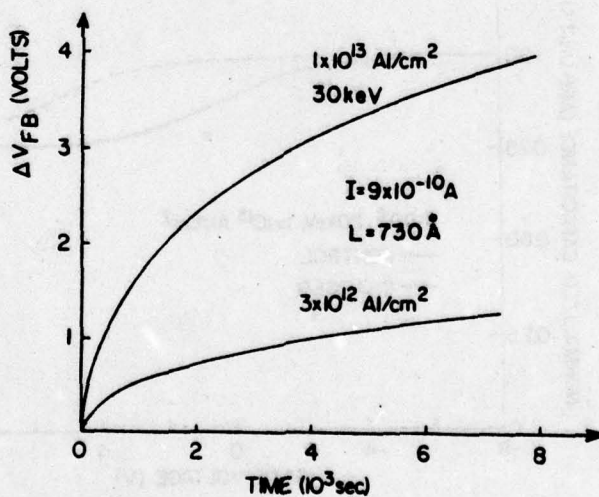


Fig. 6. Flat-band voltage shift as a function of time for various Al ion fluences. Taken from ref. 26.

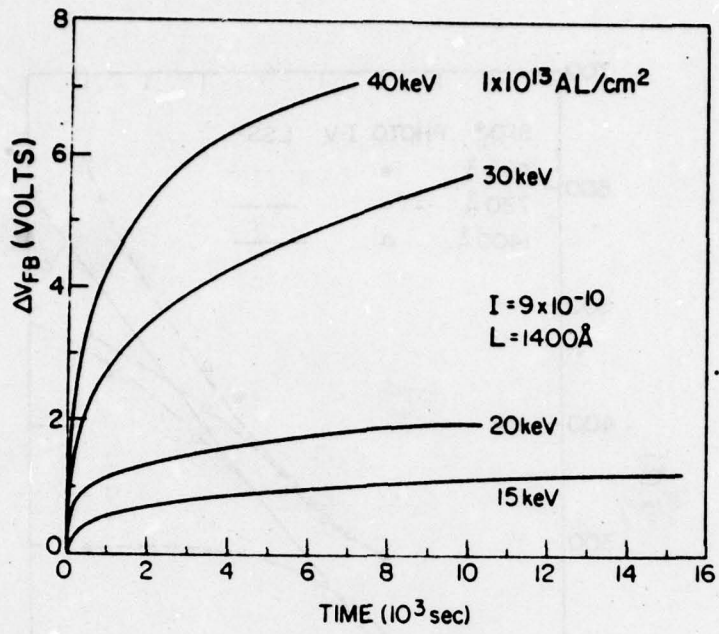


Fig. 7. Flat-band voltage shift as a function of time for various implantation energies. Taken from ref. 27.

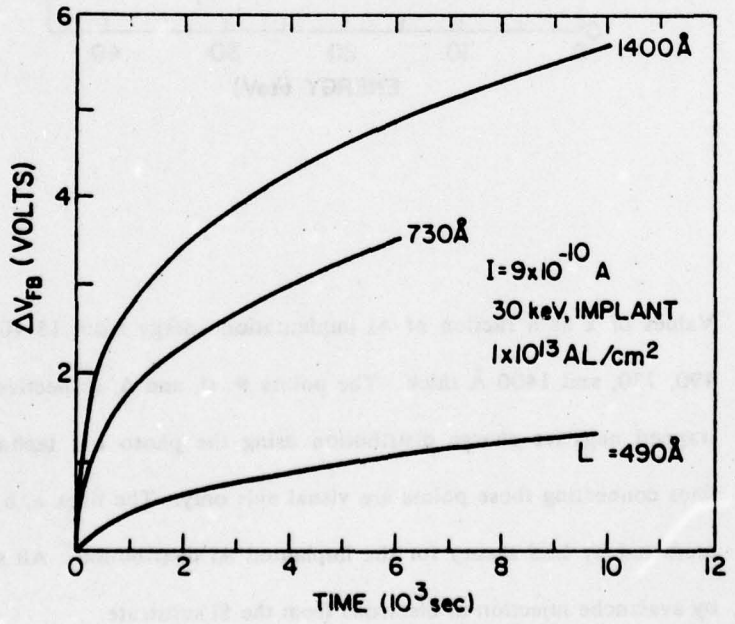


Fig. 8. Flat-band voltage shift as a function of time for various SiO_2 thicknesses. Taken from ref. 27.

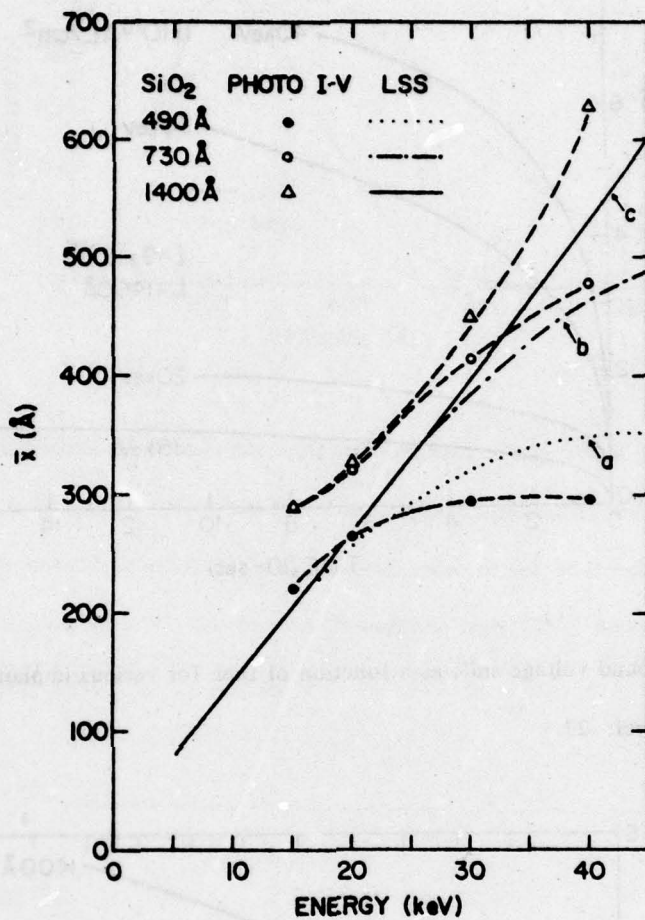


Fig. 9. Values of \bar{x} as a function of Al implantation energy from 15-40 keV for SiO₂ layers 490, 730, and 1400 Å thick. The points ●, ○, and Δ, respectively, are values for the trapped negative charge distribution using the photo I-V technique and the dashed lines connecting these points are visual aids only. The lines a, b, and c are the values predicted by LSS theory for the implanted Al distribution. All samples were charged by avalanche injection of electrons from the Si substrate.

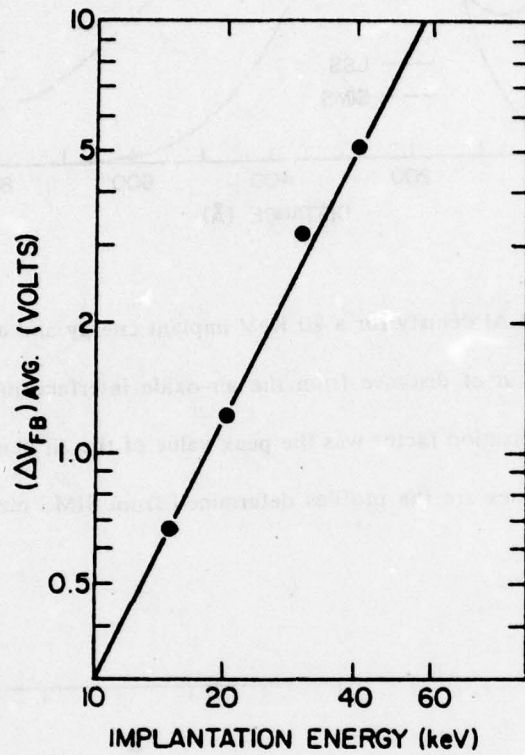


Fig. 10. Log-log plot of the average value of ΔV_{FB} for the data from Fig. 7 taken to 6500 sec. as a function of implantation energy. The average flat-band voltage shift $(\Delta V_{FB})_{avg}$ is the sum of the shifts for all the measurements divided by the number of measurements. Taken from ref. 27.

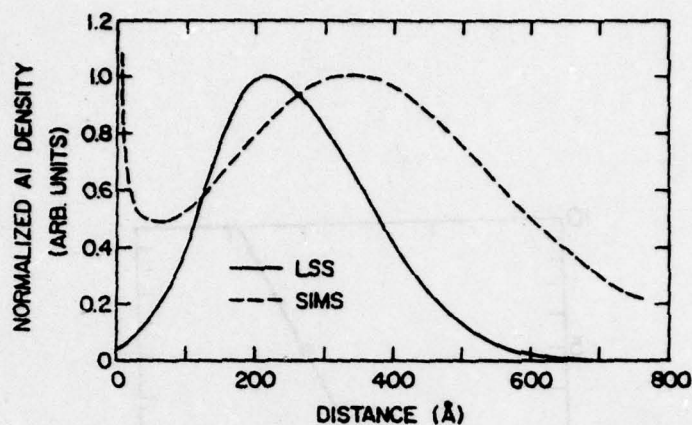


Fig. 11. Normalized Al density for a 20 KeV implant energy and a fluence of 1×10^{13} Al/cm² as a function of distance from the air-oxide interface into a SiO₂ film 770 Å thick. The normalization factor was the peak value of the Al density in the film. The dashed and solid lines are the profiles determined from SIMS measurements and LSS theory, respectively.

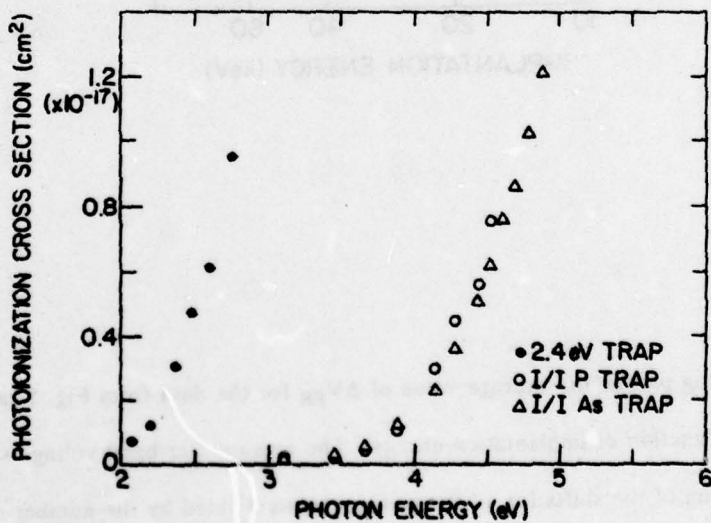


Fig. 12. Photoionization cross section as a function of energy for the 2.4 eV trap and for trapping sites related to ion implanted P and As taken from refs. 25 and 30.

TABLE I: Centroid comparison for 20 keV Al implant into SiO₂:

Oxide thickness (Å)	Centroid (Å)		
	Photo I-V	SIMS	LSS
490	265	274 ± 25	257
730	320	346 ± 25	268

TABLE II: Capture cross-sections σ_c and total number of traps per unit area N_t for the trapping sites resulting from a 30 keV Al implant with a fluence of 1×10^{13} Al/cm² and an oxide thickness of 730 Å.

σ_c (cm ²)	N_t (cm ⁻²)
1.60×10^{-15}	7.80×10^{11}
1.26×10^{-16}	1.93×10^{12}
1.40×10^{-17}	2.37×10^{12}
1.26×10^{-18}	8.47×10^{11}

Electron Trapping in SiO₂ at 295°K and 77°K

D.R. Young, E.A. Irene, D.J. Di Maria, and R.F. De Keersmaecker^a
I.B.M. T.J. Watson Research Center, Yorktown Heights, New York 10598

H.Z. Massoud^b
Applied Electronics Laboratories, Stanford University,
Stanford, California 94305

Abstract

The electron trapping behavior of SiO₂ has been measured as a function of thickness at 295°K and 77°K. The devices used were MOS devices with the SiO₂ grown thermally. The results indicate bulk traps are dominant at 295°K and traps associated with the Si-SiO₂ interface are dominant at 77°K. The effect of processing conditions was also studied and the optimum conditions are different for the two temperatures used for the measurements. These observations have been verified using a Photo I-V technique. The generation of donor states in the SiO₂ near the Si-SiO₂ interface was observed as a result of the electron current through the SiO₂.

a) Work supported in part by the Defense Advanced Research Projects Agency, the Department of Defense, monitored by the Deputy for Electronic Technology (RADC) under Contract No. F-19628-76-C-0249 Electronic Technology Laboratories.

b) Work done at IBM Research Laboratories

1. Introduction

Nicollian and Berglund¹ have published a paper describing the effect of water exposure on the electron trapping behavior of SiO₂. They reported a trap cross section of 1.5×10^{-17} cm² for water related trapping centers. Ushirokawa, Suzuki, and Warashina², have measured a cross section of 1.8 to 2.6×10^{-18} cm² for these centers. Ning and Yu³ have studied electron traps with a cross section of 3×10^{-13} cm² which they have shown to be related to the initial Si-SiO₂ interface charge. They have varied this charge by means of the annealing treatment used. Gdula³ has studied the effect of processing on the electron trapping behavior of SiO₂ over a wide range of processing conditions. His results have also shown an anomalous effect indicating that the net negative charge does not continue to increase monotonically but a maximum occurs, and then the net negative charge decreases. An enhanced electron trapping at 77°K in SiO₂ was shown in a paper by DiMaria, Aitken, and Young⁵. The recent work of Ning⁶ has shown that electrons trapped on these sites at 77°K can be detrapped at temperatures between 77°K and 295°K corresponding to energies 0.3 eV below the conduction band edge of SiO₂. An excellent review paper has recently been written by DiMaria⁷ describing the effect of "impurities" on the trapping behavior of SiO₂. In the present work, we concentrate on the trapping behavior without the intentional addition of impurities.

In this paper, we discuss the thickness dependence of the electron trapping behavior at 295°K and 77°K showing that the results are significantly

different for these temperatures. Our work further shows a difference in the effect of oxide processing conditions depending on the measurement temperature used. Photo I-V results are consistent with the results of the thickness dependence studies showing that the dominant traps at 295°K are distributed throughout the bulk of the SiO₂ while at 77°K the dominant traps are associated with the SiO₂ interface. In addition, the anomalous "turn around" effect reported by Gdula is shown to result from a positive compensating charge located at the Si-SiO₂ interface. This charge is due to the presence of states close to this interface that are generated by the injected current and can be charged and discharged at will.

II. Experimental Procedures

A. Sample Preparation

Chem-mechanically polished, <100> oriented, p-type silicon wafers (3.2 cm diameter and 0.025 cm thick) with a nominal resistivity of 0.2 ohm-cm were thoroughly cleaned by a previously described procedure⁸. The double walled fused silica tube, the three zone resistance furnace, temperature measurement, ellipsometry, and oxidation procedures were also previously described.⁸ Oxidation of silicon was carried out at 1000°C in oxygen which was supplied from a liquid source. Hydrocarbons were removed and the H₂O content of oxygen used for "dry" oxidations was <1 ppm as measured after the oxidation furnace. For "wet" oxidations, the purified oxygen was bubbled through deionized water prior to injection into the oxidation tube. The water

content of the oxygen was $\sim 10^4$ ppm for a 2 l/min oxygen flow with bubbler temperature of 22°C.

As measured by ellipsometry, the SiO₂ film thicknesses used for this study were 525 ± 20 Å and the average value for the film refractive indices were 1.465 ± 0.006 for 5461 Å light.

Initially, the samples were removed from the oxidation furnace right after the oxidation. Further work showed that the trapping rate was reduced if the samples were left in the furnace for a period of time (at least 20 minutes) with N₂ gas flowing after the O₂ was turned off. The effect of this treatment will be discussed.

Immediately after oxidation, .032" diameter, 5000 Å thick Al electrodes were electron beam evaporated onto the SiO₂-Si structure. Some samples were post metallized annealed at 450°C in a clean flowing nitrogen ambient for 20 min. The oxide on the backside of the silicon was etched off and a gallium-indium paste was used for backside electrical contact.

The overall cleanliness and the entire sample preparation process was assessed by performing capacitance - voltage (C-V) measurements on <100> 2 Ω cm p-type silicon devices processed along with the samples. The C-V measurements revealed a positive charge level of $< 5 \times 10^{10}$ charges/cm². Bias temperature stressing ($\pm 10^6$ V/cm, 200°C for 15 min. and cooling under bias) revealed a mobile positive charge level of 5×10^{10} charges/cm².

B. Measurement Procedure

The avalanche injection technique of Nicollian, Goetzberger, and Berglund⁹ was used to induce electron flow through the SiO₂. We have developed a circuit that automatically increases the applied voltage to maintain a constant average "DC" current throughout the run. A 500 kHz square wave voltage source is used instead of the sine waves used by Nicollian, Goetzberger, and Berglund. In addition, our apparatus automatically measures the flat band voltage by interrupting the avalanche process at pre-set periods that range from 15 to 100 sec. We believe this is a more reliable technique than tracking the avalanche voltage as a measure of the charge build up in the SiO₂. This data is stored in a computer. A schematic representation of our apparatus is shown in Fig. 1.

The analysis of the data is based on fitting exponentials to the results and our computer program will do this if we have up to two exponentials involved. We use the following relationships for a single trap

$$\Delta V_{FB} = \Delta V_t (1 - e^{-t/\tau}) \quad (1)$$

where ΔV_{FB} is the change from the initial value, ΔV_t is the flat band voltage change if all the traps are filled and τ is the time constant related to the trap cross section as follows:

$$\sigma = q/\tau J_G \quad (2)$$

The electronic charge is q , J_G is the average "DC" current density which was 5.78×10^{-5} amps/cm² for most of these experiments. In many cases we find it is necessary to use at least two different traps to explain the results. To fit these exponentials, we calculate dV_{FB}/dt from our data. A plot of

$$\text{Ln } (dV_{FB}/dt) \text{ vs } t \quad (5)$$

will result in a line if a single trap is involved. The slope is $-1/\tau$ and the initial value $\Delta V_t/\tau$. The slope is used (using a least squares fitting procedure) to determine τ . The intercept at $t=0$ can be used to calculate ΔV_t if τ is known. If two traps are involved a break in the curve is observed. In this case, the analysis is carried out for the later times (after the break) for the second trap.³ Correction is made for the filling of this trap that occurs up to the time of the break. The calculated exponential is subtracted from the original data and a similar analysis is carried out on this data which contains the flat band shifts due to the first trap. Finally the calculated results for the sum of the two exponentials are subtracted from the original data and the difference is plotted as a function of time. If significant structure exists in this plot, then we know that the results can not be fit by two exponentials and the results are not used. The relationship between the trap density per unit area (N) and ΔV_t is given by

$$N = \frac{\epsilon_{ox}}{qD_c} \Delta V_t \quad (6)$$

where ϵ_{ox} is the low frequency permittivity of SiO₂, q is the electronic charge and D_c is the distance to the charge centroid as measured from the metal

electrode. If D_c is not known then we refer to our effective trap density (N_{eff})

given by

$$N_{eff} = \frac{\epsilon_{ox} \Delta V_t}{q D_{ox}}$$

where D_{ox} is the oxide thickness.

III. Experimental Results

A. Effect of Processing

The change in flat band voltage (ΔV_{FB}) as a function of avalanche time is given in Fig. 2 for measurements at 295°K and 77°K. It is seen that the lowest trapping rate is observed for the dry sample with a post metallization annealing treatment. The effect of post metallization annealing is large for the dry samples but small for the wet samples. A large difference is also observed between measurements at 295°K and 77°K. These samples were removed from the oxidation tube immediately after the oxidation. Further work has shown that the trapping can be reduced if the samples remain in the oxidation tube at temperature, with the oxygen turned off, for a period of time. This will be discussed further in a subsequent section. Unless specified otherwise the samples for the measurements that follow are given a 30 min treatment in N_2 at the oxidation temperature after the oxidation is completed.

B. Dependence on SiO₂ thickness

A series of samples were made with the SiO₂ thickness varied from 235 Å to 940 Å. The results are shown in Fig. 3 for measurements at 295°K. It is seen that there is a strong dependence on oxide thickness. If the traps are located uniformly throughout the oxide and if the volume concentration is the same for all the samples then it would be expected that the flat-band voltage shifts would go as the square of the oxide thickness. If the traps are located in the vicinity of the Si-SiO₂ interface and if they have a constant areal density from sample to sample then the dependence on oxide thickness should go as the first power. The results of Fig. 3 are replotted in Fig. 4 where the flat band shifts divided by the oxide thickness are plotted as a function of time. This clearly shows that there is a stronger dependence than the first power. To investigate this further the average flat band voltage shifts (take to 3000 sec.) divided by the oxide thickness were calculated and plotted as a function of oxide thickness in Fig. 5. This curve is linear, clearly showing that the trapping rate varies as the square of the oxide thickness. Measurements were made using the Photo I-V technique^{10,11} which showed that the centroid of the trapped charge is approximately in the middle of the oxide confirming our conclusion that traps are distributed uniformly throughout the oxide. There was a slight tendency for the centroid to be slightly closer to the Al-SiO₂ interface than the Si-SiO₂ interface.

Measurements made at 77°K showed a different dependence. These results are shown in Fig. 6. In this case, the dependence on thickness was not as strong as for room temperature. In Fig. 6, the flat band voltage shift divided by the thickness is plotted as a function of time and it is seen that the results do not quite come together. However, if the square of the thickness is used (cf Fig. 8) then we obtain the reverse order indicating that this is not the correct dependence. The results can be brought together as shown in Fig. 9 if we assume the additional charge trapped at 77°K has a charge centroid $\sim 90 \text{ \AA}$ from the Si-SiO₂ interface. These results are confirmed by photo I-V measurements^{10,11} which yield a similar result.

The stronger thickness dependence for room temperature measurements as compared to 77°K results in a large difference in the electron trapping if samples with a thin (297 \AA) oxide are used as shown by Fig. 10.

C. Processing Dependence

The effect of processing conditions is also different for the two measuring temperatures. This is illustrated in Fig. 11 where it is seen that the room temperature trapping is reduced if the post oxidation annealing treatment is done at 1000°C whereas at 77°K the optimum temperature for this treatment is $\sim 800^\circ\text{C}$.

D. Anomalous Positive Charge Effect

If the avalanche currents are passed through the sample for longer times, it is observed that the flat band voltage shift does not continue to increase monotonically but that a maximum shift occurs followed by a decrease as shown by Fig. 12. This was also observed by Gdula⁴. The photo I-V technique has also been applied to this case with the results shown in Figs. 13, 14, and 15. The relatively large shifts observed by the photo I-V as compared to the C-V measurements indicate the presence of positive charge at the Si-SiO₂ interface. It is well known that the photo I-V results are not sensitive to the Si-SiO₂ interface charge whereas this charge does effect the C-V results. This work clearly shows that the "turn around effect" is due to a positive charge building up at the Si-SiO₂ interface which compensates the negative charge due to electrons trapped in the bulk of the SiO₂. It has also been observed that this effect is significantly reduced if the sample is given a prolonged post oxidation heat treatment (cf. Fig. 16). The build-up of positive charge depends on the total electronic charge flowing through the SiO₂ as shown in Fig. 17 where a comparison is made between two measurements made at 3×10^{-7} and 3×10^{-8} amps and it is seen that the results come together if the flat band voltage shifts are plotted as a function of the charge per unit are passed through the SiO₂ as shown by Fig. 17.

Further work has shown that this buildup in charge occurs even faster if the avalanche current is turned off. The change that occurs in this case depends on the charge that has flowed through the sample. The application of a

moderate field ($4-6 \times 10^6$ v/cm) can increase or decrease the positive charge as shown by Fig. 18 depending on the polarity used. The sign of this effect indicates that the charge causing these shifts comes from the Si and not from the Al or is not due to the transport of ionic species across the SiO_2 . The charging and discharging of these sites can be expedited by the use of an elevated temperature indicated by Fig. 19 and it appears that the positive charge can be eliminated under these conditions. This work indicates that donor states are generated in the vicinity of the Si-SiO₂ interface by the passage of current through the oxide and these states can be charged or discharged at will by the application of electric fields particularly at elevated temperatures. These states appear to be similar to those generated by VUV and negative gate bias reported by Weinberg and Rubloff¹². These states are not generated if the avalanche injection occurs at 77°K instead of 295°K.

E. Electron Trapping Characteristics

The effect of a positive gate bias at elevated temperature suggests the possibility of studying the electron trapping behavior without the complications of the compensating effect since a positive voltage is used for the avalanche injection process. This was done as shown by Fig. 20 and it is seen that the "turn around effect" disappears at elevated temperatures. The electron trapping characteristic for the higher temperature can be analyzed and two traps are observed with cross sections and effective densities listed below:

σ (cm ²)	N_{eff} (cm ⁻²)
3.18×10^{-19}	5.8×10^{11}
3.35×10^{-18}	8×10^{11}

F. Si Gate Process

It is interesting to note that samples made using a Si gate process instead of the Al gate do not show the turn around effect as seen by Fig. 21 and also have a smaller effective density of the second trap as shown below:

σ (cm ²)	N_{eff} (cm ⁻²)
2.40×10^{-19}	2.04×10^{11}
2.27×10^{-18}	2.76×10^{10}

The second trap is much smaller in the Si gate process. We believe this trap is due to H₂O in the SiO₂ and the lower concentration for the Si gate process is due to the high temperature used for this process (~ 900°C) which may reduce the H₂O concentration. The absence of the "turn around effect" for the Si gate also suggests that H₂O may be responsible for the "turn around effect".

IV. Conclusions

The electron trapping behavior of SiO_2 depends on the H_2O contents of the SiO_2 , the heat treatment following oxide growth, the past metallization treatment, the gate technology and on the temperature used for the measurement. When a temperature of 295°K is used for the measurement, the traps are uniformly distributed throughout the bulk of the SiO_2 . This observation is not consistent with the results of Ushirokawa, Suzuki and Warashima¹² who observed a thickness dependence of the trap concentration. The difference in the results may be due to the thinner oxides used in the present work (232 to 940 Å) as compared with their study (600 to 2000 Å) or may be done to the "wet oxides" used for most of their work. For measurements at 77°K the dominant traps are near the Si- SiO_2 interface. Donor states are created in the vicinity of the Si- SiO_2 interface by the passage of current through the SiO_2 .

V. Acknowledgments

The authors are indebted to C.M. Serrano and J.A. Calise for assistance in the measurements, to the Silicon Process Facility for making some of the samples, to A.B. Fowler and M.I. Nathan for interest and support of this work.

References

1. E. H. Nicollian and C. N. Berglund, *J. of App. Phys.* **42**, 5654 (1971).
2. A. Ushirokawa, E. Suzuki, and M. Warashima, *Jap. J. of App. Phys.* **12**, 398 (1973).
3. T. H. Ning, and H. N. Yu, *J. App. Phys.* **45**, 5373 (1974).
4. R. A. Gdula, *J. Electrochem. Soc.* **123** 42 (1976)
5. D. J. DiMaria, J. M. Aitken, and D. R. Young, *J. Appl. Phys.* **47**, 2740 (1976).
6. T. H. Ning, *J. App. Phys.* **49**, 5997 (1978).
7. D. J. DiMaria, in *Proceedings of the International Topical Conference of the Physics of SiO₂ and Its Interfaces*, edited by S. T. Pantelides (Pergamon Press, New York 1978) p. 160.
8. E. A. Irene, *J. Electrochem. Soc.* **121**, 1613 (1974).
9. E. H. Nicollian, A. Goetzberger, and C. N. Berglund, *App. Phys. Lett.* **15**, 174 (1969).
10. R. J. Powell, C. N. Berglund, *J. App. Phys.* **42**, 4390 (1971)
11. D. J. DiMaria, *J. App. Phys.* **47**, 4073 (1976).

12. Z. A. Weinberg, G. W. Rubloff, in **Proceedings of the International Topical Conference of the Physics of SiO₂ and Its Interfaces**, edited by S.T. Pantelides, (Pergamon Press, New York 1978) p. 24.

Figure Captions

- Fig. 1. Schematic Drawing of Apparatus Used for Avalanche Injection.
- Fig. 2. Flat Band Voltage Shift (ΔV_{FB}) as a function of time for a constant avalanche current. Sample removed immediately from oxidation chamber after oxidation. Measurement made at room temperature (295°K).
- Fig. 3. ΔV_{FB} as a function of time for various oxide thicknesses. The post oxidation treatment (POA) was at 1000°C for 1 hour and the post metallization treatment (PMA) was at 400°C for 20 minutes.
- Fig. 4. Results of Fig. 3 replotted with the ordinate $\Delta V_{FB}/D_{ox}$.
- Fig. 5. Average ΔV_{FB} (taken to 3000 sec.) taken from results of Fig. 3 as a function of D_{ox} .
- Fig. 6. ΔV_{FB} as a function of time for measurements made at 77°K.
- Fig. 7. $\Delta V_{FB}/D_{ox}$ as a function of time.
- Fig. 8. $\Delta V_{FB}/(D_{ox})^2$ as a function of time.
- Fig. 9. $\Delta V_{FB}/(\sqrt{D_{ox}} - 9 \times 10^{-7})$ as a function of time.
- Fig. 10. Comparison of flat band voltage shifts for measurements at 77°K and 295°K. Oxide thickness 297 Å.

- Fig. 11. Effect of post oxidation annealing temperature on flat band voltage shifts for measurements at 295°K and 77°K.
- Fig. 12. Flat band voltage as a function of time showing "turn around effect".
- Fig. 13. Photocurrent as a function of gate voltage curve for positive gate voltage made before avalanche injection (solid circles) and after injection (open circles).
- Fig. 14. Photocurrent as a function of gate voltage for negative gate voltage.
- Fig. 15. Capacity as a function of gate voltage curves made before avalanche injection (solid line) and after avalanche injection (dashed line).
- Fig. 16. Effect of post oxidation heat treatment (POA) on "turn around effect".
- Fig. 17. V_{FB} as a function of charge/unit area
- Fig. 18. Effect of electric field on V_{FB} after avalanche injection.
- Fig. 19. Increased effect due to elevated temperature
- Fig. 20. Elimination of "turn around effect" at elevated temperatures.
- Fig. 21. ΔV_{FB} as a function of time for sample made with silicon gate process.

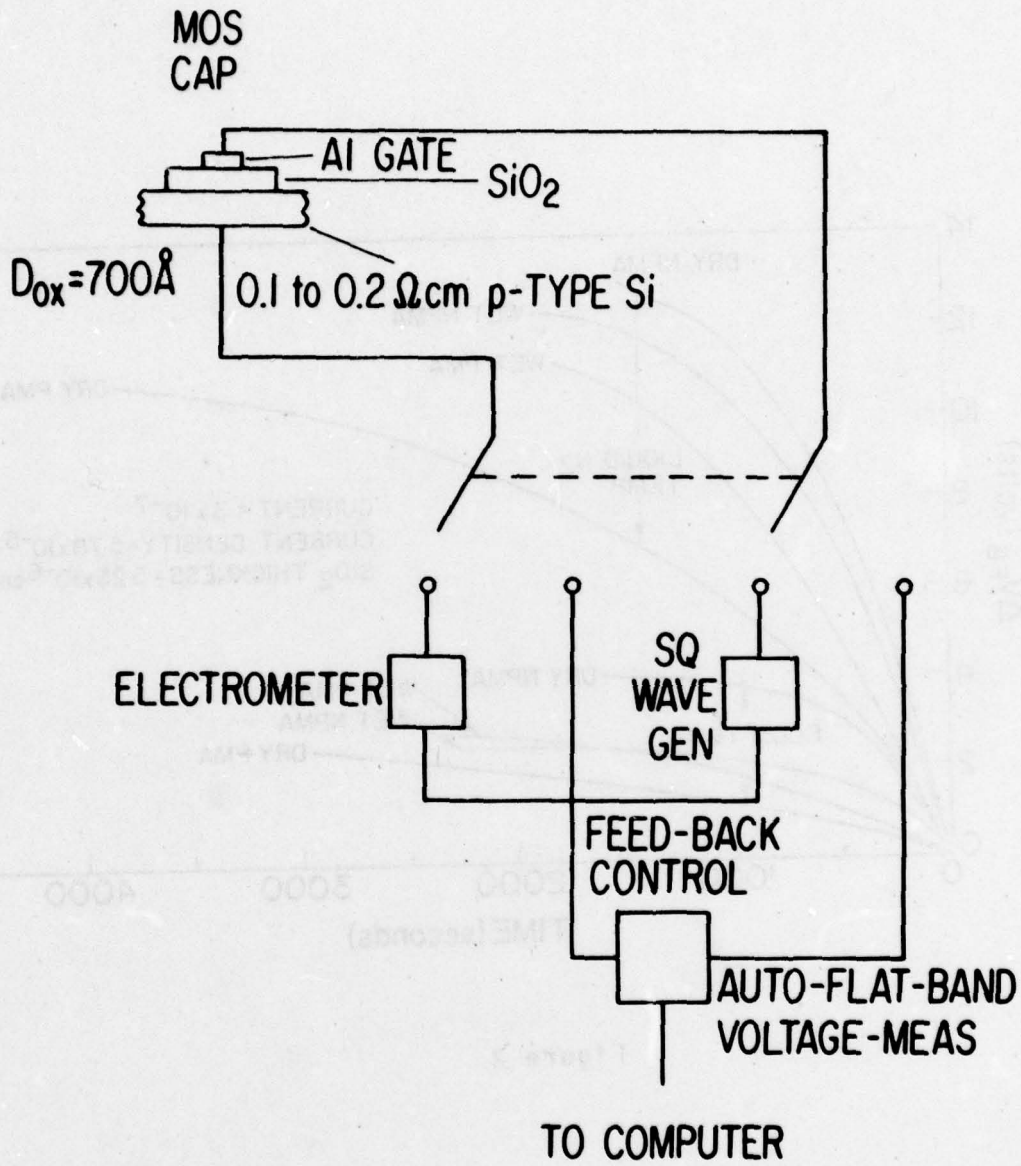


Figure 1

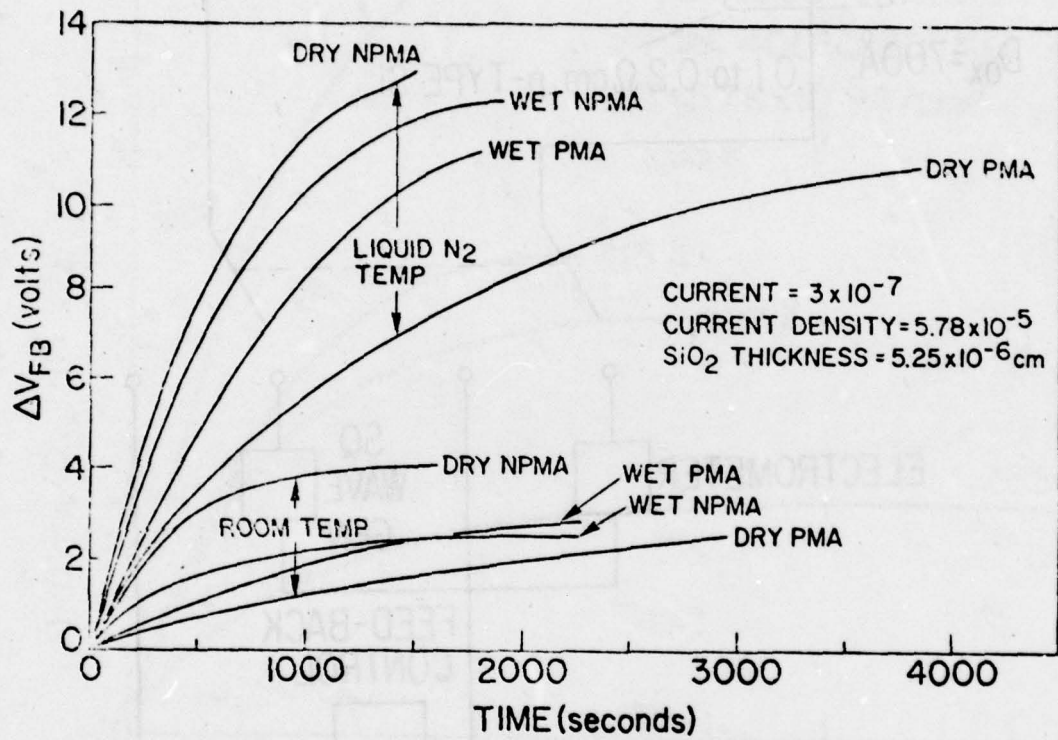


Figure 2

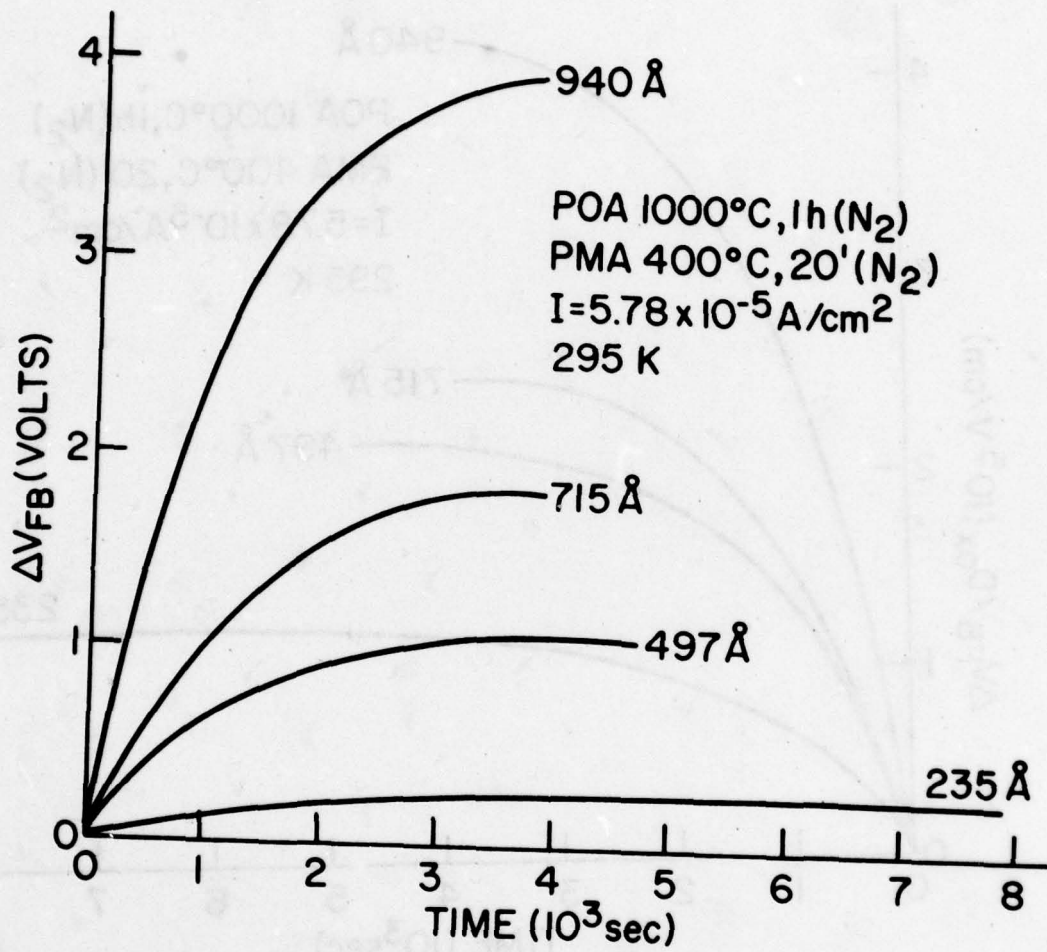


Figure 3

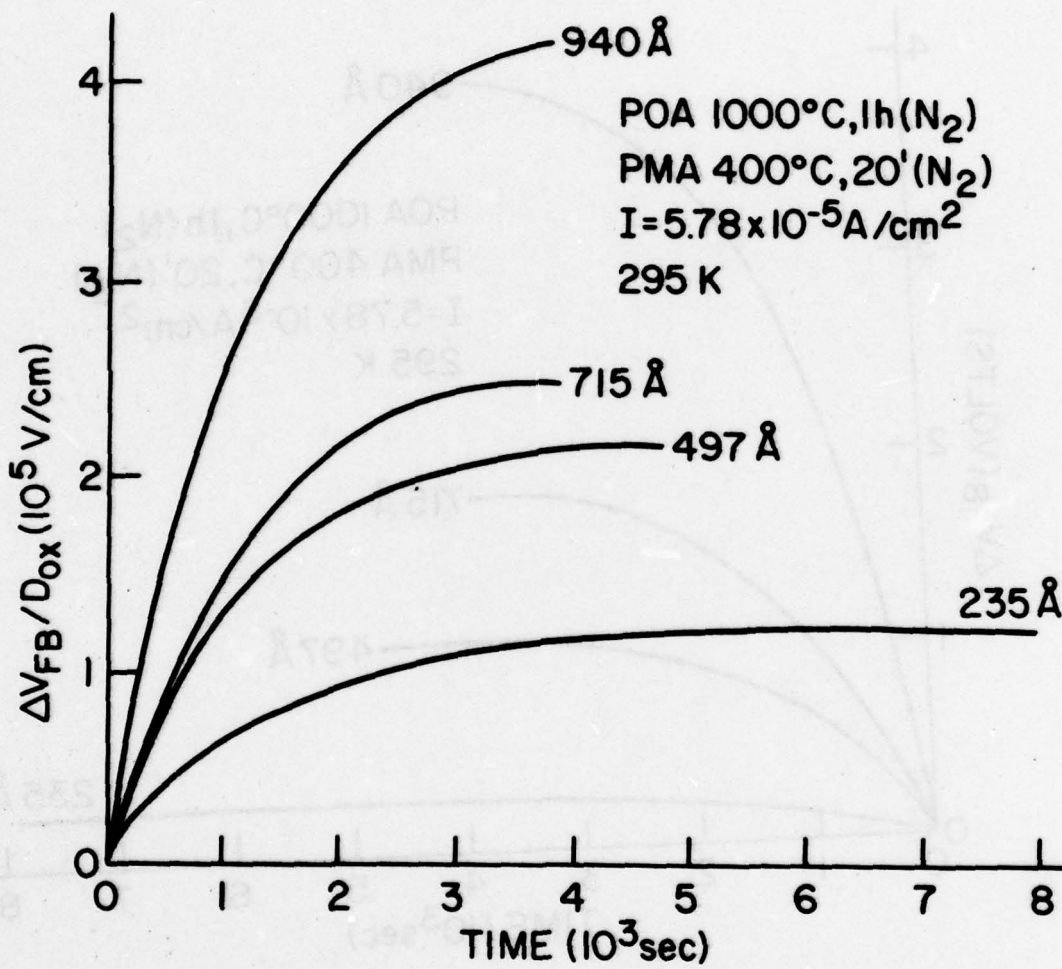


Figure 4

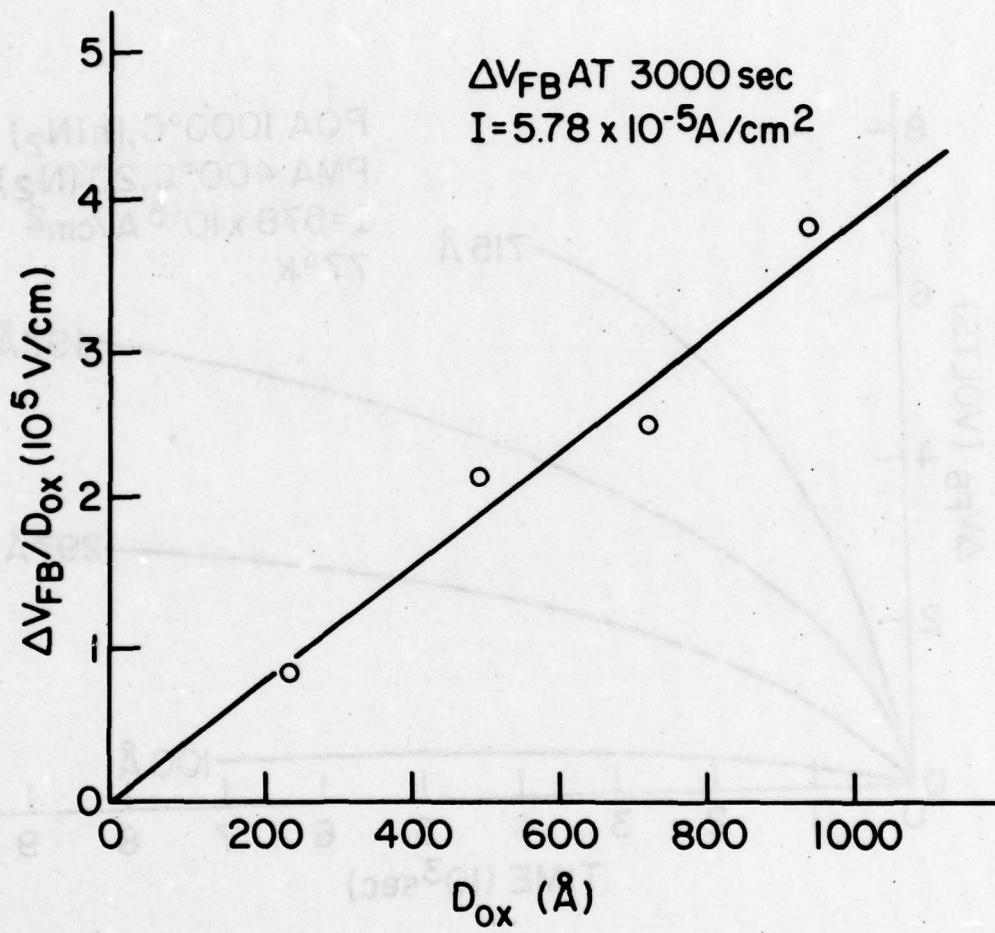


Figure 5

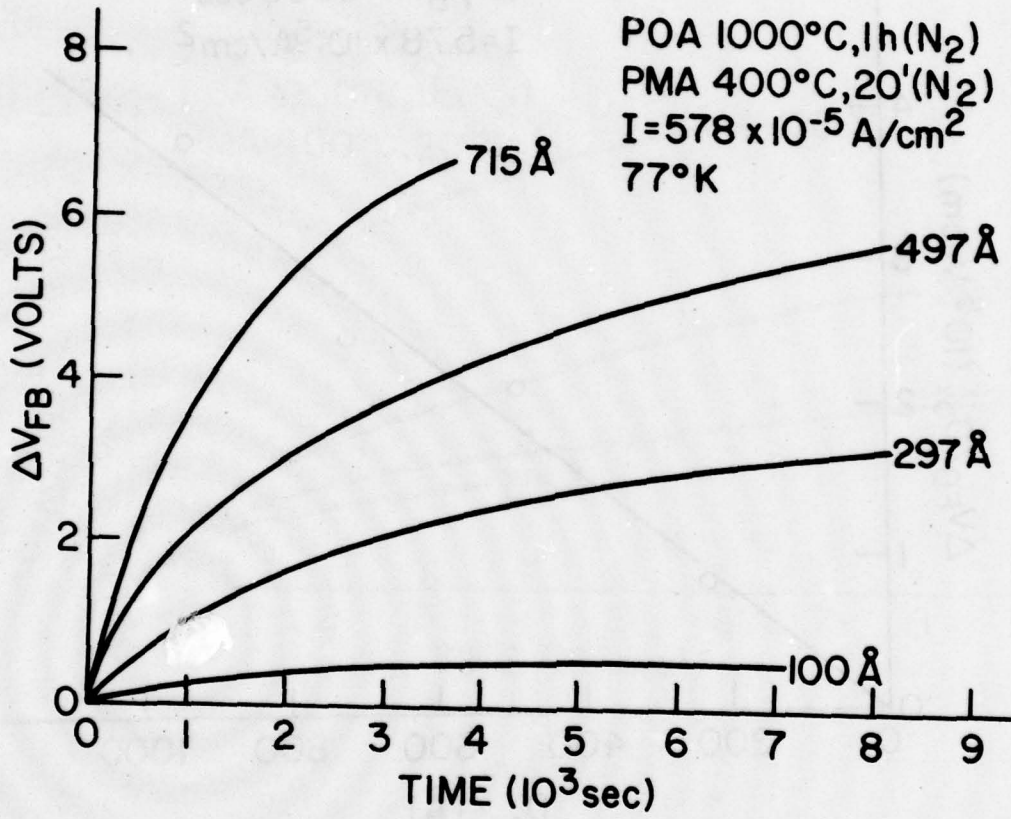


Figure 6

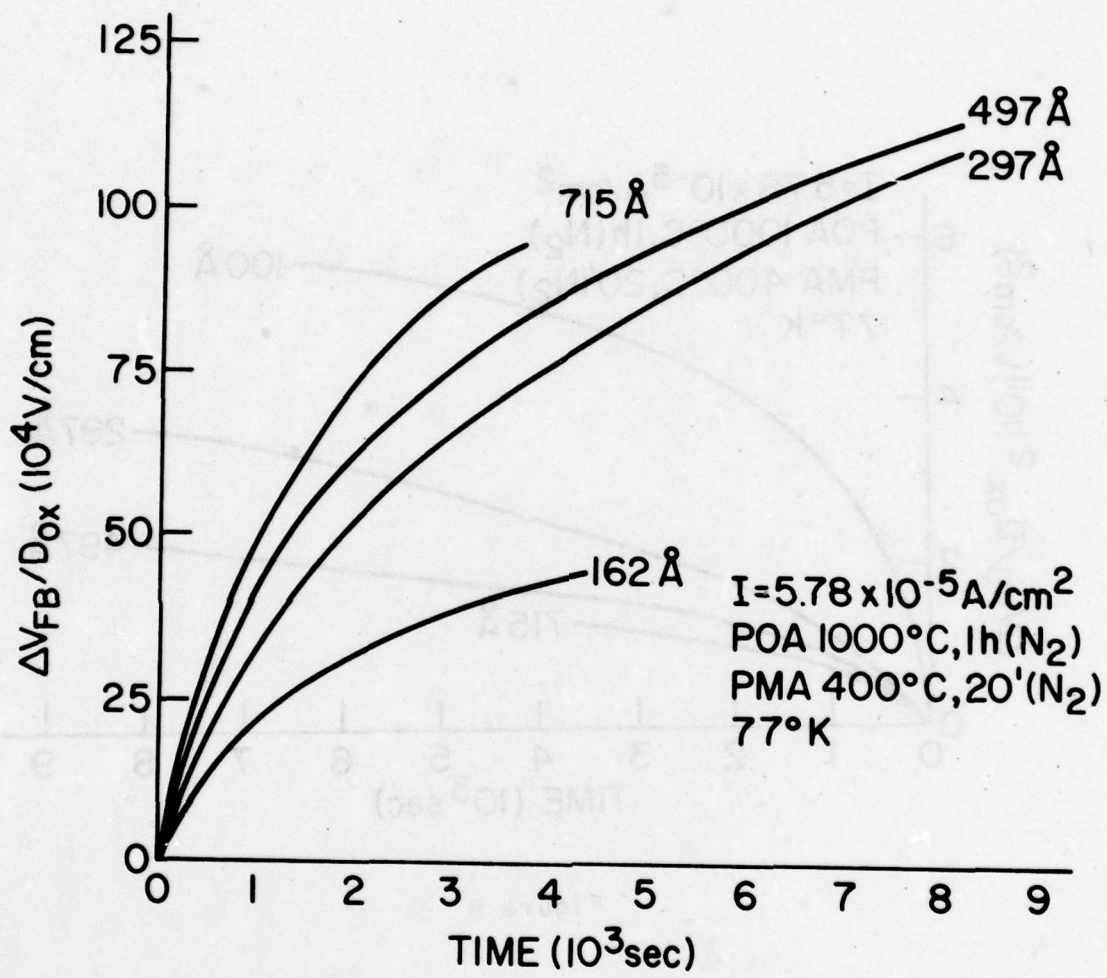


Figure 7

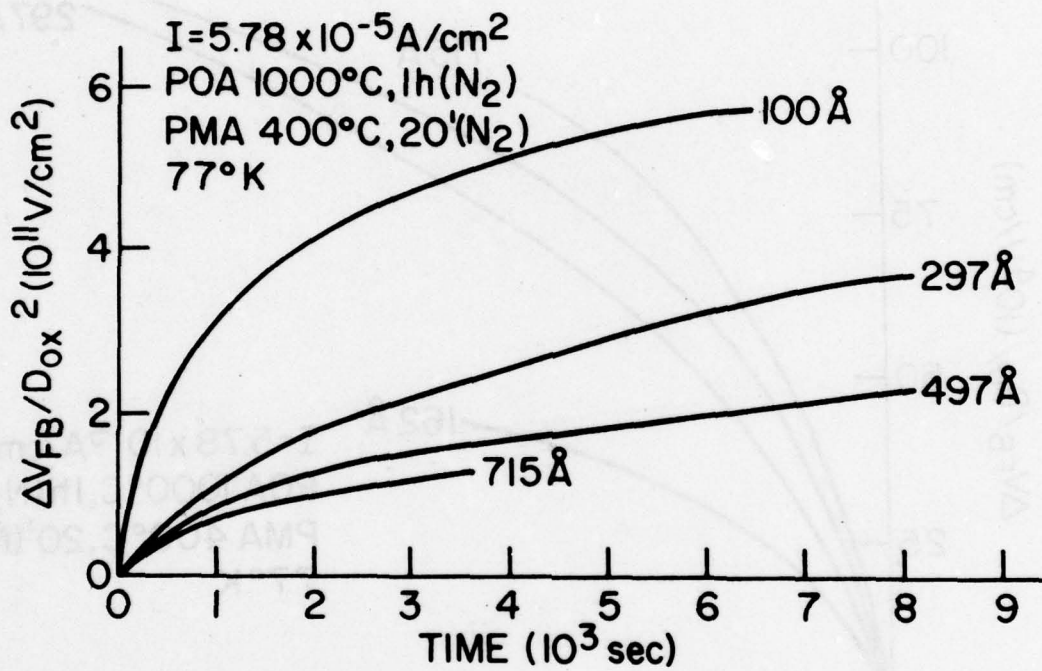


Figure 8

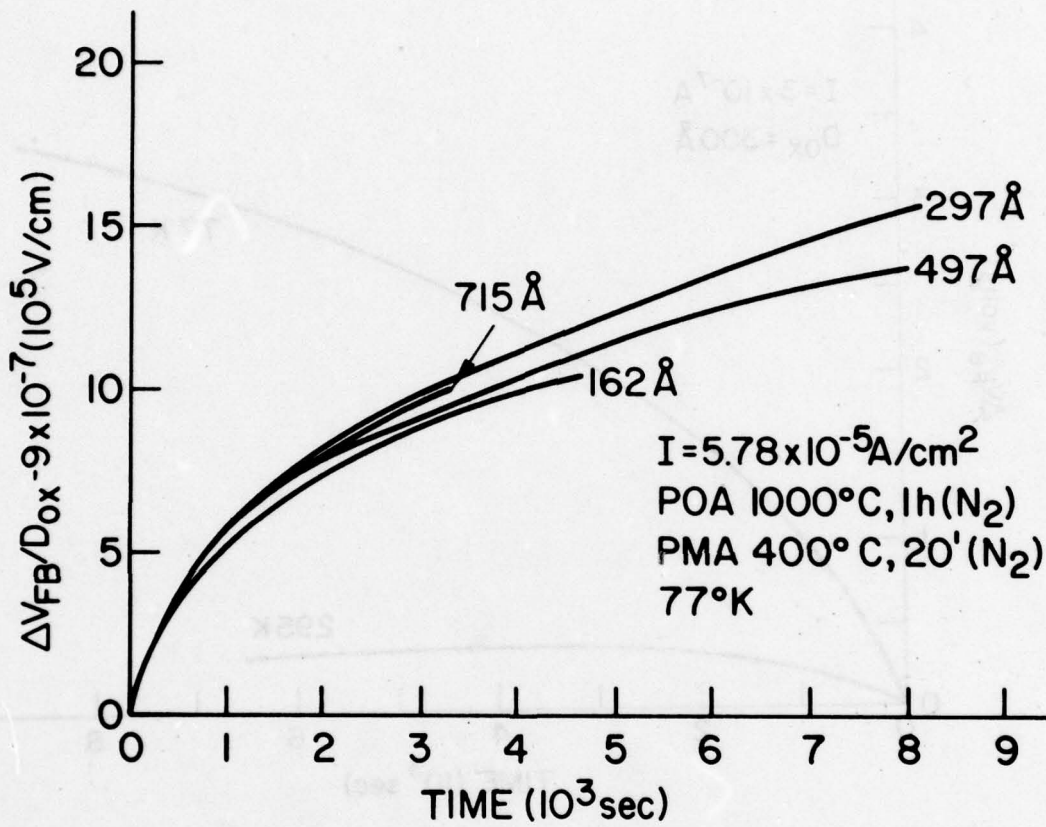


Figure 9

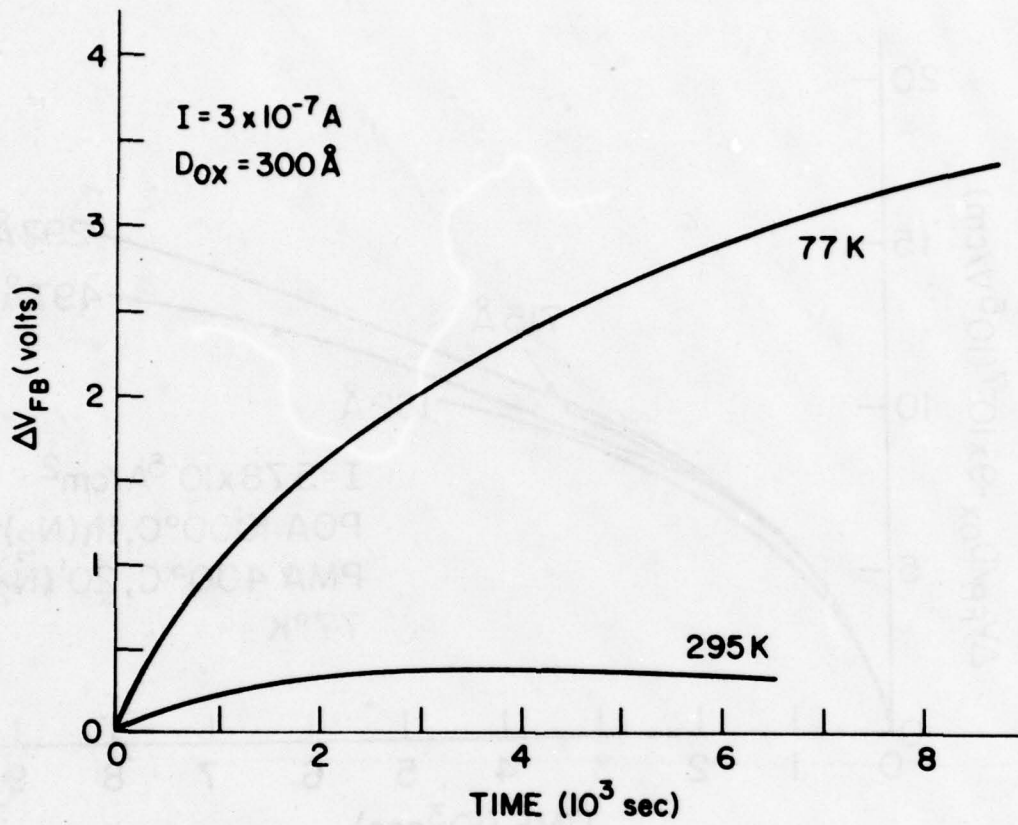


Figure 10

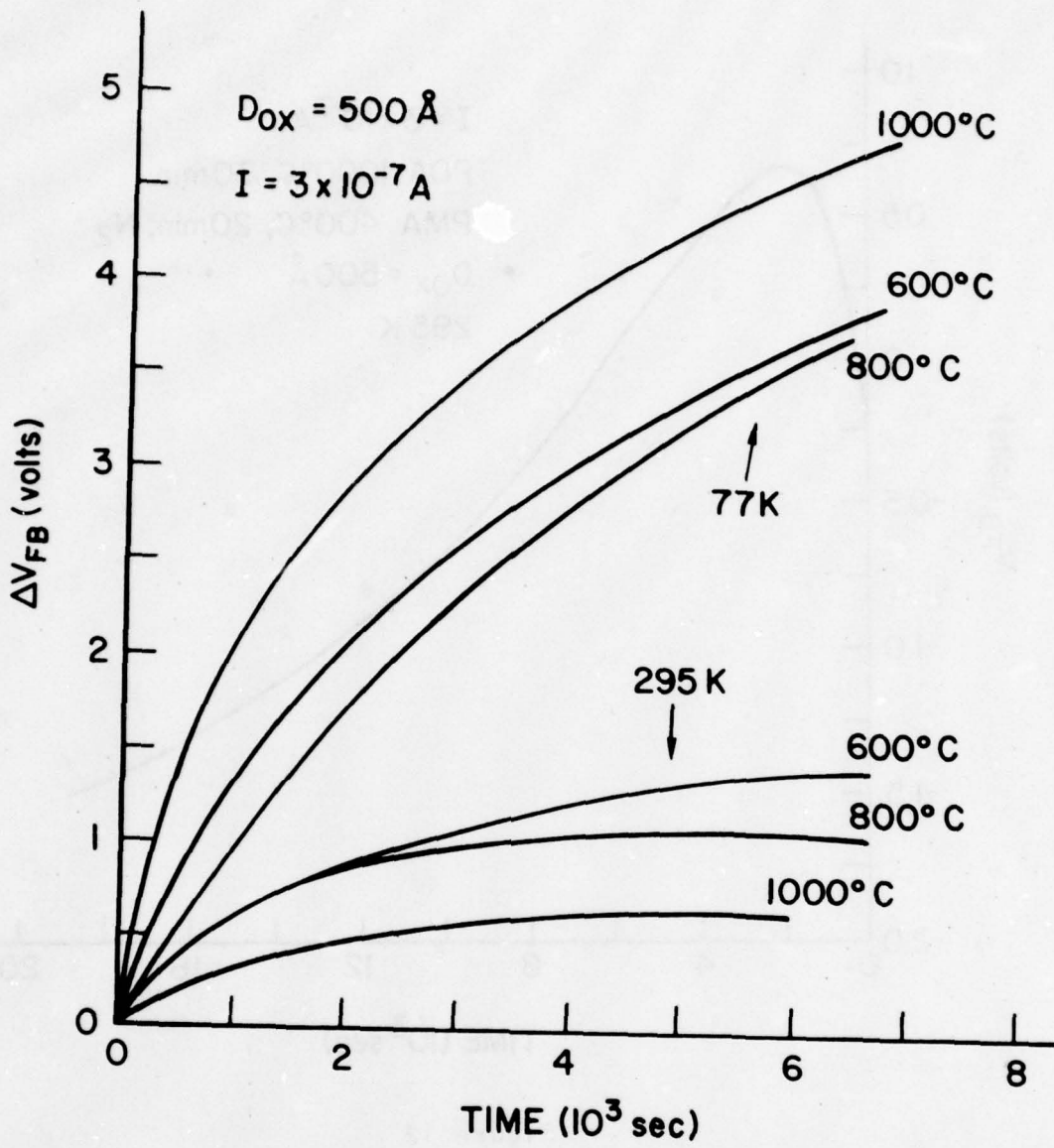


Figure 11

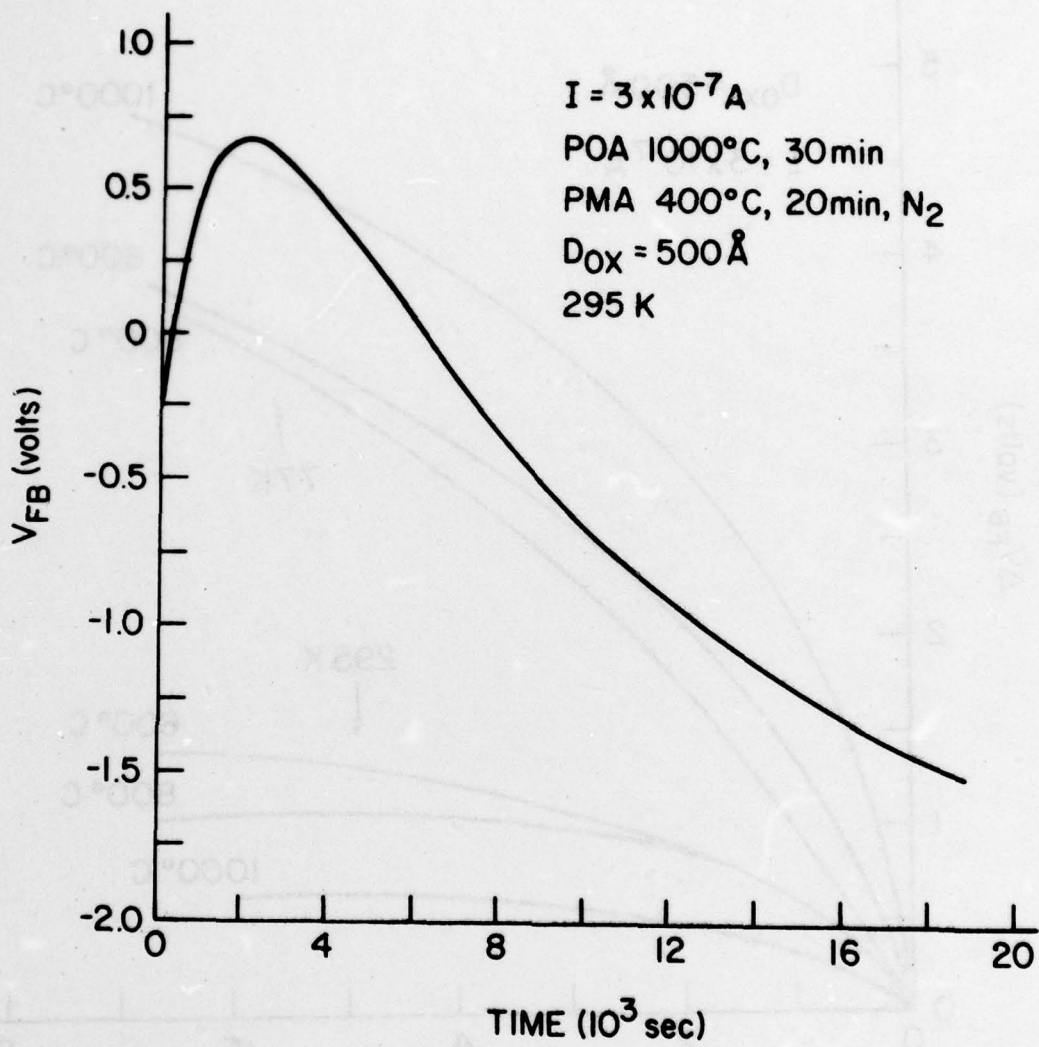


Figure 12

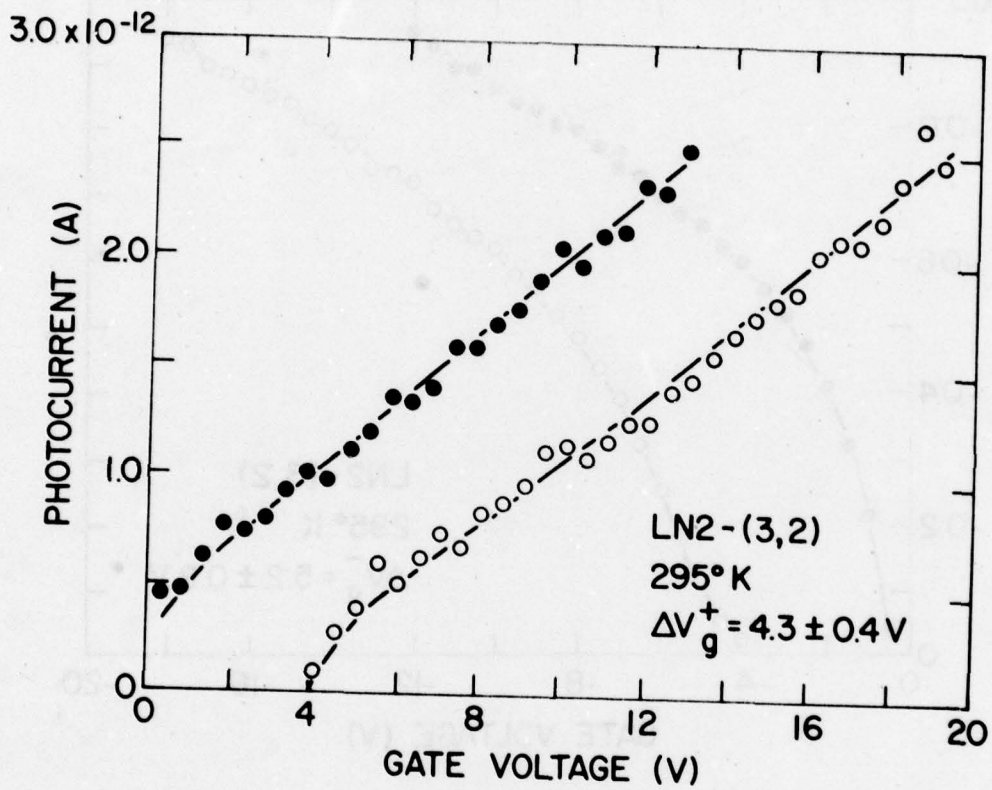


Figure 13

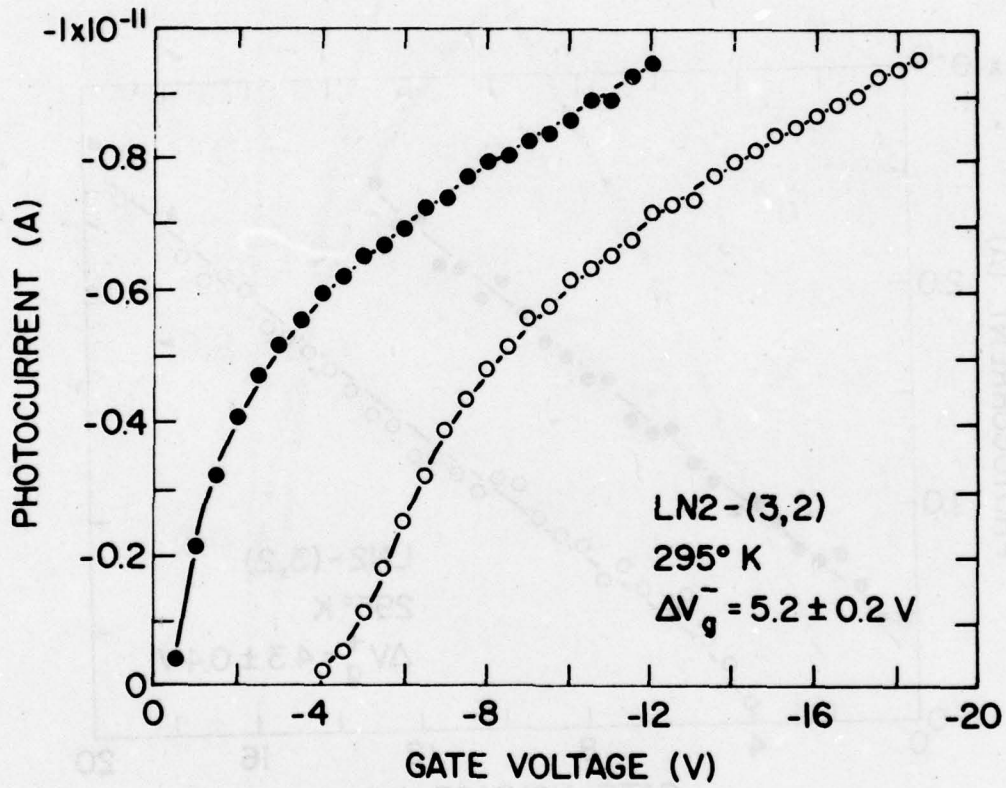


Figure 14

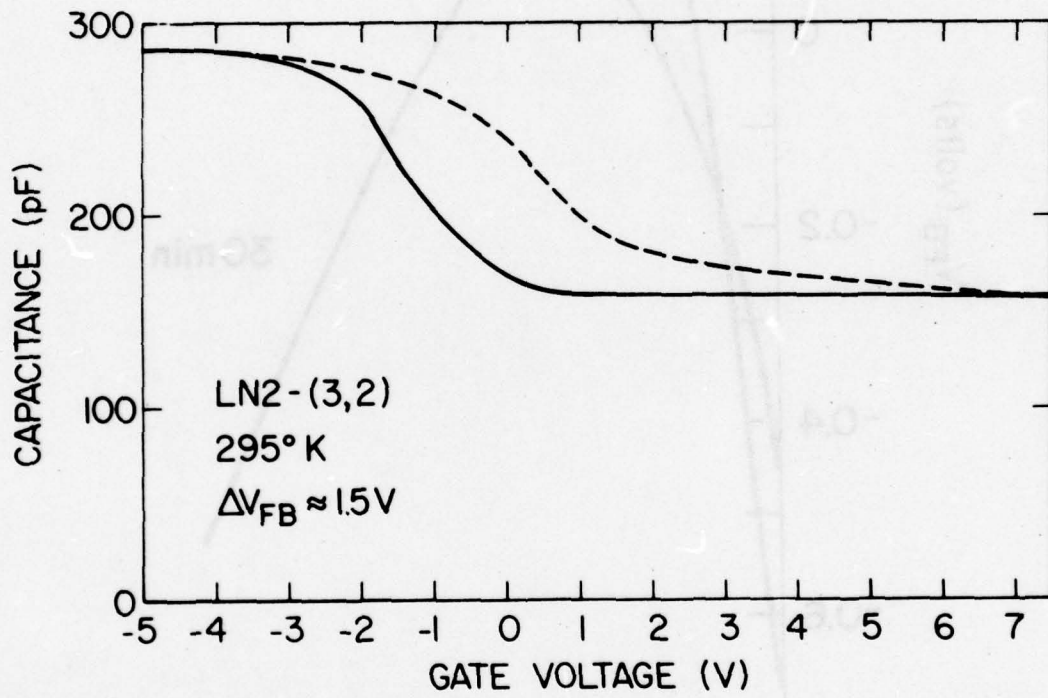


Figure 15

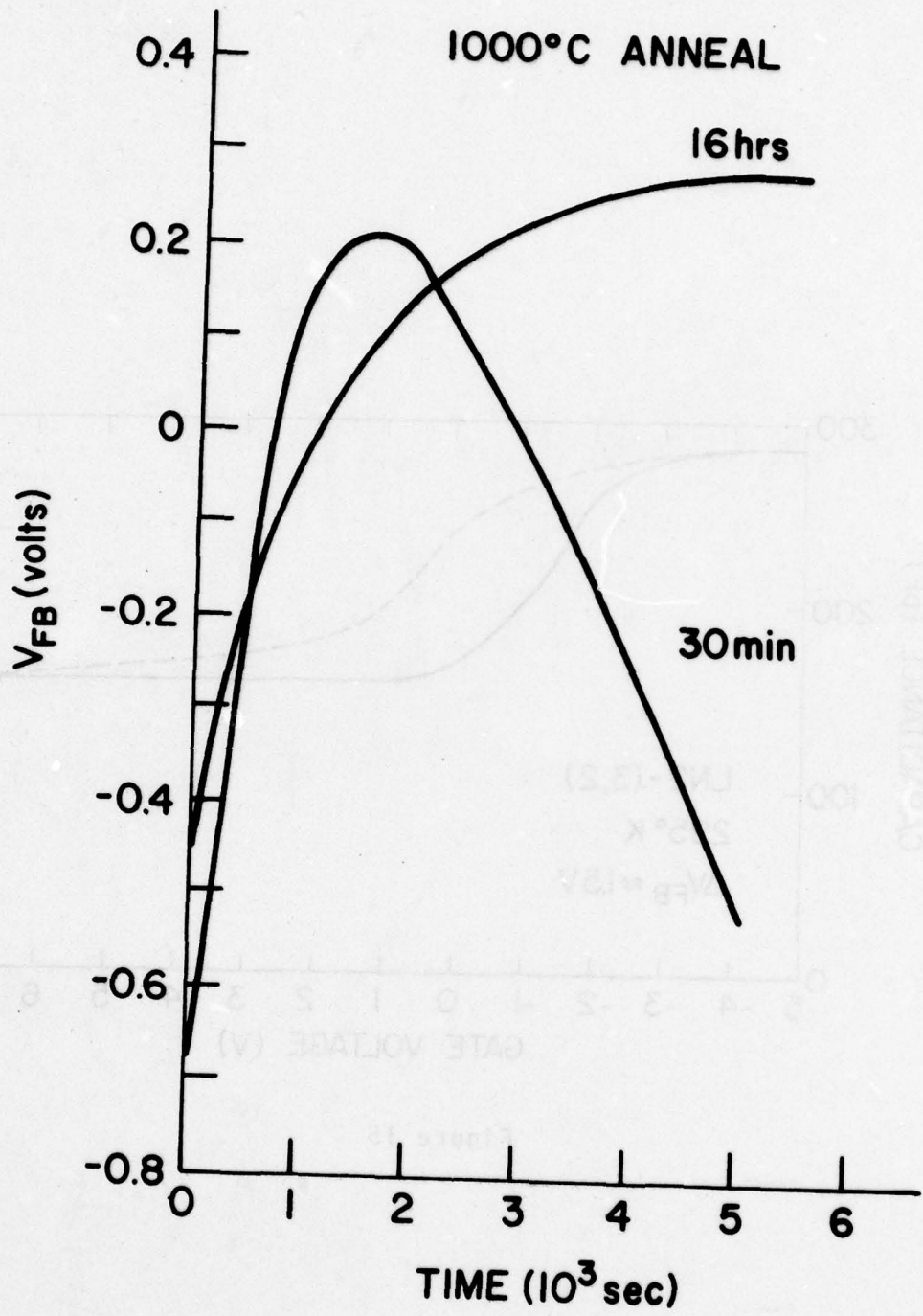


Figure 16

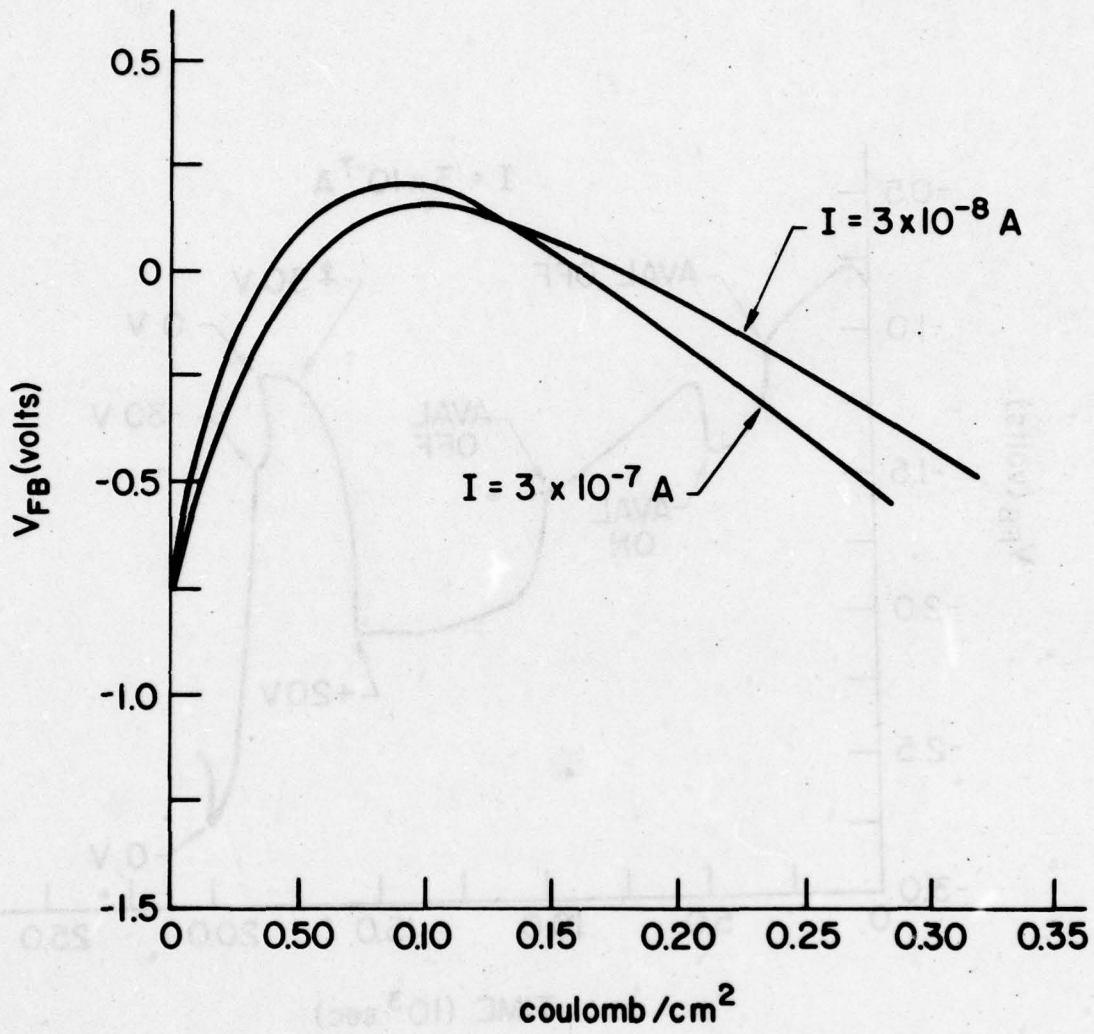


Figure 17

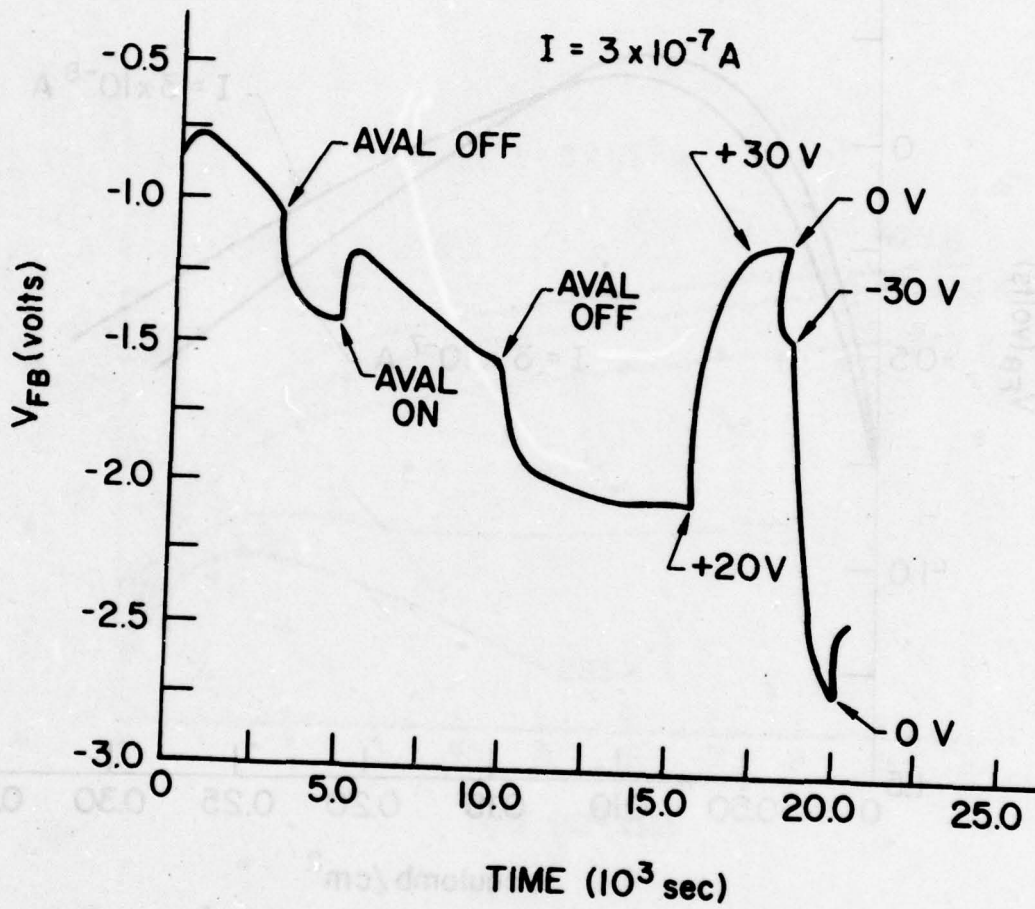


Figure 18

500 Å SiO₂ DRY PROCESS

POA 1000°C, 30 min, N₂

PMA 400°C, 20 min, F.G.

I = 3 x 10⁻⁷ A

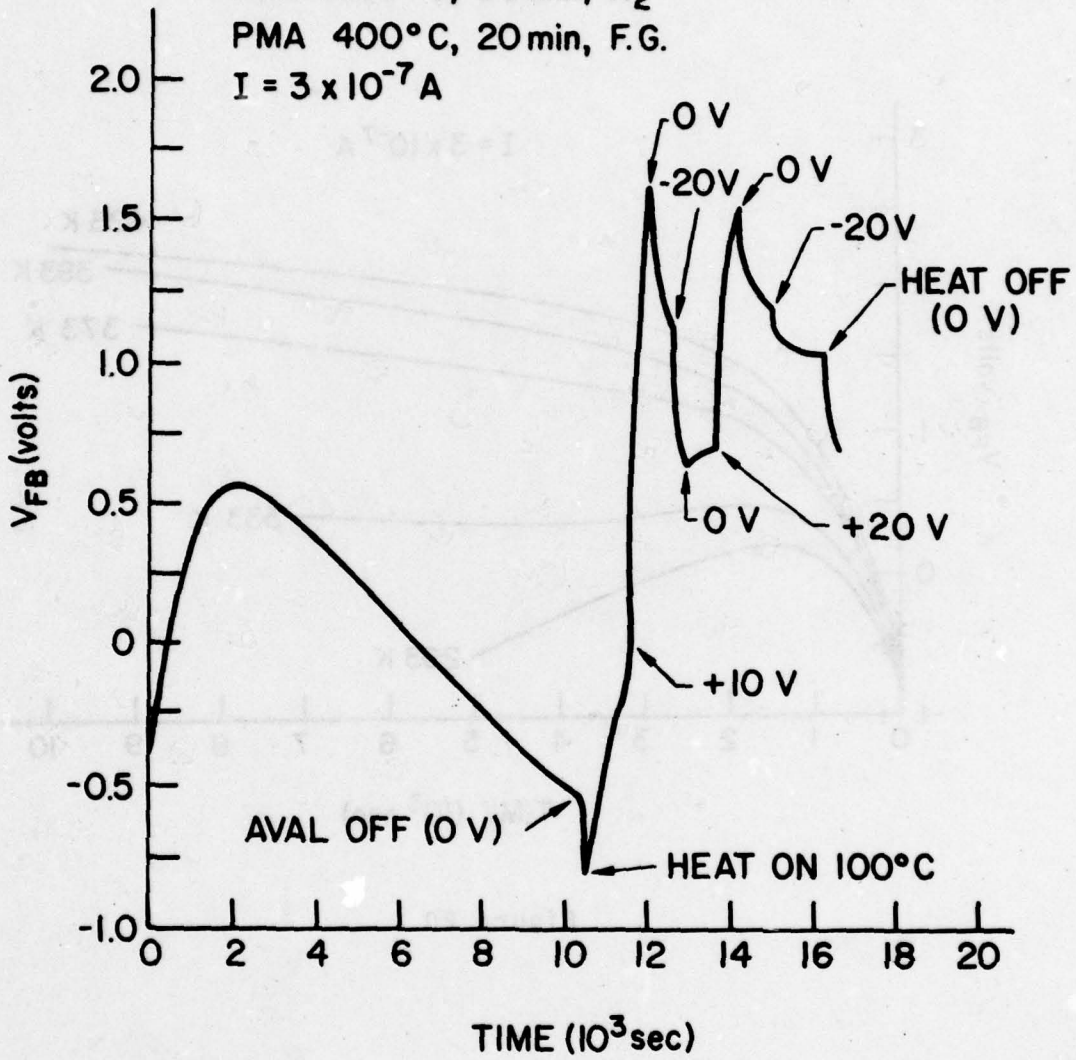


Figure 19

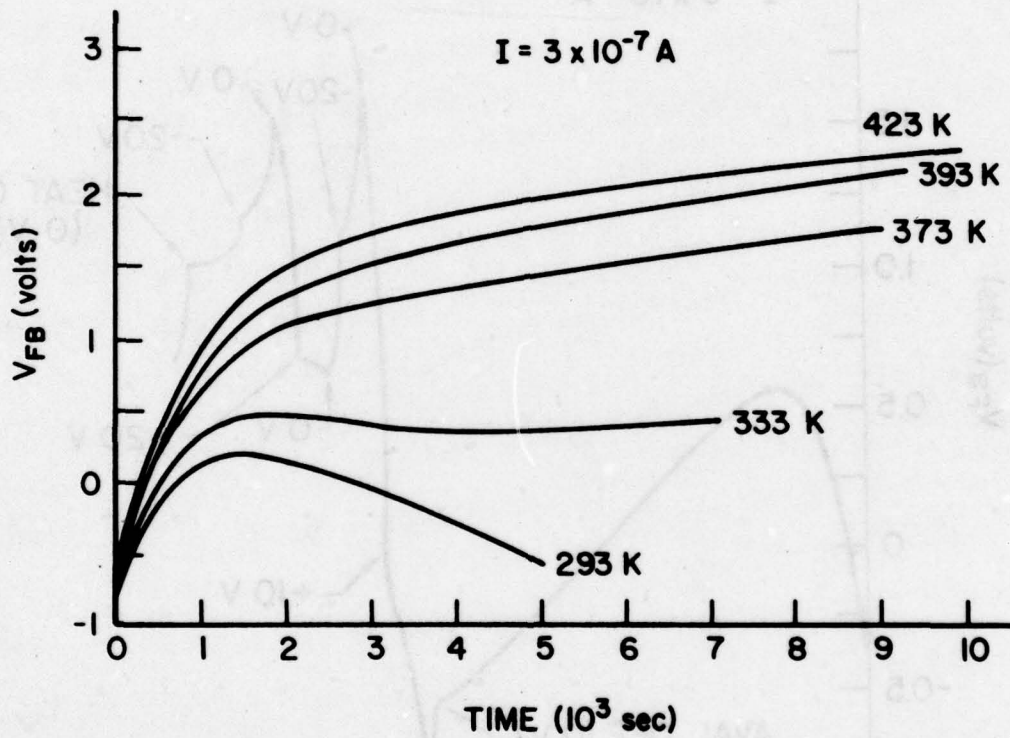


Figure 20

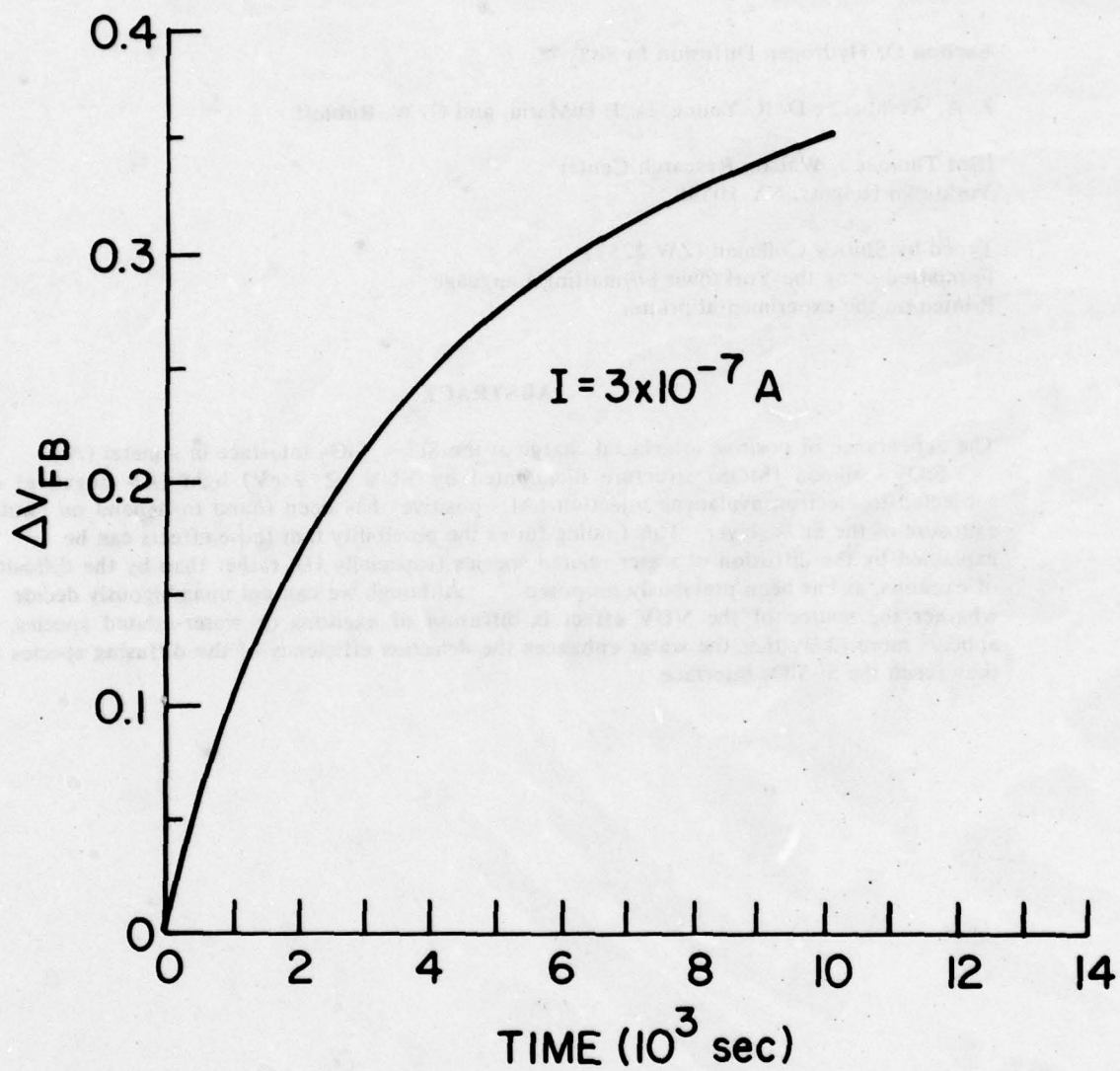


FIGURE 21

Exciton Or Hydrogen Diffusion In SiO₂ ?*

Z. A. Weinberg , D. R. Young, D. J. DiMaria, and G. W. Rubloff.

IBM Thomas J. Watson Research Center
Yorktown Heights, NY 10598

Typed by Shirley Coleman (ZW.2251)
Formatted using the Yorktown Formatting Language
Printed on the experimental printer

ABSTRACT

The appearance of positive interfacial charge at the Si - SiO₂ interface in a metal (Al) - SiO₂ - silicon (MOS) structure illuminated by VUV (≥ 9 eV) light (Al- negative) or subjected to electron avalanche-injection (Al - positive) has been found to depend on water exposure of the SiO₂ layer. This finding raises the possibility that these effects can be explained by the diffusion of water-related species (especially H), rather than by the diffusion of excitons, as has been previously proposed^{1,2}. Although we can not unambiguously decide whether the source of the VUV effect is diffusion of excitons or water-related species, it appears more likely that the water enhances the *detection* efficiency of the diffusing species as they reach the Si-SiO₂ interface.

* This research was supported in part by the Defense Advanced Research Projects Agency and monitored by the Deputy for Electronic Technology, RADC, under Contract F19628-76-C-0249.

Exciton Or Hydrogen Diffusion In SiO₂ ?*

Z. A. Weinberg, D. R. Young, D. J. DiMaria, and G. W. Rubloff.

IBM Thomas J. Watson Research Center

Yorktown Heights, NY 10598

ABSTRACT

The appearance of positive interfacial charge at the Si - SiO₂ interface in a metal (Al) - SiO₂ - silicon (MOS) structure illuminated by VUV (≥ 9 eV) light (Al - negative) or subjected to electron avalanche-injection (Al - positive) has been found to depend on water exposure of the SiO₂ layer. This finding raises the possibility that these effects can be explained by the diffusion of water-related species (especially H), rather than by the diffusion of excitons, as has been previously proposed^{1,2}. Although we can not unambiguously decide whether the source of the VUV effect is diffusion of excitons or water-related species, it appears more likely that the water enhances the *detection* efficiency of the diffusing species as they reach the Si-SiO₂ interface.

- * This research was supported in part by the Defense Advanced Research Projects Agency and monitored by the Deputy for Electronic Technology, RADC, under Contract F19628-76-C-0249.

It has been previously proposed that several effects related to charge trapping at the interfaces of MOS (metal - SiO₂ - silicon) structures may be the result of migration of stable excitons across relatively long distances in the oxide^{1,2}. We have recently found that these effects are influenced by water exposure during processing, which raises the possibility that they are caused by diffusion of water-related species, such as hydrogen, instead of excitons. Alternatively, the exciton model may still be correct, the water merely affecting the efficiency of exciton detection at the interface. We have investigated this issue by performing various experiments on both "dry" and "wet" samples, as described in this communication. In spite of our inability to resolve the issue at the present time, we present the experimental results and discuss their implications because the possibility of exciton migration is of fundamental importance both to the understanding of various trapping and radiation effects in MOS structures and to theoretical studies of SiO₂. In fact, recent advances³⁻⁵ in the theory of the electronic structure of SiO₂ strongly support the long standing belief that features in its optical spectra are excitonic in origin⁶ and that the absorption edge is dominated by an exciton which produces the first absorption peak at 10.45 eV⁷.

To investigate the effect of water, samples were prepared by the oxidation of silicon wafers in a "dry" O₂ ambient followed by a 5-min anneal in N₂, both done at 1000°C. After oxidation, several wafers were placed in boiling deionized water for 5 min; samples from these wafers are referred to, herein, as "wet". The silicon wafers were n- or p- type, .1 - .2 Ωcm, and (100) oriented. The oxide thickness was 105 nm. All wafers were metallized together by an array of aluminum dots, 15 nm thick, and 1.25 mm in diameter. There was no post-metallization anneal.

The experimental findings which need an explanation are the "negative-bias VUV effect" and the "avalanche-injection turn-around effect"; both effects refer to the appearance of positive charge at the Si - SiO₂ interface. The former effect occurs in samples which are illuminated by ionizing ($h\nu \geq 9\text{eV}$) vacuum-ultraviolet (VUV) radiation with the Al electrode

biased negatively^{1,2}, and the latter effect occurs in samples subjected to injection of electrons from the Si into the SiO₂ by the avalanche-injection technique⁸ in which the Al is biased positively. It should be noted that in both experiments electrons constantly flow through the Si - SiO₂ interface and annihilate part of the positive charge being trapped there. This annihilation, or electron-hole recombination, depends on the applied electric field and its cross-section decreases with increased field.⁹ The positive charge remaining after the charging treatment can be further reduced, but not entirely removed, by electron injection at low fields from internal-photoemission at $h\nu < 5.5$ eV. It is reasonable to assume that the part of the positive charge that can not be annihilated is due to traps situated very close to the Si - SiO₂ interface which act as surface states, with other traps being distributed further from the interface and acting as oxide charge. With this interpretation the distinction between surface-states and oxide charge is merely a function of their proximity to the interface; it is more commonly assumed however, that the distinction arises from differences in chemical (or bonding) origins¹⁰. Except for the annihilation experiment we have not separated these two components and therefore we shall refer below to the accumulative positive charge as the "interfacial charge."

In order to determine whether the trapping efficiency for holes at the Si - SiO₂ interface has been affected by the water treatment, we have also performed hole injection experiments by either hole avalanche - injection¹¹ or by drifting holes under positive bias in the VUV experiments¹². In addition, we have used the photo I-V technique to determine the location of the various trapped charges in the oxide^{13,14}. We next present the experimental results with an emphasis on the comparison between the "wet" and "dry" samples.

1) *VUV experiments.* Samples were illuminated by VUV photons with the Al electrode biased either negatively (Fig. 1) or positively (Fig. 2). A mask was used to shield the unmetallized surface of the oxide and to collect secondary photoemitted electrons. The data of Figs. 1 and 2 show the rate of accumulation of positive interfacial charge (at the Si - SiO₂ interface) as

a function of photon energy. More experimental details are given in the figure captions. For the "negative-bias VUV effect" shown in Fig. 1, the data for the "wet" samples show an enhanced trapping relative to the "dry" samples by a factor of approximately 10, over the entire spectrum. To facilitate the discussion below, the absorption length (L) of the light in the oxide is also shown in Fig 1. These data were measured on thin oxide membranes produced by etching a window in the silicon substrate.^{7,15} In the positive bias experiment (Fig 2), holes are drifted toward the Si - SiO₂ interface and the "wet" samples show an enhancement of hole trapping by a factor of about 4 over the "dry" samples. The data, as indicated by error-bars, are somewhat less accurate because the hole current was not constant and has exhibited some decay with time because of hole trapping at the Al - SiO₂ interface.

2) *Avalanche-injection of electrons and holes.* The a.c. avalanche-injection technique has been described in detail elsewhere⁸. In this technique, hot carriers are injected (in pulses) from the Si into the SiO₂, over the interface energy-barrier. Either electrons ($+V_G$) or holes ($-V_G$) can be injected from p- or n- type substrates, respectively. In these experiments the oxide current is kept constant by automatic adjustment of the applied voltage. The data for electron injection (Fig. 3) and hole injection (Fig. 4) are shown by plotting the shifts of C-V curves as a function of time. The "turn-around effect", seen in Fig. 3, is the result of the initial trapping of electrons on sites distributed in the oxide bulk which is surpassed, after a period of time, by the accumulation of positive interfacial charge. Note that negative C-V shifts ($-\Delta V$) indicate positive trapped charge and vice versa. Fig. 4 shows the rate of hole trapping at the Si - SiO₂ interface for avalanche-injection of holes. Because of some difficulties with keeping the hole current constant, the data show somewhat larger errors, as indicated in the figure.

3) *Photo I-V Measurements.* With a technique which has been described extensively elsewhere^{13,14}, current-voltage (I-V) characteristics of electron internal-photoemission (IPE) from both electrodes are compared before and after the charging treatment. Since IPE is

sensitive to the field near the injecting electrode, shifts or distortions in the curves provide information on the location of the trapped charge.

Tables I and II summarize the amount of trapped charge per unit area in the oxide layer for wet and dry samples after avalanche injection of the indicated number of electrons per unit area. For the low current avalanche injection conditions in Table I (4×10^{-8} A for 600 sec), the wet oxide traps more electrons than the dry oxide and has its centroid closer to the Al - SiO₂ as expected. For the high current avalanche injection conditions in Table II (3×10^{-7} A for 2000 sec), a similar behavior between wet and dry is seen for the amount and location of the negative trapped charge. However, for the conditions of Table II a large positive charge is also found very near the Si - SiO₂ interface as discussed in the preceding section on avalanche injection. Separation of the positive interface charge from the bulk negative charge requires both the C-V and photo I-V techniques as discussed in previous publications^{8,13,14}. The wet sample has more trapped positive charges than the dry sample. This behavior was also observed in previous sections for hole trapping near the Si - SiO₂ interface after hole avalanche injection from the Si (see Fig. 4) or hole generation across the SiO₂ bandgap (see Figs. 1 and 2). If the dry oxide MOS samples were annealed in forming gas at 400°C for 20 minutes after Al metallization, both negative and positive trap charging under similar conditions to those in Tables I and II are reduced by approximately a factor of 0.5. Clearly, the data presented here shows a strong correlation of the "avalanche-injection turn-around effect" with the presence of water in the SiO₂ layer.

Discussion

The finding that water influences the "negative bias VUV effect" and the "avalanche-injection turn-around effect" may indicate that these effects originate from the diffusion of water-related species. Since both effects occur under opposite polarities, the diffusion of H (atomic hydrogen) may be responsible for both, rather than the diffusion of excitons as has

been previously suggested.^{1,2} Free hydrogen could be generated by SiO₂ exciton decay, hole trapping, electron trapping, or photon absorption at water-related centers. A possible explanation in terms of the drift of OH⁻ under one polarity ("VUV effect") and H⁺ for the other polarity ("avalanche-injection effect") is discounted because the former effect was found to decrease when the applied field was increased¹ and because OH⁻ is a rather large ion.

The H⁻ diffusion model runs into a difficulty, however, when the spectral dependencies of Fig. 1 are considered. As seen in the figure for $h\nu > 10$ eV the effect follows the behavior of the optical absorption length (L) and decreases even more sharply when the light is absorbed closer to the Al electrode (the dip near 10.5 eV). Going to lower photon energies, as L becomes larger than the oxide thickness, the effect decreases because of smaller total absorption in the oxide. This light absorption in the oxide produces a more pronounced effect when the absorption takes place nearer the Si-SiO₂ interface (i.e. when L is larger). The water content is larger near the Al electrode, especially in the "wet" samples as has actually been shown by the photo I-V results. If water-related species were the *source* of the effect, we would expect that: (1) the effect would be stronger at smaller L, particularly for the "wet" samples, and (2) the shape of the "wet" curve in Fig. 1 would differ from that of the "dry" curve in showing a relatively enhanced effect at smaller L. Neither expectation is fulfilled by the data.

In fact the "wet" and "dry" curves of Fig. 1 show mainly a change in scale, which could result if only the *detection* efficiency of the effect was influenced by the water. With this interpretation the exciton model may still be the correct explanation for the *source* of the effect. The fact that hole trapping at the Si - SiO₂ interface has been affected by the water treatment is seen in the experiments where holes are transported across the interface: the positive bias VUV experiment (Fig. 2) and the hole avalanche-injection experiment (Fig. 4). The "wet" versus "dry" enhancement of the "negative-bias VUV effect" of Fig 1 is stronger than the enhancement of hole trapping seen in Figs. 2 and 4. This may indicate that the

trapping efficiency for excitons at the interface is more sensitive to the water treatment than the trapping efficiency of holes. One may ask how the water can affect the interface so strongly. This may result from water molecules diffusing to the interface. Alternatively, water reaction at the Al-SiO₂ interface, which is believed to produce hydrogen¹⁶, could lead to hydrogen diffusion through the SiO₂ to the Si-SiO₂ interface and modify its trapping efficiency. With the latter mechanism, aluminum-oxide (or hydroxyl) trapping centers, would also be generated near the Al - SiO₂ interface. These centers may be responsible for the "avalanche-injection turn-around effect" as either electrons or excitons, trapped there, may produce a hole that drifts under the positive applied voltage to the Si - SiO₂ interface. It should be noted that close to the Al electrode it is easier for excitons to dissociate into free electrons and holes, than in the oxide bulk.

In conclusion, we can not unambiguously decide whether the source of the VUV effect is diffusion of excitons or water-related species. However, it appears more likely that the water enhances the *detection* efficiency of diffusing species as they reach the Si-SiO₂ interface. This would mean that the enhancement of both the VUV effect and the avalanche-injection turn-around effect by water exposure during processing may result from increased conversion efficiency in producing positive charge at the Si-SiO₂ interface.

Acknowledgements

We are grateful to E. A. Irene and D. W. Dong for their support in supplying samples. The experimental help of J. A. Calise, F. L. Pesavento, and the Si facility at IBM are greatly appreciated. One of us (ZAW) wishes to acknowledge helpful discussions with J. N. Zemel and C. Svensson about the role of hydrogen in SiO_2 .

References

- 1) Z. A. Weinberg and G. W. Rubloff, *Appl. Phys. Lett.* **32**, 184 (1978)
- 2) Z. A. Weinberg and G. W. Rubloff, in *The Physics of SiO₂ and Its Interfaces*, ed. by S. T. Pantelides, p. 24 (Pergamon, New York, 1978)
- 3) J. R. Chelikowsky and M. Schluter, *Phys. Rev. B* **15**, 4020 (1977).
- 4) S. T. Pantelides, in *The Physics of SiO₂ and Its Interfaces*, ed. by S. T. Pantelides, p 80 (Pergamon, New York, 1978).
- 5) D. L. Griscom, *J. Non-Crystalline Solids*, **24**, 155 (1977).
- 6) E. Loh, *Solid State Commun.* **2**, 269 (1964).
- 7) Z. A. Weinberg and G. W. Rubloff, to be published.
- 8) D. R. Young, E. A. Irene, D. J. DiMaria, H. Z. Massoud, and R. F. DeKeersmaecker, The Electrochemical Society Spring Meeting, Seattle, Washington, 1978 (unpublished).
- 9) T. Ning, *J. Appl. Phys.* **47**, 3203 (1976).
- 10) C. T. Sah, *IEEE Trans. on Nuclear Science*, **NS-23** 1563 (1976).
- 11) J. M. Aitken and D. R. Young, *IEEE Trans. Nucl. Sci.* **NS-24**, 2128 (1977).
- 12) Z. A. Weinberg, *Appl. Phys. Lett.* **27**, 437 (1975).
- 13) D. J. DiMaria, *J. Appl. Phys.* **47**, 4073 (1976).
- 14) D. J. DiMaria, Z. A. Weinberg, J. M. Aitken, *J. Appl. Phys.* **48**, 898 (1977).
- 15) R. J. Powell and M. Morad, *J. Appl. Phys.* **49**, 2499 (1978).
- 16) P. Balk, The Electrochemical Society Fall Meeting, Buffalo, N.Y., 1965, paper No. 111.

Figure Captions

- Fig. 1 The "negative bias VUV effect." The data show the accumulation of positive charge at the Si - SiO₂ interface as a function of photon energy. The Al bias was $V_G = -12$ V. Negative C-V shifts ($-\Delta V$) indicate positive trapped charge. The plotted shifts were scaled to give the equivalent of 1 min of illumination at an incident photon flux which produces a current of 5×10^{-11} A in the oxide for $h\nu \geq 10$ eV. The absorption length of the light in SiO₂ (L , the inverse of the absorption coefficient) is also shown (the righthand scale). "Wet" oxides were immersed in boiling deionized water, for 5 min, prior to metallization.
- Fig. 2 Hole trapping in the oxide under VUV illumination and positive bias, $V_G = 12$ V. The normalization to incident photon flux and to time of illumination are the same as in Fig. 1.
- Fig. 3 The "avalanche-injection turn-around effect." The data show the time dependence of voltage shifts of the C-V curves in samples subjected to (pulsed) avalanche-injection of electrons from the Si into the oxide. Note that positive ΔV indicates negative trapped charge. The time-averaged current through the oxide was 3×10^{-7} A and was kept constant by a continuous adjustment of V_G (42 to 54 V).
- Fig. 4 Avalanche-injection of holes from the Si (n-type) into the oxide. The currents were 3×10^{-11} A and V_G was adjusted between -42 and -55 V. The larger errors bars result from some difficulties in keeping the current constant.

TABLE I

Trapping Comparison Between Wet and Dry Oxides for

1.2×10^{16} Avalanche Injected Electrons per cm^2

	N_e (cm^{-2})	\bar{x}_e (cm) [†]
Wet	$1.37 \pm .01 \times 10^{12}$	$4.3 \pm .3 \times 10^{-6}$
Dry	$7.6 \pm .1 \times 10^{11}$	$5.1 \pm .5 \times 10^{-6}$

[†] N_e = total number of trapped electrons per unit area

\bar{x}_e = centroid of trapped electron distribution measured from

Al - SiO_2 interface.

TABLE II

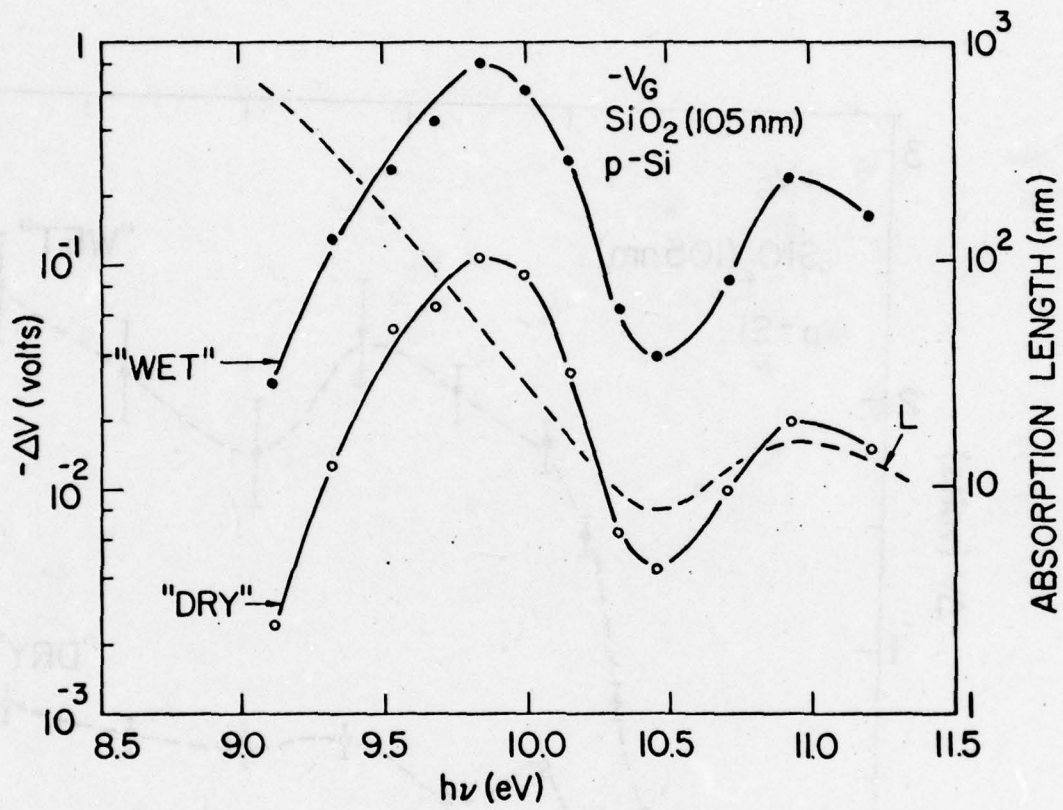
Trapping Comparison Between Wet and Dry Oxides for
 3.0×10^{17} Avalanche Injected Electrons per cm^2

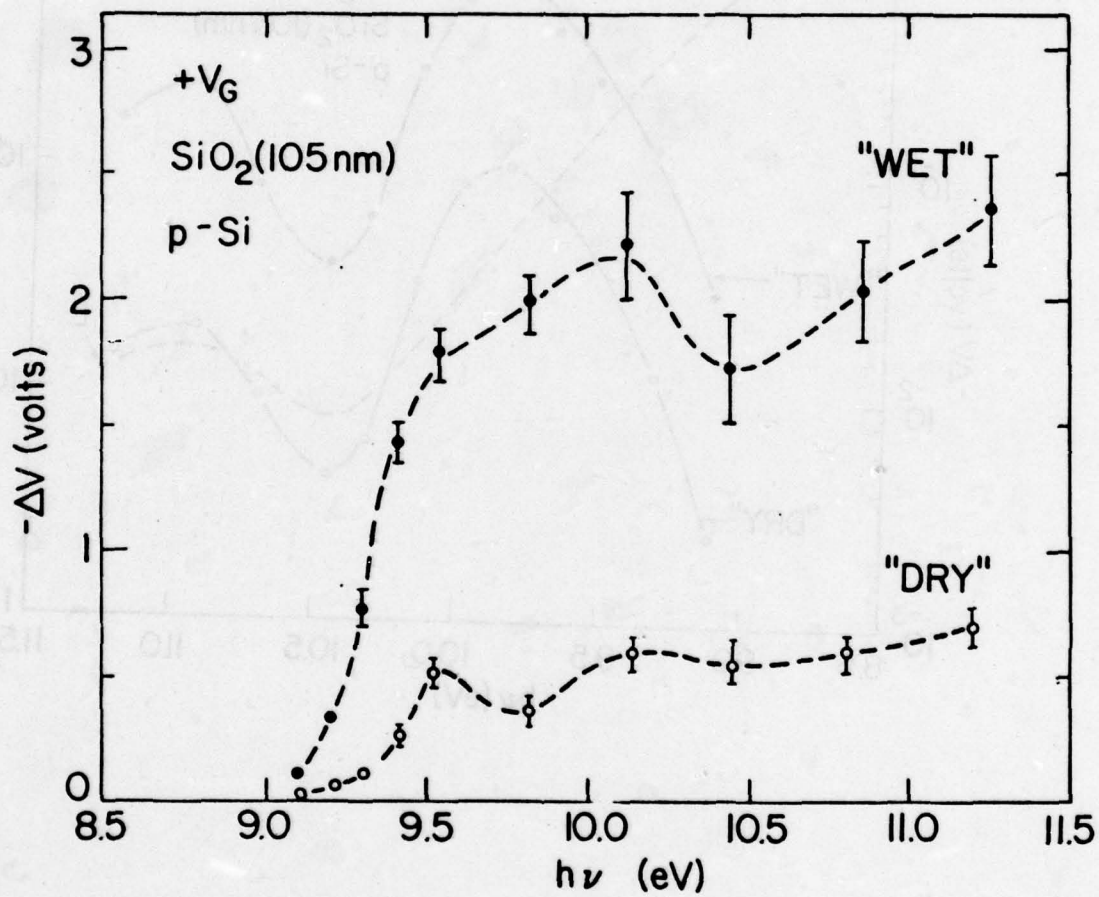
	N_e (cm^{-2})	\bar{x}_e (cm)	N_h (cm^{-2})	\bar{x}_h (cm) [†]
Wet	$9.19 \pm .02 \times 10^{12}$	$3.9 \pm .1 \times 10^{-6}$	$2.4 \pm .4 \times 10^{12}$	$1.00 \pm .05 \times 10^{-5}$
Dry	$7.82 \pm .04 \times 10^{12}$	$4.5 \pm .1 \times 10^{-6}$	$1.8 \pm .4 \times 10^{12}$	$1.00 \pm .05 \times 10^{-5}$

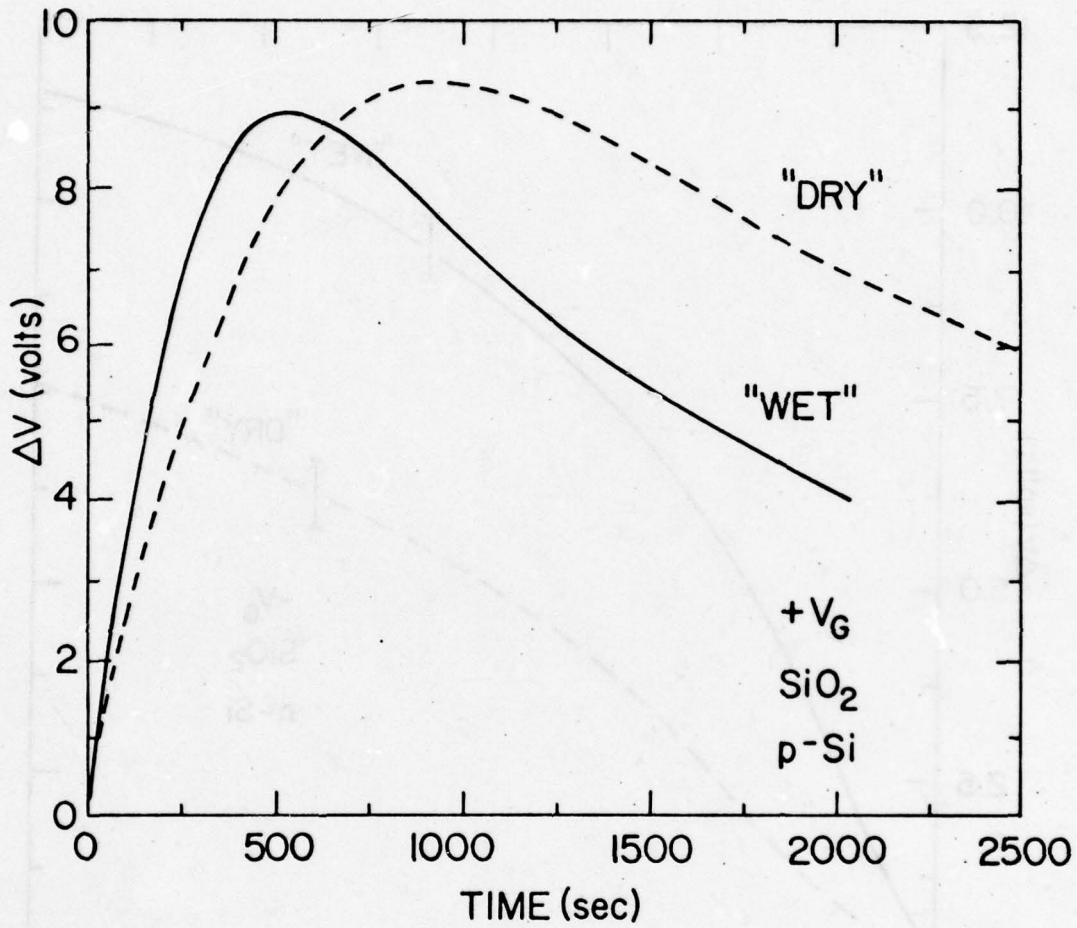
[†] N_h = total number of trapped positive charges per unit area

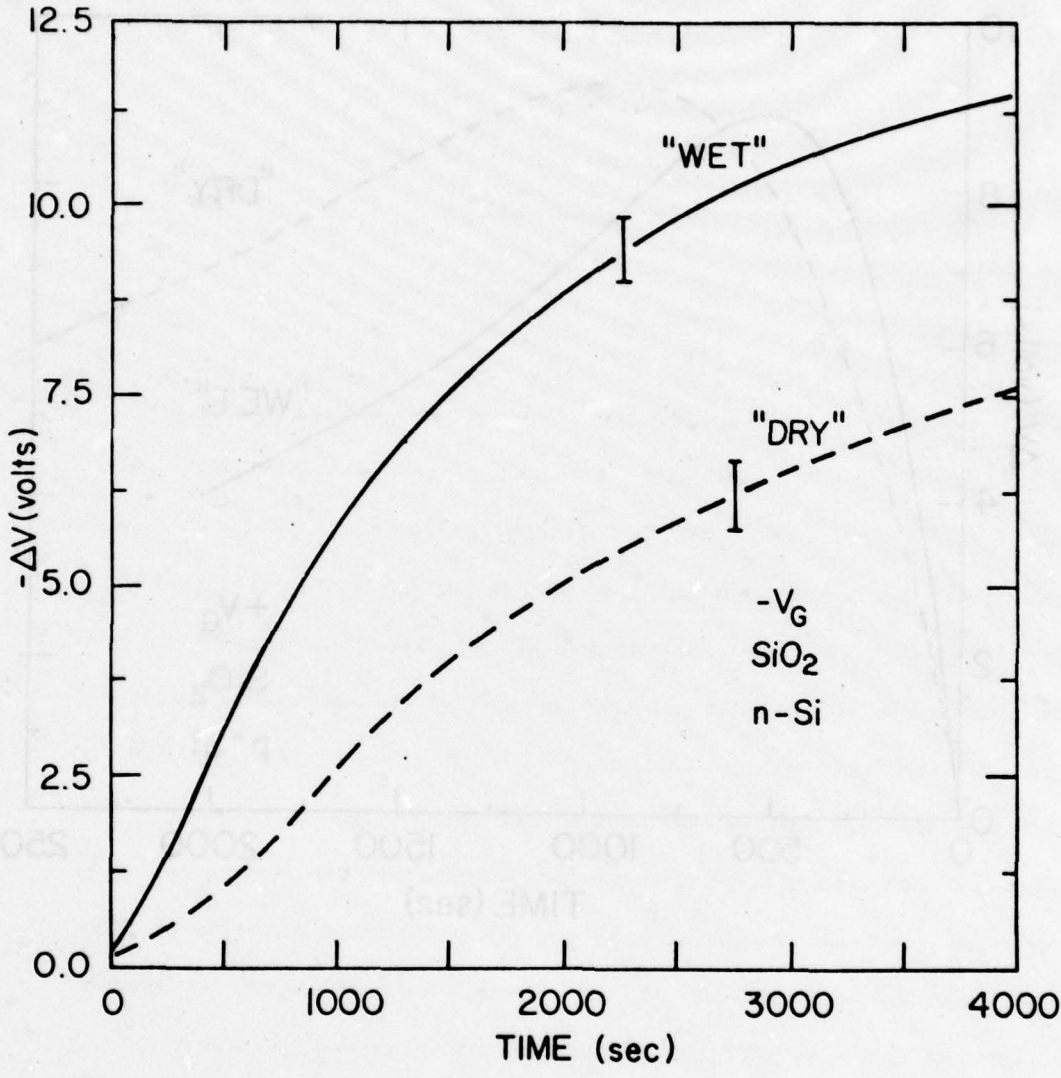
\bar{x}_h = centroid of trapped positive charge distribution measured from

Al - SiO_2 interface.









RADIATION DAMAGE IN SILICON DIOXIDE FILMS EXPOSED TO REACTIVE ION ETCHING*

by

D.J. DiMaria, L.M. Ephrath and D.R. Young
IBM Thomas J. Watson Research Center
Yorktown Heights, NY 10598

Technical Assistance of:
F.L. Pesavento, J.A. Calise, and the
Silicon Process Studies Group

Typed by Candi Brown (DD.2218)

ABSTRACT

The enhanced electron trapping characteristics and the location of this trapped charge in an SiO₂ layer exposed to either CF₄, O₂, or Ar plasmas in a Reactive Ion Etching (RIE) system are reported. Capacitance-voltage (C-V) and photocurrent-voltage (photo I-V) techniques were used to monitor charge trapping and location after the samples were incorporated into metal-oxide-semiconductor (MOS) capacitors. Using a CF₄ plasma which etches SiO₂, trapping sites caused by penetrating radiation were observed. These traps were removed by annealing at temperatures $\geq 600^\circ\text{C}$ for 30 min in N₂ prior to metallization. These bulk SiO₂ trapping sites showed no strong dependence on whether the samples were placed on the anode or cathode in the RIE chamber, implying no preferred directionality in the photons which are believed to generate them. With an O₂ or an Ar plasma which does not etch SiO₂, an additional trapping layer within about 100 Å of the exposed SiO₂ surface caused by penetration of energetic ions (≤ 400 eV) was detected. Trapping in this layer was greatly reduced by a 1000°C anneal in N₂ for 30 min, and almost entirely removed by a buffered HF dip which etches about 100 Å of SiO₂. Samples placed on the anode (ground plane) of the RIE system which would see energetic secondary electrons, but only relatively low energy ions (approximately 20 eV), also had electron trapping sites near the exposed surface; however, the trapping in this layer was greatly reduced compared with samples placed on the cathode.

* This research was supported in part by the Defense Advanced Research Projects Agency and monitored by the Deputy for Electronic Technology, RADC, under contract F19628-76-C-0249.

RADIATION DAMAGE IN SILICON DIOXIDE FILMS EXPOSED TO REACTIVE
ION ETCHING*

by

D.J. DiMaria, L.M. Ephrath and D.R. Young

IBM Thomas J. Watson Research Center

Yorktown Heights, NY 10598

ABSTRACT

The enhanced electron trapping characteristics and the location of this trapped charge in an SiO₂ layer exposed to either CF₄, O₂, or Ar plasmas in a Reactive Ion Etching (RIE) system are reported. Capacitance-voltage (C-V) and photocurrent-voltage (photo I-V) techniques were used to monitor charge trapping and location after the samples were incorporated into metal-oxide-semiconductor (MOS) capacitors. Using a CF₄ plasma which etches SiO₂, trapping sites caused by penetrating radiation were observed. These traps were removed by annealing at temperatures $\geq 600^\circ\text{C}$ for 30 min in N₂ prior to metallization. These bulk SiO₂ trapping sites showed no strong dependence on whether the samples were placed on the anode or cathode in the RIE chamber, implying no preferred directionality in the photons which are believed to generate them. With an O₂ or an Ar plasma which does not etch SiO₂, an additional trapping layer within about 100 Å of the exposed SiO₂ surface caused by penetration of energetic ions (≤ 400 eV) was detected. Trapping in this layer was greatly reduced by a 1000°C anneal in N₂ for 30 min, and almost entirely removed by a buffered HF dip which etches about 100 Å of SiO₂. Samples placed on the anode (ground plane) of the RIE system which would see energetic secondary electrons, but only relatively low energy ions

* This research was supported in part by the Defense Advanced Research Projects Agency and monitored by the Deputy for Electronic Technology, RADC, under contract F19628-76-C-0249.

(approximately 20 eV), also had electron trapping sites near the exposed surface; however, the trapping in this layer was greatly reduced compared with samples placed on the cathode.

1. Introduction

Reactive Ion Etching (RIE) is currently used in processing for silicon technology. RIE is a dry etching technique that is capable of etching densely packed micron dimension structures such as the 8K bit memory chip [1] which was based on a 1.25 micron dimension, polysilicon gate, FET technology. In RIE, wafers are loaded on an rf cathode and etched in a low pressure discharge of a gas such as CF_4 [2,3]. In this configuration, the directional etching that is required for the delineation of fine lines is observed; that is, the etch profile is nearly vertical and there is no undercut of the etch mask.

In this work, RIE induced radiation damage was studied by etching SiO_2 films in a CF_4 plasma or by exposing them to an O_2 plasma which does not etch SiO_2 but is used to strip resist and clean wafers. Trapping studies are then carried out. Traps are introduced by the impinging ions, electrons, and/or high energy photons as shown schematically in Fig. 1. The ions which have significant energies are implanted into the SiO_2 film. The atomic displacement damage caused by the ions as well as the implanted ions themselves can form trapping sites for electrons or holes [4,5]. High temperature annealing (1000°C in N_2) removes the atomic displacement damage, but trapping sites related to the implanted ions are still present [5]. Ions, electrons, and high energy photons generate positively charged traps (trapped holes) and uncharged (neutral) sites [5-9]. The trapped holes are generated when electron-hole pairs are created in the SiO_2 by ionization across the bandgap with the energetic particles or light, and some of these holes are captured from the oxide valence band into energetically deep trapping sites, near the Si- SiO_2 interface [9]. These trapped holes are removed by low temperature annealing (400°C [7]), and therefore they are not particularly a problem and will not be considered further. The neutral centers which can capture electrons are also believed to be created by the bandgap ionization process, but they are more difficult to anneal out [7,8]. They require a 600°C anneal and therefore can not be removed (as can the trapped holes) when Al electrodes or contacts are already in place [7].

The neutral traps and traps caused by or related to the implanted ions, both of which capture electrons in SiO_2 films, will be investigated here for various RIE conditions; for example, CF_4 etching of SiO_2 as compared to O_2 clean-up of hydrocarbons from the surface of etched SiO_2 . The neutral traps in the RIE samples will be shown to be introduced by photons with energies ≤ 800 eV. The similarity of these traps with bulk neutral traps induced by high energy x-rays or electron beams [6,8] will also be demonstrated. These traps cause an accelerated space charge build-up in the SiO_2 layer and lead to device degradation and failure particularly in metal-oxide-semiconductor (MOS) field effect transistors (FETs) where channel hot electron effects are present during operation [10].

In the following section, the experimental set-up for the RIE chamber will be discussed as well as the sample fabrication. Then, the experimental techniques used to study trapping and charge location will be discussed followed by the experimental results and their implications for the samples under study here.

II. Experimental

A. RIE System

The Reactive Ion Etching system used in this work is shown in Fig. 2. The substrates were loaded onto an 18 cm diameter aluminum plate. The aluminum plate was mechanically and electrically connected to the water cooled copper rf cathode. A perforated anode plate which was attached to the grounded chamber was placed 3.3 cm from the cathode in order to confine the plasma to the volume between the cathode and the anode. The anode plate did not confine the plasma completely (a weak glow was visible in the rest of the chamber), but it was used so that wafers could be monitored visually during etching and also to ensure an adequate and uniform supply of etchant in the vicinity of the wafers. The chamber was evacuated with a 6 inch oil diffusion pump and then backfilled with 40 sccm CF_4 , O_2 , or Ar to establish a dynamic pressure of 3.33 Pa (25 millitorr). During etching, 0.25 W/cm^2 is

delivered to the cathode. Under these conditions, the peak-to-peak voltage is 800 V. The dc voltage at the cathode is approximately one half of the peak-to-peak voltage [11]. The etch rate of silicon dioxide in CF_4 is about 500 Å/min. Silicon dioxide is not chemically attacked in the O_2 and Ar plasma, but it is removed by physical sputtering at a rate of about 25 Å/min.

B. Sample Preparation

Dry SiO_2 films of 1500 Å thickness were grown on boron doped, $\langle 100 \rangle$ orientation, 0.1 to 0.5 Ω-cm resistivity silicon substrates. The oxide films were then exposed to a CF_4 , O_2 or Ar plasma. The films exposed to the CF_4 plasma were etched back to approximately 1000 Å. Other films were exposed to O_2 and Ar plasmas for 1 to 10 minutes. The wafers were then cleaned to remove metals and hydrocarbons from the surface of the SiO_2 in alkali and acid peroxide solutions using a procedure similar to that used by Irene [12] but without HF. Some wafers received a buffered HF dip at this point in order to remove ~ 100 Å from the surface of the oxide. After cleaning, some wafers were annealed in a N_2 ambient for 1/2 hour. Annealing temperatures ranged from 600 to 1000°C. Circular Al dots, 135 Å in thickness and 5.2×10^{-3} cm² in area, were then evaporated in vacuum from resistively heated Ta boats or rf heated crucibles. Finally, the backs of the wafers were stripped and metallized and a forming gas anneal at 400°C for 20 minutes was carried out.

C. Techniques

To investigate the enhanced electron trapping characteristics of SiO_2 layers exposed to plasmas in an RIE system, avalanche injection [13,14] and internal photoemission [15-17] techniques were used to inject electrons from the contacts of the MOS structures into the SiO_2 . The experimental apparatus for avalanche injection [18] and internal photoemission [19] have been described in other publications. As the electrons traversed the film in the presence of an applied electric field, some of the carriers were trapped into sites created by the RIE conditions. This trapping was not particularly sensitive to the mode of carrier injection:

avalanche from the Si or internal photoemission from the Al or Si. The trapping rate was not particularly sensitive to the average field in the oxide layer which is consistent with the weak field dependence of the capture process for radiation induced neutral traps recently reported by Ning [8]. This weak field dependence is in contrast to the strong field dependence of electron capture on trapped holes [5,8,9].

The build-up of this trapped charge was sensed through the internal electric field it generates near the contacts by the capacitance-voltage (C-V) [20,21], and photocurrent-voltage (photo I-V) [9,22,23] techniques which are well described in the literature. Typical C-V and photo I-V data before and after charging of samples exposed to CF_4 or O_2 plasmas are shown in Figs. 3-8 and Figs. 9-11, respectively. The voltage shifts between the C-V curves depend on $\bar{x}Q$ where Q is the charge per unit area and \bar{x} is the charge centroid in the oxide layer measured with respect to the Al-SiO₂ interface [20,21]. The voltage shifts between photo I-V data for both positive and negative polarity allow separate determination of \bar{x} and Q [9,22]. The combination of the C-V and photo I-V techniques can also be used to separate Si-SiO₂ interface trapping from bulk SiO₂ trapping [9,22,23]. Also by studying charge build-up as a function of time, electron capture cross sections σ_c and trap densities N_t can be determined [5]. These quantities (\bar{x} , Q , σ_c , and N_t) will be used to characterize the different traps created by the exposure to RIE plasmas in the following sections. Only a very small amount of trapping was seen for the charging conditions used on samples fabricated in an identical manner, but not exposed to RIE (for example, see Fig. 12).

III. Results and Discussion

A. CF₄ Plasma

C-V and photo I-V data characteristic of SiO₂ films etched in a CF₄ plasma with the samples placed on the cathode are shown in Figs. 3-8 before and after some of the trapping sites were charged by internal photoemission or avalanche injection. The C-V flat-band voltage shift [20,21] and the average photo I-V voltage shifts for positive and negative gate polarity [9,22] are recorded in the figure captions. This data is characteristic of a bulk SiO₂ negative trapped charge distribution with some slight increase in trapping near the Al-SiO₂ interface [22,23]. From the values for the average positive and negative photo I-V shifts (ΔVg^+ and ΔVg^- , respectively) and the photo I-V relationship $\bar{x}/L = (1 - \Delta Vg^- / \Delta Vg^+)^{-1}$ where L is the total oxide thickness, a value indicative of bulk oxide charge ($\bar{x}/L \lesssim 0.5$) is obtained as listed in the figure captions. Comparison of Figs. 3-5 and Figs. 6-8 show that the centroid of the trapped charge distribution is independent of the injecting interface and the number of injected carriers.

Fig. 12 shows the trapped electronic charge build-up in the SiO₂ layer as a function of the number of injected electrons for a sample etched in CF₄ as compared to a sample from the same batch that was not exposed to RIE. Clearly the etched film shows enhanced trapping. This type of data was used to determine the capture cross sections and the trap densities reported here using well established procedures [5]. The electron capture cross sections for those traps have values between 10^{-14} – 10^{-17} cm² with trap densities varying between 10^9 – 10^{11} cm⁻². The traps could be removed by a 600°C premetallization anneal in N₂ for 1/2 hr.

All these characteristics seen on samples subjected to RIE with CF₄ are very similar to those seen in trapping studies on the neutral traps introduced into the SiO₂ with 20-keV x-rays or 25 keV electrons where the x-rays or electrons would uniformly penetrate the oxide layer before being absorbed in the underlying Si substrate [6-8,24]. Note the similarity of the data

of Fig. 12 with Fig. 2 of Reference 4 and Fig. 2 of Reference 5 where clearly the radiation induced neutral traps start to fill after at least 10^{14} electrons/cm² have been injected.

As mentioned previously, a series of experiments were performed to verify that CF₄ RIE samples had the same trapping and charge centroid characteristics as MOS structures exposed to a penetrating electron beam. After exposure of MOS structures with 525 Å and 1095 Å thick dry SiO₂ layers, positively charged trapped holes were removed with an anneal at 400°C in forming gas for 20 min so that the radiation induced neutral-centers could be studied separately. Figs. 13-15 show C-V and photo I-V data for neutral centers generated by $\geq 10^{22}$ electrons/cm² from a 20 keV electron beam. These data show for the first time that the radiation induced neutral center first reported by Aitken et al. [6-8] is a bulk SiO₂ trapping site. \bar{x}/L is approximately 0.5, independent of oxide thickness. Note the similarity of Figs. 13-15 with Figs. 3-8. If the radiation induced neutral traps are related to the bandgap ionization process as speculated [5], subtle differences in the \bar{x}/L ratio between the CF₄ RIE and e-beam irradiated samples are expected due to differences in the absorption coefficient of SiO₂ for the photon energies involved in the RIE process (≤ 800 eV) and for the electron energy involved in the e-beam exposure (20 keV). The high energy e-beam induced neutral traps should have a larger value of \bar{x}/L because the electrons penetrate more deeply. This is seen experimentally (see figure captions for Figs. 5, 8, and 15). The electron capture cross sections (from 10^{-14} to 10^{-18} cm² [6-8]) for the e-beam irradiated samples were very similar to the CF₄ RIE samples. As can be seen in Figs. 13-15, there is no noticeable dependence of the charge centroid on the extent of the number of filled traps which implies that all the different cross section traps have the same spatial distributions. This observation is also similar for CF₄ RIE samples (See Figs. 3-8). After the first charging in Figs. 13-15, all traps with capture cross sections $\geq 10^{-16}$ cm² were filled; and after the second charging all traps with capture cross sections, $\geq 10^{-18}$ cm² were filled. A control sample, which was from the same wafer but not e-beam irradiated, charged under similar conditions to those in Figs. 13-15 trapped $\leq 25\%$ of the total negative bulk charge found in the e-beam irradiated

samples. The traps in the control sample are the well known water related sites [5] with a centroid location of also ≈ 0.5 of the oxide thickness.

The etching action of the CF_4 plasma seems to be removing most of the ion implanted region near the exposed SiO_2 surface which is seen on samples exposed to O_2 or Ar plasmas as discussed in the next section. The only trapping sites apparently created during RIE in CF_4 are those caused by some form of penetrating radiation which in this case must be photons with energies less than 800 eV. Electrons with energies ≤ 800 eV which are attainable during the negative portion of the rf cycle would not penetrate very deeply into the SiO_2 layer [25].

A series of experiments designed to test if the radiation in the RIE chamber had a strong directional dependence were also performed. Here SiO_2 samples were placed on the anode (ground plane) and cathode of the RIE system and exposed to a CF_4 plasma which would etch approximately 500 Å of SiO_2 from the sample placed on the cathode (1 min exposure). Samples placed on the anode were not etched significantly. Also, one of the samples placed on the anode had about 100 Å of SiO_2 removed with buffered HF after CF_4 plasma exposure. No pronounced differences were seen in the electron trapping characteristics and charge location of these samples, implying an absence of any preferred directionality of the photons creating the neutral trapping sites.

B. O_2 or Ar Plasma

Samples placed on the cathode and exposed to an O_2 or an Ar plasma displayed C-V and photo I-V characteristics after electron charging like those in Figs. 9-11. Another gas (Ar) besides O_2 which does not etch SiO_2 was used to determine the effect on trapping caused by the type of gas plasma. These data in Figs. 9-11 are characteristic of strong trapping predominantly in a layer close to the exposed surface [9,22]. This trapping layer was created by low energy (less than 400 eV) ion implantation into the SiO_2 of the positively charged ions generated in the RIE chamber. From the photo I-V relationship and the values given for the

average value of ΔVg^+ and the maximum observed value of ΔVg^- , the centroid \bar{x} for the data of Figs. 9-11 is within approximately 100 Å of the exposed surface. The electron capture cross sections for these sites have values ranging from about 10^{-14} to 10^{-18} cm² with trap densities $>10^{13}$ cm⁻². These are very efficient trapping centers with an initial capture probability (product of the capture cross section and number of traps per unit area [5]) of $>50\%$. The trapping probability was deduced by measuring the ratio of the build-up of the number of trapped charges determined from C-V or photo I-V voltage shifts to the number of injected electrons from the Si substrate [5]. The numbers for the trapping probability were also independently confirmed by comparing the current measured in the external circuit for photoinjection from the Al electrode on identical samples with and without the O₂ plasma induced traps which are near the Al-SiO₂ interface. Because of the high capture probability, the numbers determined for the capture cross sections reported here which assume an approximately spatially constant current density flowing through the trapping region must be regarded with a certain amount of caution. These numbers for the cross sections are used here only as a *guide in comparing trapping on these sites to other known trapping centers*. Trapping on neutral bulk sites (as in the case with CF₄) was also occurring, however this could be separated from the larger amount of trapping in the ion implanted region.

No strong dependence on the gas (O₂ or Ar) or the time of exposure (1-10 minutes) of the trapping in this ion implanted layer was seen. The lack of the dependence of charge trapping on the gas used in the RIE system (O₂ or Ar) indicates that most of these sites are caused by the atomic displacement damage created by the impinging ions. The lack of dependence on time suggests that this damage must saturate in a short period of time due to the heavy bombardment of energetic ions. The number of positive ions incident on the sample in 1 min could be as large as 2.3×10^{17} cm⁻² for 0.25 W/cm² delivered to the cathode with a dark space dc voltage drop of ≈ 400 V. Samples exposed to O₂ and annealed prior to metallization at 1000°C in N₂ for 1/2 hr. showed greatly reduced trapping in the implanted region. This is characteristic of films ion implanted with impurities such as Al, As, and P where it is

believed from experimental evidence that this annealing treatment removes the displacement damage and the resulting electron trapping is mostly characteristic of the implanted ion [5,18].

In some cases, the chemical surface cleaning step after RIE which removes metals and hydrocarbons was omitted on samples exposed to CF_4 and O_2 plasmas. This resulted in a further increase in trapping very near the exposed surface and suggests the need for this step in processing. If a sample exposed to O_2 was given a buffered HF dip to remove about 100 Å of SiO_2 , the trapping associated with the ion implanted region is no longer present as expected, but the bulk radiation induced neutral traps are still present.

Samples placed on the anode of the RIE system in an O_2 plasma for 10 min. showed greatly reduced electron trapping in a layer close to the exposed surface. Here electrons and very low energy ions (less than 20 eV) in addition to photons strike the surface. Part of the trapping in this surface layer could be due to neutral traps created by the impinging electrons which are strongly absorbed.

IV Conclusions

The importance of trapping sites generated by CF_4 RIE or by O_2 clean-up of SiO_2 layers in RIE systems has been demonstrated. The small amount of trapping (trap densities of $\approx 10^{11} \text{ cm}^{-2}$) seen in CF_4 etched films can be removed with a 600°C anneal prior to metallization. These bulk oxide traps can not be removed by chemical etching of a surface layer of the oxide. SiO_2 films that are exposed to O_2 plasmas (used to strip resist and remove hydrocarbons from the SiO_2 surface by CO_2 evolution) showed a high density of traps near the exposed surface due to damage from implanted ions from the plasma. This trapping layer could be effectively removed by chemical etching about 100 Å of the SiO_2 layer with buffered HF. However, it is preferable to clean wafers and strip resist in a plasma asher. There are commercially available barrel type reactors in which ion energies are approximately 20 eV as compared to ion energies as large as 400 eV in the RIE system used in this study. Some trapping still occurs in this

surface layer even after high temperature annealing at 1000°C. The chemical surface cleaning of plasma exposed films was shown to be important in removing a possible layer of hydrocarbons and metals which are believed to contribute to additional trapping when this cleaning is absent.

The results reported here are for worst case damage of SiO₂ during RIE. In a usual processing sequence for delineating the gate, the oxide is shielded by the gate electrode material except at the edges of the gate oxide. It would be necessary in the future to evaluate edge effects and the degree of shielding by the gate electrode with a particular device and processing sequence in mind. If proper high temperature annealing can not be carried out after RIE processing of more realistic structures containing SiO₂ layers (for example, MOS-FETs) where metal layers are already present prior to RIE, then other means of removing the traps must be found. One such possible means might be rf annealing recently described by T.-P. Ma and W. H.-L. Ma [26].

Acknowledgements

The authors wish to acknowledge the critical reading of this manuscript by R.F. DeKeersmaecker and M.I. Nathan; the experimental assistance of F.L. Pesavento and J.A. Calise; the sample preparation by the Silicon Process Studies Group; and the assistance of J.M. Aitken in preparing the electron beam irradiated samples.

References

- 1.) H.N. Yu, R.H. Dennard, T.H.P. Chang, C.M. Osburn, V. DiLonardo, and H.E. Luhn, J. Vac. Sci. Technol. 12, 1197 (1975).
- 2.) G. Schwartz, L.B. Zielinski and T. Schopen, in Etching for Pattern Definition, ed. by H.G. Hughes and M.J. Rand (the Electrochemical Society, Inc., Princeton, N.J., 1976), p. 122.
- 3.) L.M. Epharth, J. Electron. Mat. 7, 415 (1978).
- 4.) N.M. Johnson, W.C. Johnson, and M.A. Lampert, J. Appl. Phys. 46, 1216 (1975).
- 5.) D.J. DiMaria, in Proceedings of the International Topical Conference on the Physics of SiO₂ and Its Interfaces, ed. by S.T. Pantelides (Pergamon Press, New York, 1978), p. 160 and references therein.
- 6.) J.M. Aitken and D.R. Young, J. Appl. Phys. 47, 1196 (1976).
- 7.) J.M. Aitken, D.R. Young, and K. Pan, J. Appl. Phys. 49, 3386 (1978).
- 8.) T.H. Ning, J. Appl. Phys. 49, 4077 (1978).
- 9.) D.J. DiMaria, Z.A. Weinberg, and J.M. Aitken, J. Appl. Phys. 48, 898 (1977), and references therein.
- 10.) T.H. Ning, C.M. Osburn, and H.N. Yu, J. Electron. Mat. 6, 65 (1977).
- 11.) H.R. Koenig and L.I. Maissel, IBM J. Res. Develop. 14, 168 (1970).
- 12.) E.A. Irene, J. Electrochem. Soc. 121, 1613 (1974).
- 13.) A. Goetzberger and E.H. Nicollian, J. Appl. Phys. 38, 4582 (1967).
- 14.) E.H. Nicollian and C.N. Berglund, J. Appl. Phys. 41, 3052 (1970).
- 15.) R. Williams, Phys. Rev. 140, A569 (1965).
- 16.) B.E. Deal, E.H. Snow, and C.A. Mead, J. Phys. Chem. Solids 27, 1873 (1966).
- 17.) A.M. Goodman, Phys. Rev. 144, 588 (1966).
- 18.) D.R. Young, D.J. DiMaria, and W.R. Hunter, J. Electron. Mater. 6, 569 (1977).
- 19.) D.J. DiMaria and P.C. Arnett, IBM J. Res. Dev. 21, 227 (1977).

- 20.) A.S. Grove, Physics and Technology of Semiconductor Devices (Wiley, New York, 1967), Chap. 9.
- 21.) S.M. Sze, Physics of Semiconductor Devices (Wiley-Interscience, New York, 1969), Chap. 9.
- 22.) D.J. DiMaria, J. Appl. Phys. 47, 4073 (1976).
- 23.) R.J. Powell and C.N. Berglund, J. Appl. Phys. 42, 4390 (1971).
- 24.) J.M. Aitken, 20th Electron. Mat. Conf., Santa Barbara, California, June 1978, Abstract No. L-3, unpublished.
- 25.) J.P. Mitchell and P.K. Wilson, Bell Syst. Tech. J. 46, 1 (1967).
- 26.) T-P. Ma and W. H-L. Ma, Appl. Phys. Lett. 32, 441 (1978).

Figure Captions

- Fig. 1: Energy band diagram for thermal SiO₂ layer on an underlying Si substrate exposed to low energy positive ions and photons which are present in an RIE system.
- Fig. 2: Schematic diagram of RIE system used in this series of experiments.
- Fig. 3: High frequency (1 MHz) capacitance as a function of gate voltage before (solid line) and after (broken line) partial electronic charging of some of the radiation induced neutral traps in the bulk of the SiO₂ layer. The oxide layer of this sample was etched from 1500 Å to 860 Å in a CF₄ plasma. Approximately 2.5×10^{14} electrons/cm² were injected into the SiO₂ layer by internal photoemission from the Al electrode. This sample only had a 400°C, 20 min., forming gas anneal after metallization. The flat-band voltage shift due to charging is $\Delta V_{FB} = 0.3 \pm 0.1$ V.
- Fig. 4: Current measured in the external circuit for 5 eV light as a function of positive gate voltage (Si-injecting) for the same sample before and after charging as in Fig. 3. The solid circles represent the as-fabricated structure and the open circles represent the same sample after partial charging. The lines connecting the data points are visual aids only. The average positive photo I-V shift between these curves is $\Delta V_g^+ = 0.4 \pm 0.1$ V.
- Fig. 5: Current measured in the external circuit for 4.5 eV light as a function of negative gate voltage (Al-injecting) for the same sample before and after charging as in Fig. 3. The average negative photo I-V shift between these curves is $\Delta V_g^- \approx -0.6 \pm 0.2$ V. The centroid determined from the photo I-V voltage shifts is 345 ± 120 Å.
- Fig. 6: High frequency (1 MHz) capacitance as a function of gate voltage before and after charging of the radiation induced neutral traps in the bulk of the SiO₂ of a sample similar to that used in Fig. 3. The oxide layer of this sample was

etched from 1500 Å to 945 Å in a CF₄ plasma. Approximately 4×10^{15} electrons/cm² were avalanche injected into the SiO₂ layer from the Si substrate. The flat-band voltage shift due to charging is $\Delta V_{FB} = 1.0 \pm 0.1$ V.

Fig. 7: Current measured in the external circuit for 5 eV light as a function of positive gate voltage (Si-injecting) for the same sample before and after charging as in Fig. 6. The average positive photo I-V shift between these curves is $\Delta V_g^+ = 1.0 \pm 0.1$ V.

Fig. 8: Current measured in the external circuit for 4.5 eV light as a function of negative gate voltage (Al-injecting) for the same sample before and after charging as in Fig. 6. The average negative photo I-V shift between these curves is $\Delta V_g^- = -1.7 \pm 0.1$ V. The centroid determined from the photo I-V voltage shifts is 350 ± 35 Å.

Fig. 9: High frequency (1 MHz) capacitance as a function of gate voltage before and after partial electronic charging of some of the radiation induced neutral traps in the bulk of the SiO₂ layer and traps near the exposed oxide surface caused by damage due to the ion implantation of oxygen. The oxide layer of this sample was exposed to an O₂ plasma for 10 min after which the SiO₂ was 1455 Å thick. This sample was charged under approximately the same conditions as in Fig. 3. This sample had only a 400°C, 20 min., forming gas anneal after metallization. The flat-band voltage shift due to charging is $\Delta V_{FB} = 0.4 \pm 0.1$ V.

Fig. 10: Current measured in the external circuit for 5 eV light as a function of positive gate voltage (Si-injecting) for the same sample before and after charging as in Fig. 9. The average positive photo I-V shift between these curves is $\Delta V_g^+ = 0.6 \pm 0.1$ V.

Fig. 11: Current measured in the external circuit for 4.5 eV light as a function of negative gate voltage (Al-injecting) for the same sample before and after

charging as in Fig. 9. The maximum negative photo I-V shift between these curves is $\Delta V_{gmax}^- \geq -8$ V. The maximum centroid determined from the photo I-V voltage shifts is 100 ± 15 Å.

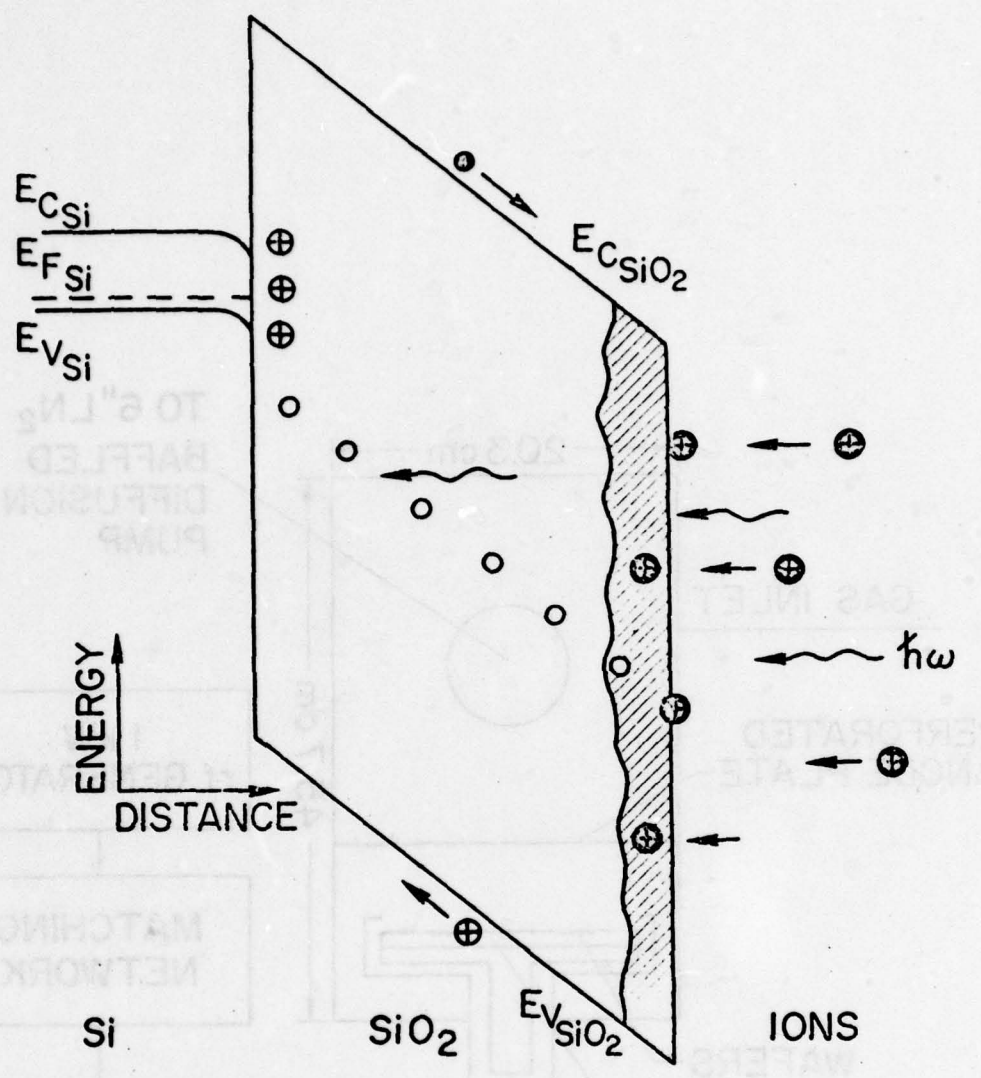
Fig. 12: The number of negative charges per unit area as a function of the number of injected electrons for a control and a sample similar to that used in Fig. 3. An avalanche current of 2×10^{-10} A was used to charge the traps. The control RIE2F had the same processing as RIE2B except for the CF_4 exposure. The negative charge trapping in RIE2B is due to the radiation induced neutral centers, while that in RIE2F is due to the neutral centers normally present in the oxide layer.

Fig. 13: High frequency (1 MHz) capacitance as a function of gate voltage before (solid line) and after (broken and dot-dash lines) electronic charging of radiation induced neutral traps. The 525 Å thick oxide layer of this sample was exposed to a 20 keV electron beam with a fluence of $\geq 10^{22}$ electrons/cm². The MOS structure was annealed at 400°C for 20 min. in forming gas after exposure. The 1st and 2nd charging correspond to the MOS sample after avalanche injection of 1.25×10^{16} and 1.5×10^{17} electrons/cm² from the Si substrate. The flat-band voltage shifts with respect to the uncharged virgin sample for the first partial trap charging and the additional second trap charging are $\Delta V_{FB} = 0.5 \pm 0.1$ V and 2.0 ± 0.1 V, respectively.

Fig. 14: Current measured in the external circuit for 5 eV light as a function of positive gate voltage (Si-injecting) for the same sample before and after charging as in Fig. 13. The average positive photo I-V shifts with respect to the uncharged virgin sample for the first charging (open circles) and the second charging (open triangles) are $\Delta V_g^+ = 0.5 \pm 0.1$ V and 2.1 ± 0.1 V, respectively.

Fig. 15: Current measured in the external circuit for 4.5 eV light as a function of negative gate voltage (Al-injecting) for the same sample before and after

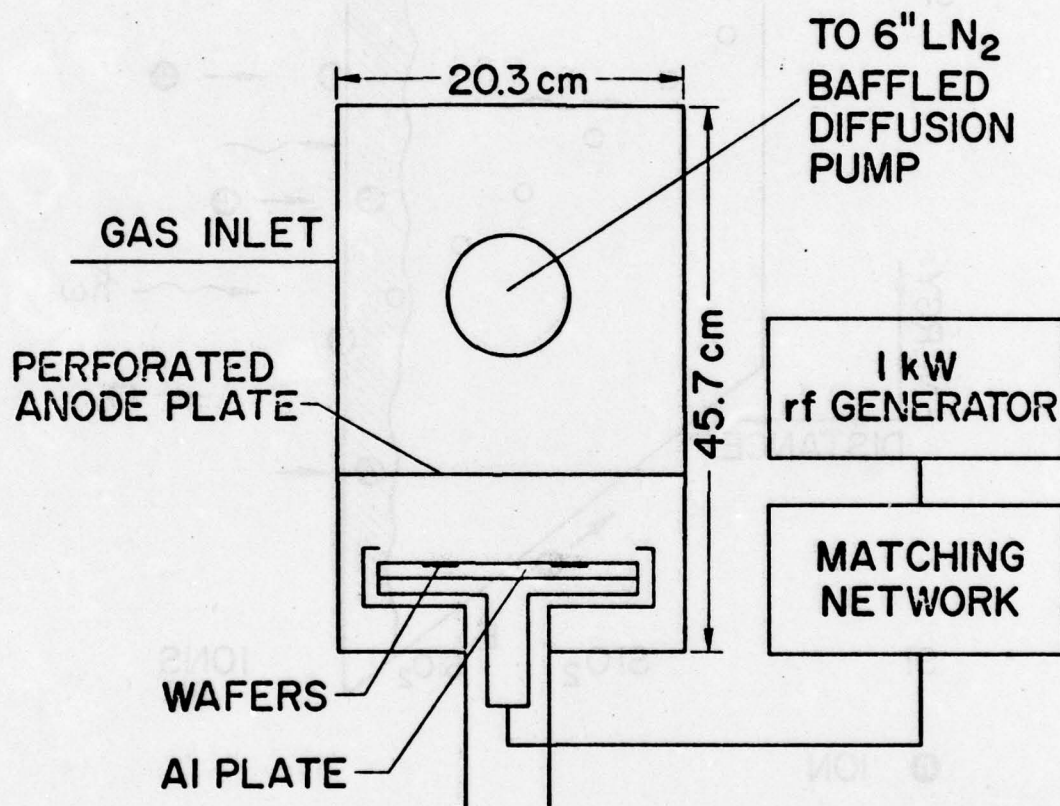
charging as in Fig. 13. The average negative photo I-V shifts with respect to the uncharged virgin sample for the first charging and second charging are $\Delta V_g^- = -0.4 \pm 0.1$ V and -2.0 ± 0.1 V, respectively. The centroids determined from the photo I-V voltage shifts are 290 ± 60 Å for the first charging and 270 ± 15 Å for the second charging.

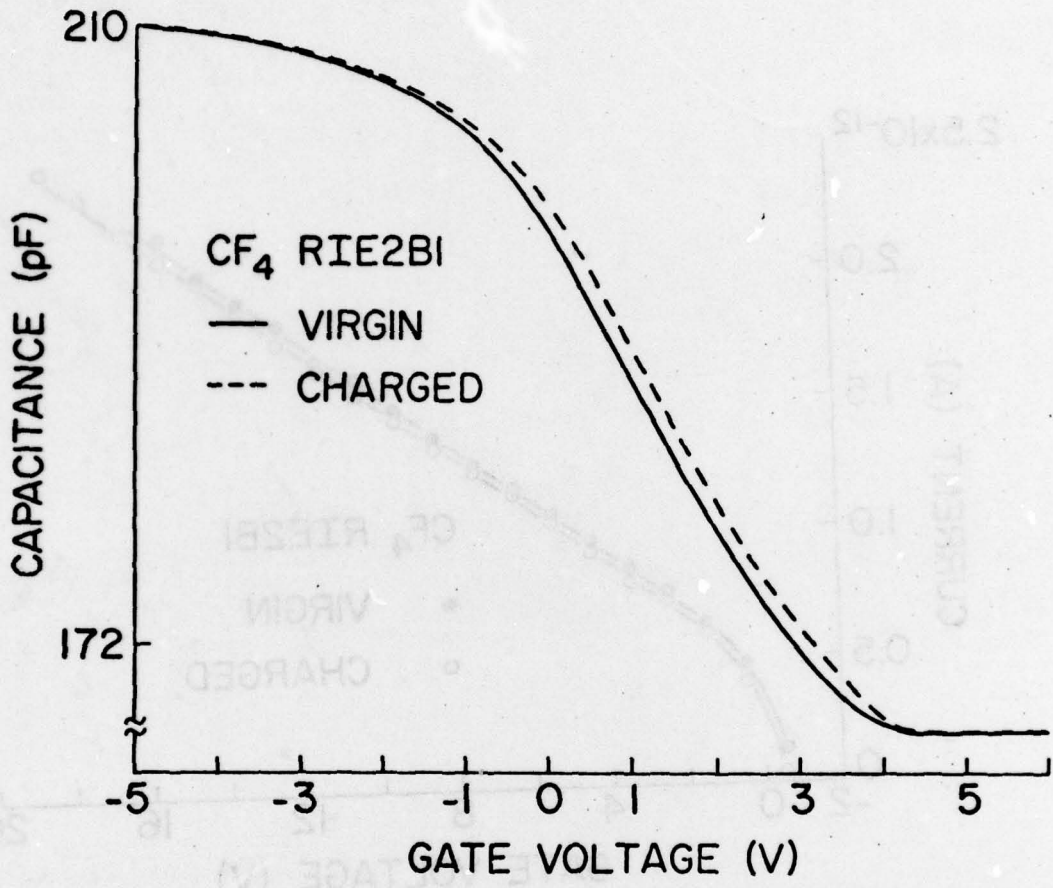


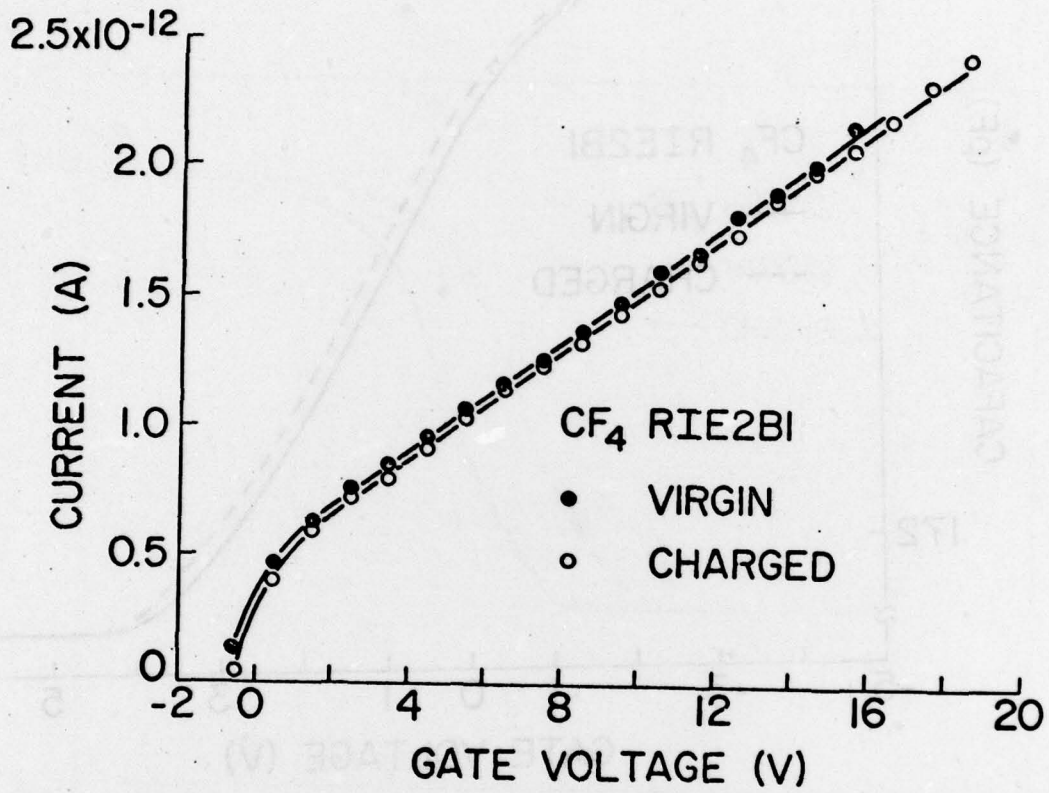
ENERGY
DISTANCE

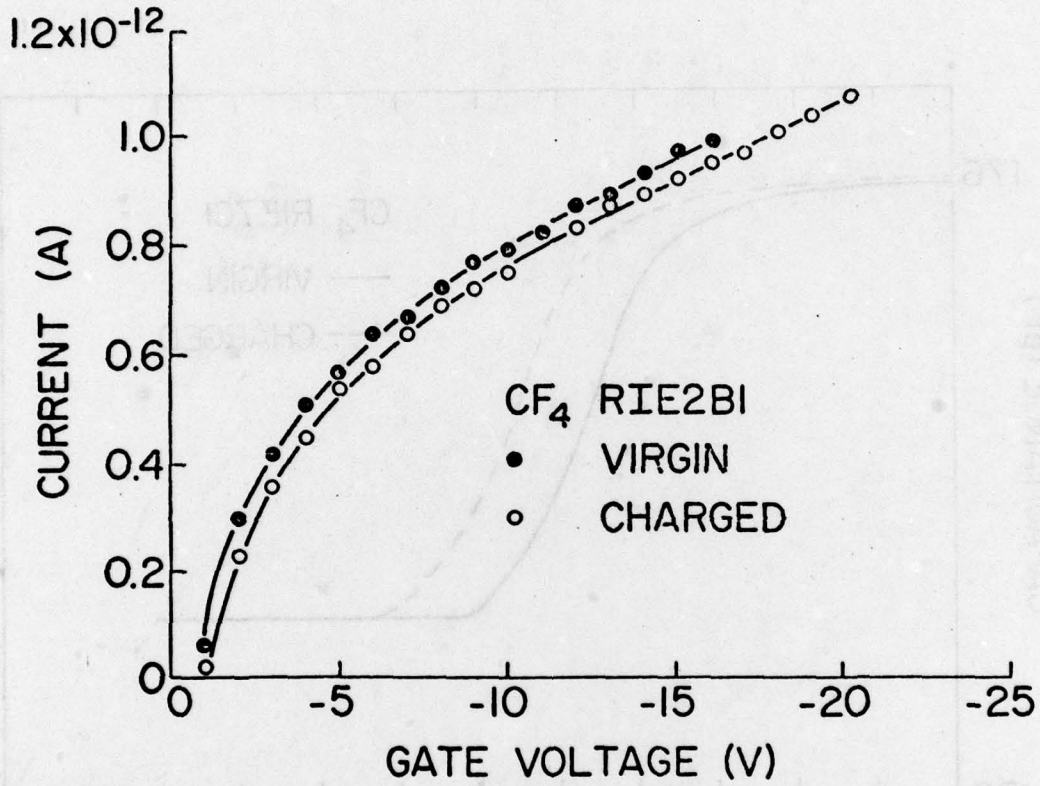
Si SiO₂ IONS

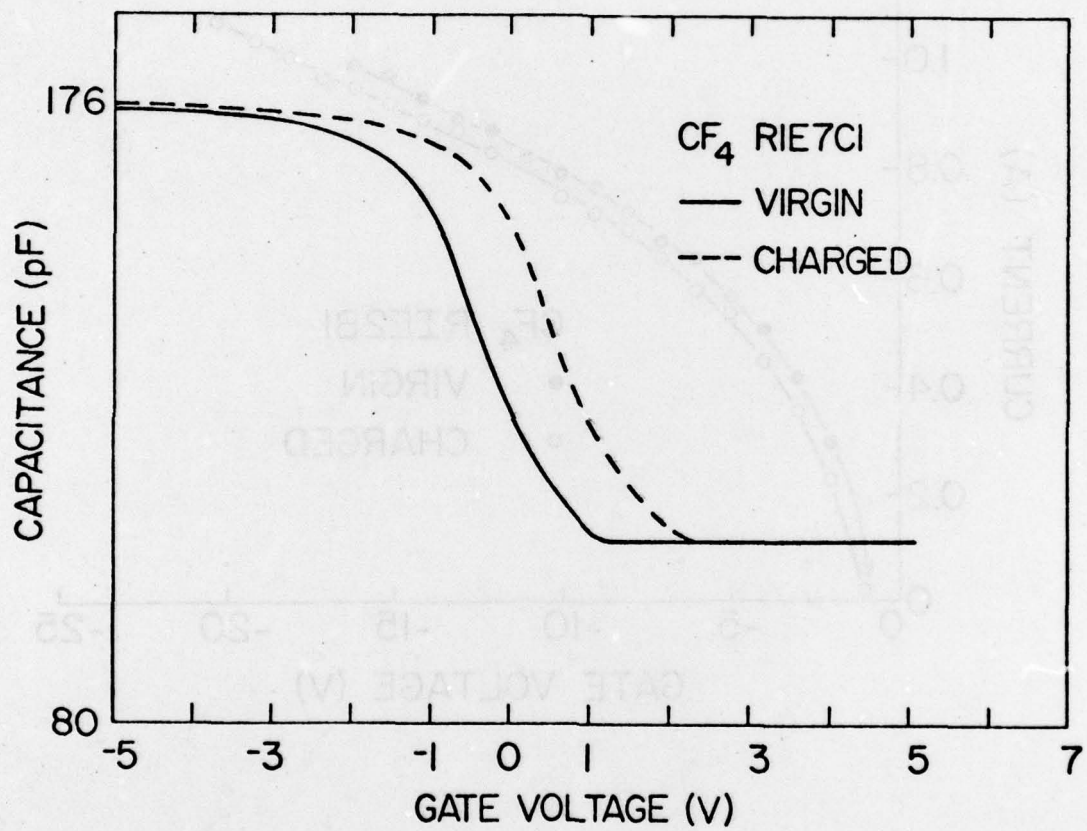
- ⊕ ION
- NEUTRAL TRAP
- ⊕ HOLE
- ELECTRON
- ////// DAMAGE
- ~> PHOTON

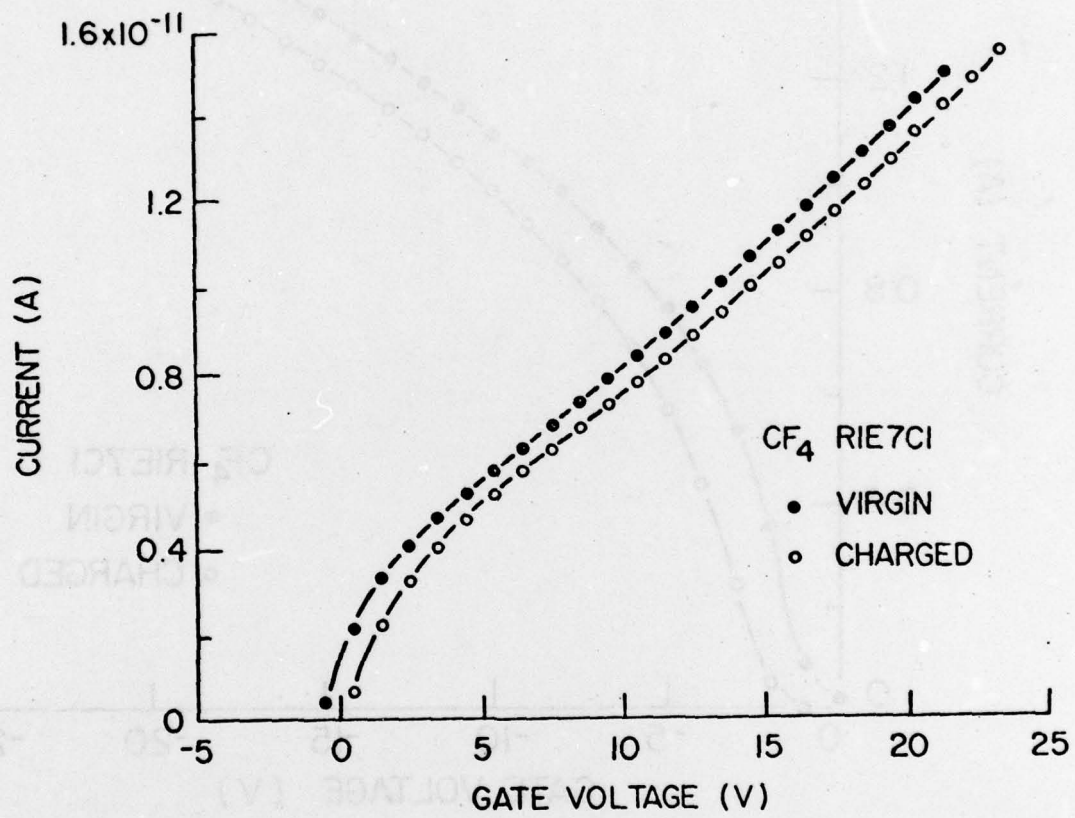


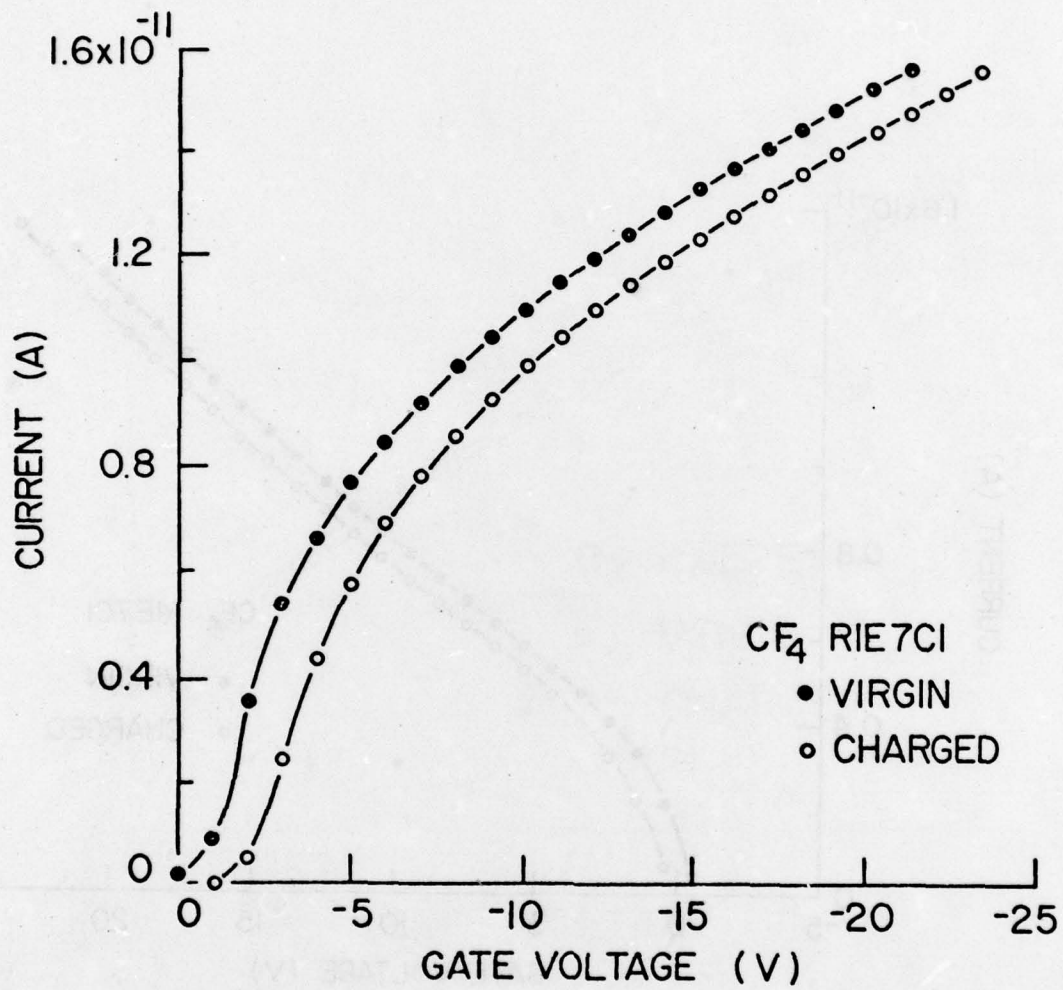


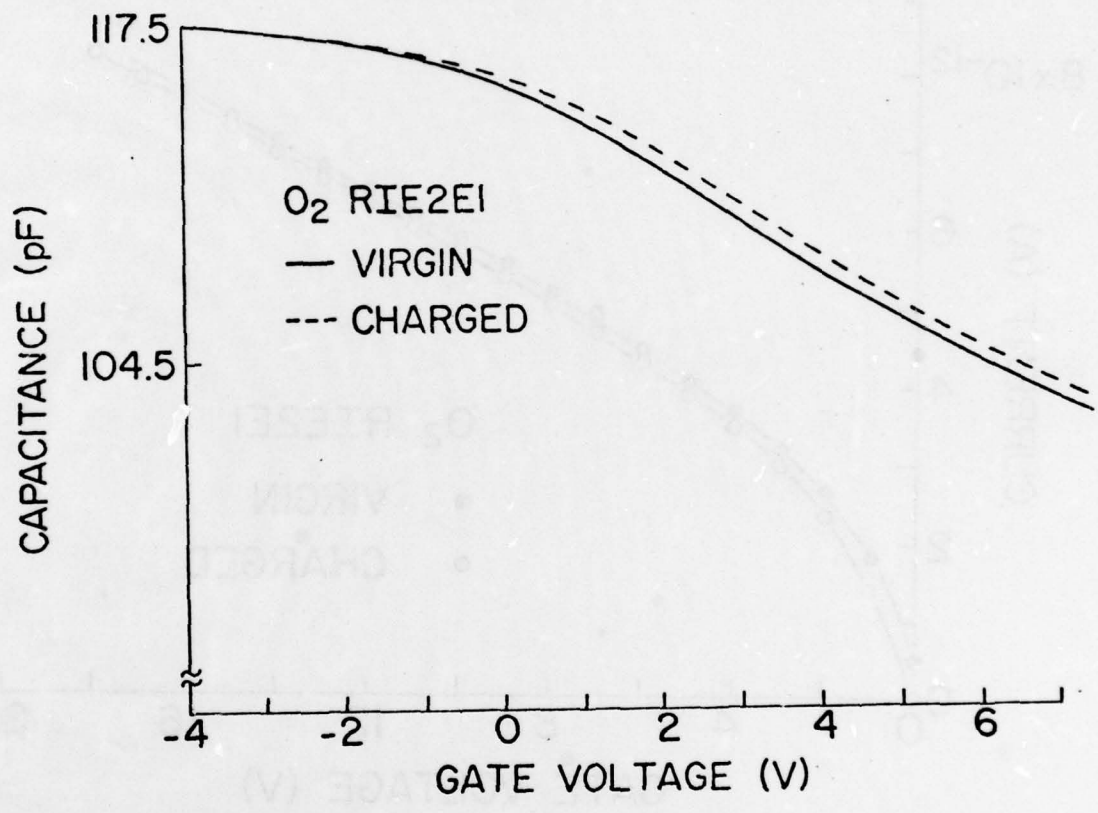


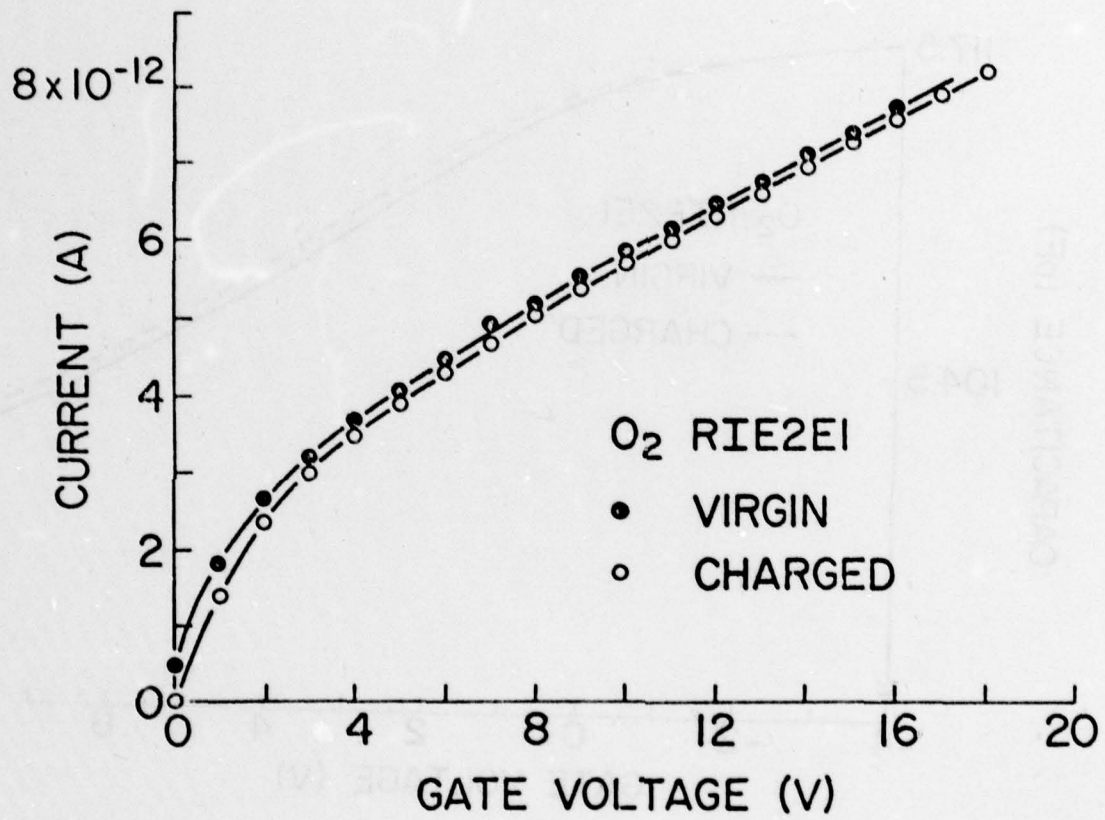


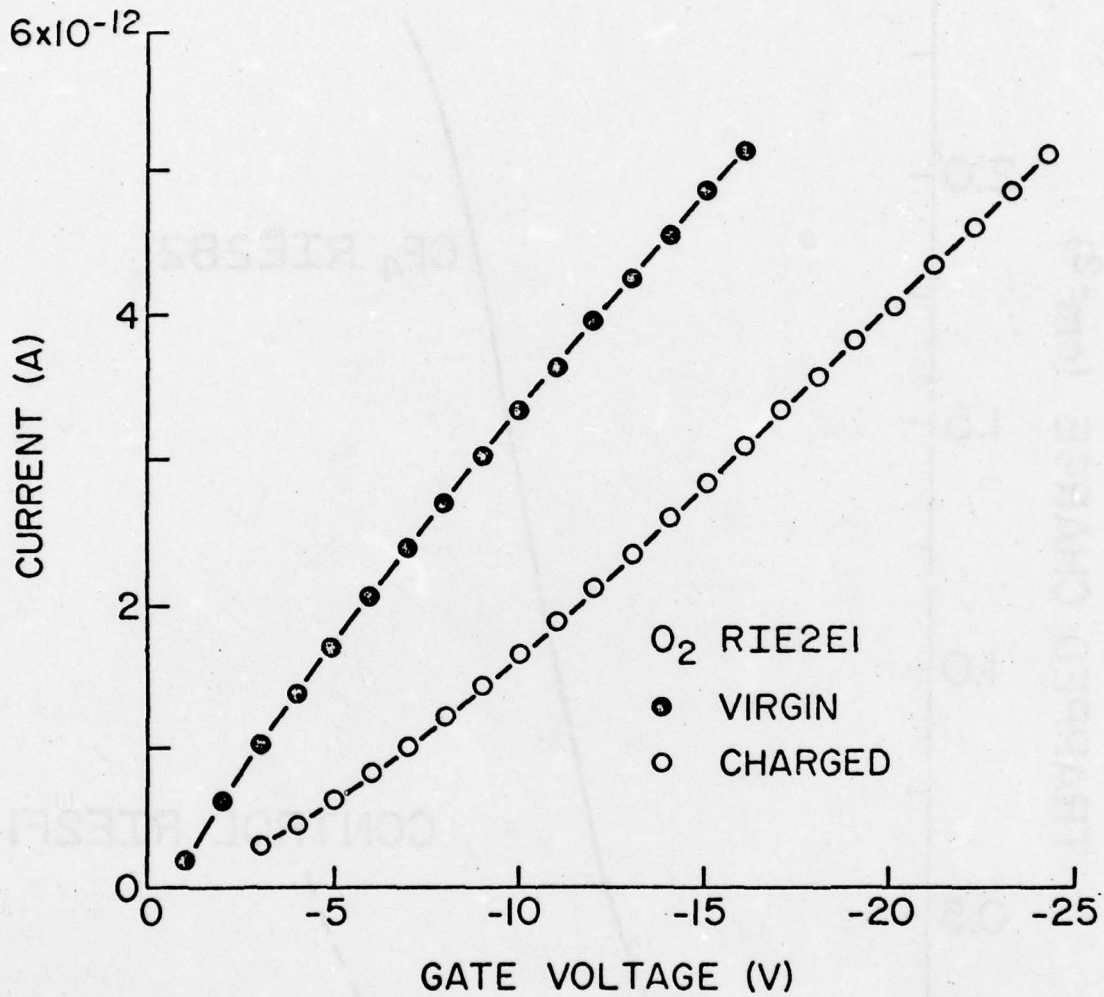


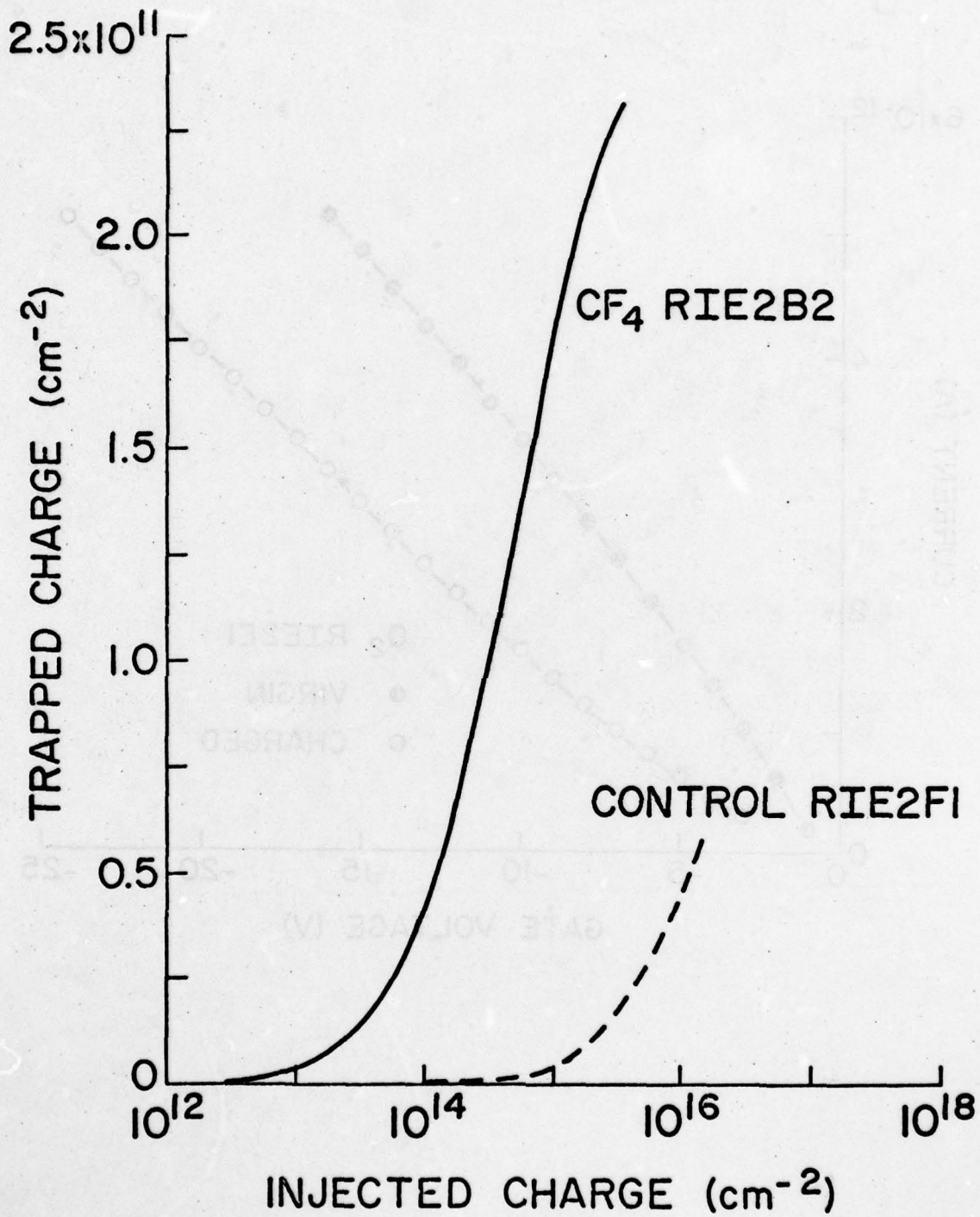


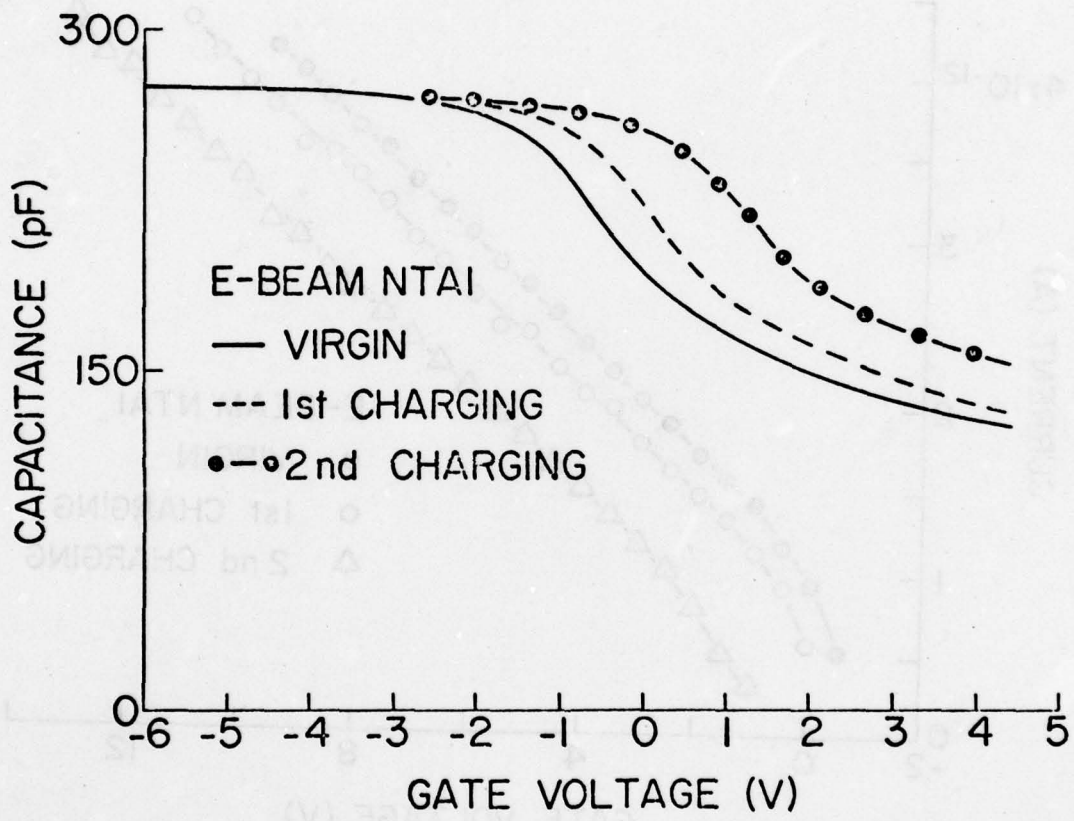


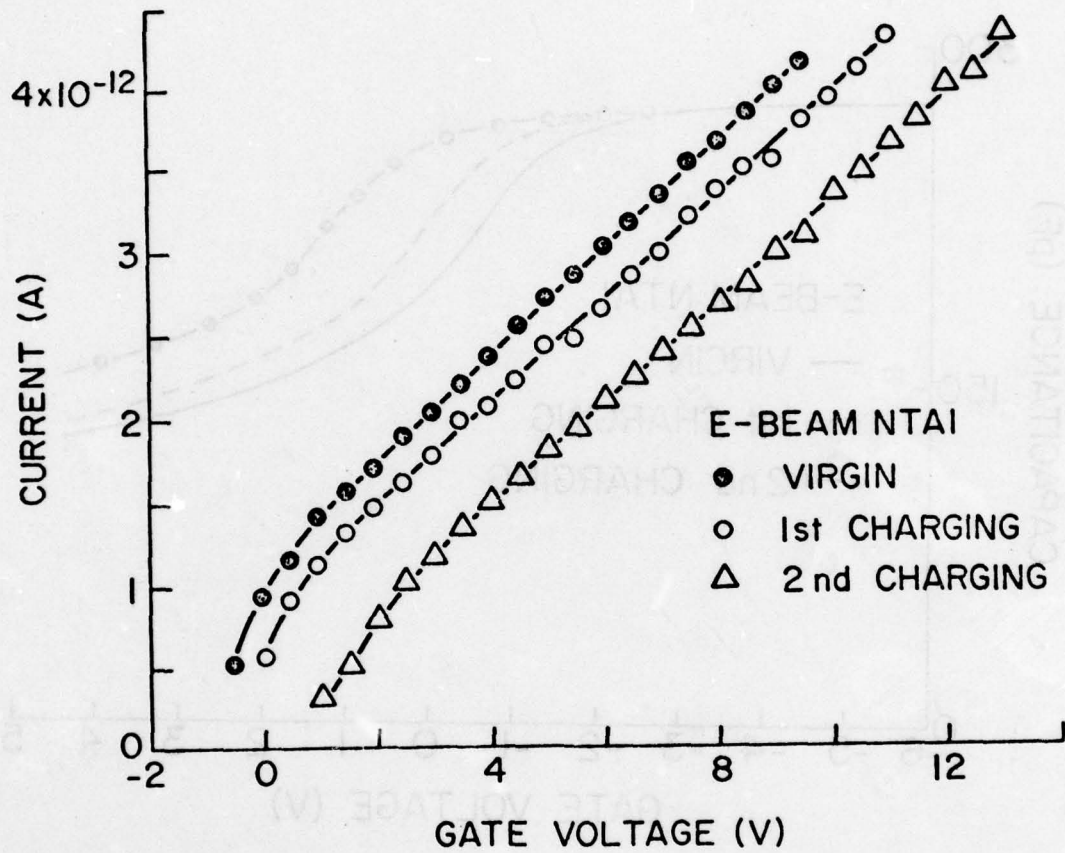


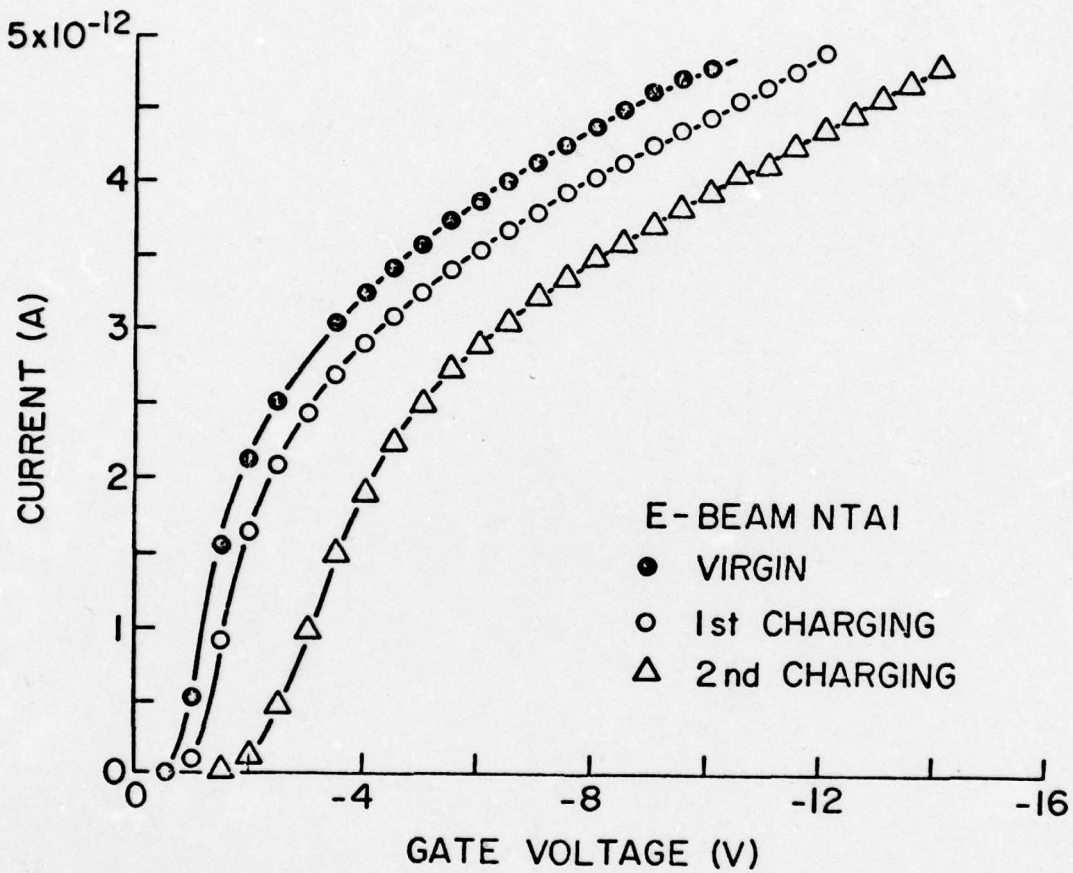












MISSION
of
Rome Air Development Center

RADC plans and executes research, development, test and selected acquisition programs in support of Command, Control Communications and Intelligence (C³I) activities. Technical and engineering support within areas of technical competence is provided to ESD Program Offices (POs) and other ESD elements. The principal technical mission areas are communications, electromagnetic guidance and control, surveillance of ground and aerospace objects, intelligence data collection and handling, information system technology, ionospheric propagation, solid state sciences, microwave physics and electronic reliability, maintainability and compatibility.

**Printed by
United States Air Force
Hanscom AFB, Mass. 01731**